Topographical organisation of non-cholinergic neurons in the pedunculopontine nucleus

Cristina Martínez González

Brasenose College

Thesis submitted for the degree of Doctor of Philosophy at the University of Oxford

Michaelmas Term 2012

Topographical organisation of non-cholinergic neurons in the pedunculopontine nucleus

Cristina Martínez González

Brasenose College, Oxford

Thesis submitted for the degree of Doctor of Philosophy, Michaelmas Term 2012

ABSTRACT

The pedunculopontine nucleus (PPN) is a brainstem structure involved in motor control, sleep and arousal. The boundaries of the PPN are defined by its cholinergic neurons, but it also contains GABAergic, glutamatergic and calcium-binding protein-positive neurons. To further understand the physiological roles of the PPN it is necessary to understand which neuronal subtypes are present in the PPN and how they are connected with other regions of the brain in normal and pathological conditions. In order to address these issues, the total numbers, distributions and neurochemical phenotypes of neurons, positive for the calcium-binding proteins calbindin and calretinin, were studied in the rat PPN.

Sagittal, perfuse-fixed rat brain sections were double or triple-immunolabelled to reveal the cholinergic marker choline acetyltransferase (ChAT) with calbindin and/or calretinin. A stereological approach revealed that calbindin- and calretinin-positive neurons account for a large proportion of PPN neurons, but they rarely co-express ChAT. A combination of immunolabelling for calbindin or calretinin with *in situ* hybridisation for GAD65/67 or VGluT2 mRNAs revealed that about one third of the calbindin- and calretinin-expressing neurons are GABAergic and preferentially located in the rostral PPN, whereas approximately two thirds are glutamatergic and principally located in the caudal PPN.

Additionally, retrograde tracer injections in the subthalamic nucleus (STN) and the gigantocellular nucleus (GiN) showed that the majority of PPN neurons, projecting to one or both of these nuclei, were not cholinergic (70-90%). Less than 10% of STN-projecting neurons expressed calbindin or calretinin and 5% of the GiN-projecting neurons contained calretinin but none contained calbindin. Finally, the expression of the immediate early gene, Egr1, a marker of neuronal activation, was evaluated in STN- and GiN-projecting neurons of the PPN in control and 6-OHDA lesioned animals. No statistically significant differences, in the number of Egr1-positive neurons, were observed between control and 6-OHDA lesioned animals.

These findings show that calbindin- and calretinin-positive neurons are abundant in the PPN, heterogeneously distributed and display a GABAergic or glutamatergic phenotype. Additionally, calbindin- and calretinin-positive neurons represent only a minority of the PPN neurons projecting to either the STN, GiN or both nuclei. Results also suggest that the hyperactivity seen in the PPN in the 6-OHDA model of Parkinson's disease may not necessarily be due to the neurons projecting to the STN and/or GiN.

Overall, this thesis supports the notion that the PPN is composed of a rich diversity of neuronal cell-types, which are heterogeneously distributed along its rostro-caudal axis. The heterogeneous neurochemistry, connectivity and physiology of these neurons allow the PPN to influence a wide range of brain regions through a variety of pathways presumably underlying its various functional roles.

Acknowledgments

First to all I will like to thank my supervisors Prof. J. Paul Bolam and Dr. Juan Mena-Segovia for their invaluable support, teaching and encouragement to achieve excellence in science all these years.

Thanks to Paul for being a fantastic mentor and a truly great person to learn from, for his infinite patience reading this thesis, and for sharing his knowledge and his amazing enthusiasm for science.

Thanks to Juan for all his exhaustive teaching, mentoring and patience, for his encouragement and training to achieve this thesis, and for his friendship and support throughout these years.

Thanks to Jonny, my beloved husband who makes my life a bit brighter every day we share together, thanks for all your love, friendship and support.

To Jorge, my grandfather, thank you for all your valuable teachings as a father, for all your support and love in my life, for your patience, advice and for always believing in me.

To Blanca, my mum, thank you for your support, love and encouragement all my life.

To Rogelio, my dad, thank you for our coffee conversations and friendship.

To Martha and Adriana, thank you for being the best aunties ever.

To all my family, thank you for your love and support.

To my dear old friends from home, to Rosana, Rosario, Rocio, Eda, Maritrini, Luis and Paco, thank you for the good old days, the laughs and the eternal friendship.

To my friends from the unit, Icnelia, Eleftheria, Natalie, Megan, Maria, Ben, Adam Kouichi, Andy, Nico, Pete, Chad, Federica, Lema, Katja, Kristina, Ruth, Thomas, Pablo, Tommas, Anna, Linda, Judith, Foad and James, thank you for your friendship and for making this unit a fantastic place to work.

To Ben, Liz, Gareth, Katie and Caroline, thank you for your excellent technical assistance and help, that makes every day in the lab possible.

To Mary, Jo, Rob, Chad and Jenny thanks for your great administrative and IT support all these years.

Thank you to Professor Peter Somogyi for the encouragement to do great science and for the opportunity to work in such as remarkable scientific unit.

Table of contents

i. Abstract 2

ii. Acknowledgments 3

iii. Table of contents 4

iv. Abbreviations 8

1. GENERAL INTRODUCTION 10

1.1. Opening remarks 11

1.2. Introduction to the pedunculopontine nucleus 11

1.2.1. Localisation of the PPN 11

1.2.2. Subdivisions of the PPN 13

1.3. Neuronal diversity 15
1.3.1. Cholinergic neurons 15
1.3.2. GABAergic neurons 16
1.3.3. Glutamatergic neurons 17
1.3.4. Calcium-binding proteins in the PPN 18
1.3.4.1. Calbindin 19
1.3.4.2. Calretinin 20
1.3.4.3. Parvalbumin 21

1.4. Electrophysiological properties of PPN neurons 21

1.5. Efferent connectivity of the PPN 22
1.5.1. PPN efferents to the basal ganglia 23
1.5.1.1. PPN efferents to the striatum 23
1.5.1.2. PPN efferents to the subthalamic nucleus 24
1.5.1.3. PPN efferents to the entopeduncular nucleus/internal globus pallidus 24
1.5.1.4. PPN efferents to the substantia nigra 25
1.5.2. PPN efferents to the ventral tegmental area 26
1.5.3. PPN efferents to the thalamus 27
1.5.4. PPN efferents to the tectum 29
1.5.5. PPN efferents to the forebrain 29
1.5.6. PPN efferents to the brainstem and PPN descending projections 30
1.5.7. Summary 30

1.6. Afferent connectivity of the PPN 33
1.6.1. PPN afferents from the basal ganglia 33
1.6.1.1. PPN afferents from the subthalamic nucleus 33
1.6.1.2. PPN afferents from the entopeduncular nucleus/internal globus pallidus 33
1.6.1.3. PPN afferents from the substantia nigra *pars* reticulata 34
1.6.2. PPN afferents from the cerebral cortex 34
1.6.3. PPN afferents from other brain regions 34
1.6.4. Summary 35

1.7. Functional roles of the PPN 38
1.7.1. Locomotion 38
1.7.2. REM sleep and sleep-wake cycles 39

1.8. The basal ganglia 40

1.9. Parkinson's disease 41
1.9.1. Parkinson's disease progression 43
1.9.2. Parkinson's disease models 44
1.9.3. PPN and Parkinson's disease 45
1.9.4. Deep brain stimulation of the PPN 45

1.10. Aims of the Thesis 47

2. MATERIALS AND METHODS 48

2.1. Introduction 49

2.2. Chapter 3 methods 49
2.2.1. Perfusion, fixation and sectioning of brain tissue 49
2.2.2. Immunoperoxidase reactions 49
2.2.3. Image acquisition and identification of immunopositive neurons 51
2.2.4. Measurement and comparison of somatic diameter 51
2.2.5. Segmentation of the PPN for stereological analysis 52
2.2.6. Stereological estimation of total cell numbers and densities 54
2.2.7. Statistical analyses of cell numbers and densities 55

2.3. Chapter 4 methods 55
2.3.1. Analysis of double-immunoperoxidase labelling 55
2.3.2. *In situ* hybridisation 55
2.3.3. Immunoperoxidase labelling (subsequent to *in situ* hybridisation) 57
2.3.4. Quantification of *in situ* hybridisation and immunoperoxidase labelling 58
2.3.5. Triple immunofluorescent labelling 59

2.4. Chapter 5 methods 60
2.4.1. Tracer injections in the STN and GiN 60

2.4.2. Processing tissue for tracer injections 61
2.4.3. Immunofluorescent labelling of calbindin, calretinin and ChAT in STN- and GiN-projecting neurons 61
2.4.4. Analysis of immunofluorescent and retrograde labelled PPN neurons 62
2.4.5. 6-hydroxydopamine lesions 63
2.4.6. Behavioural evaluation of 6-OHDA lesioned animals 65
2.4.7. Tracer injections in control and 6-OHDA lesioned animals 65
2.4.8. Egr1 immunolabelling in tracer-injected, control and lesioned animals 66

3. CALBINDIN- AND CALRETININ-POSITIVE NEURONS IN THE PPN 68

3.1. Introduction 69

3.2. Summary of methods 70

3.3. Results 72
3.3.1. Morphology of calbindin- and calretinin-positive neurons 72
3.3.2. Estimated total number of calbindin- and calretinin-positive neurons 75
3.3.3. Distribution of calbindin- and calretinin-positive neurons in the PPN 75
3.3.4. Density analysis of calbindin- and calretinin-positive neurons in the PPN 77

3.4. Discussion 80

4. SUBPOPULATIONS OF CALBINDIN AND CALRETININ NEURONS IN THE PPN CONTAIN CHOLINERGIC, GABAERGIC AND GLUTAMATERGIC MARKERS 82

4.1. Introduction 83

4.2. Summary of methods 84

4.3. Results 87
4.3.1. Few calbindin-positive neurons contain the cholinergic marker ChAT 87
4.3.2. A small proportion of calretinin-positive neurons are cholinergic 89
4.3.3. Triple-immunofluorescent labelling of calbindin, calretinin and ChAT 91
4.3.4. GABAergic and glutamatergic neurons of the PPN 93
4.3.5. Distribution of calbindin-positive neurons containing GAD65/67 or VGluT2 mRNA 95
4.3.6. Distribution of calretinin-positive neurons containing GAD65/67 or VGluT2 mRNA 96

4.6. Discussion 101
4.6.1. Few calbindin- and calretinin-positive neurons in the PPN are cholinergic 101
4.6.2. Calbindin- and calretinin-positive neurons of the PPN express GABAergic or glutamatergic markers 102

4.6.3. Calbindin- and calretinin-positive neurons of the rostral and caudal PPN 102

5. CONNECTIVITY OF THE PPN WITH THE SUBTHALAMIC AND GIGANTOCELLULAR NUCLEI 104

5.1. Introduction 105

5.2. Summary of methods 106
5.2.1. Neurochemical phenotypes of STN- and GiN-projecting PPN neurons 106
5.2.2. Activation of PPN projection neurons in control and lesioned rats 107

5.3. Results 111
5.3.1. The STN and GiN are targets of PPN projection neurons 111
5.3.2. Cholinergic PPN neurons project to the STN and GiN 112
5.3.3. Projections of calbindin- and calretinin-positive neurons of the PPN 116
5.3.4. The expression of the immediate early gene Egr1 in PPN projection neurons of control and 6-OHDA lesioned animals 118

5.4. Discussion 121

6. GENERAL DISCUSSION 125

6.1. Overview of the chapters 126
6.1.1. Introduction 126
6.1.2. Chapter 3: Calbindin- and calretinin-positive neurons in the PPN 126
6.1.3. Chapter 4: Neurotransmitters expressed by calbindin- and calretinin-positive neurons of the PPN 127
6.1.4. Chapter 5: Connectivity and activation of PPN neurons 129
6.1.5. Summary 131

6.2. Technical considerations 132
6.2.1. *In situ* hybridisation 132
6.2.2. Retrograde tracer injections 134
6.2.3. Immediate early gene expression 135

6.3. Future directions 135
6.3.1. Further stereological analyses of PPN neurons 135
6.3.2. Electrophysiological characterisation of PPN neuron subtypes 136
6.3.3. Establishing the neurotransmitters of PPN projection neurons 137
6.3.4. Immediate early gene-expression in the PPN 138

7. REFERENCES 139

Abbreviations

6-OHDA	6-hydroxydopamine
ANOVA	analysis of variance
AP-1	activator protein-1
BSA	bovine serum albumin
CCK	cholesystokinin
ChAT	choline acetyltransferase
CL	centrolateral thalamic nucleus
CM	centromedian thalamic nucleus
Cp	cerebellar peduncle
CPu	caudate putamen or striatum
DA	dopaminergic
DAB	diaminobenzidine
DBS	deep brain stimulation
DG	dorsal geniculate thalamic nucleus
DR	dorsal raphé
EC	enthorinal cortex
EF-hand motifs	alpha helices E and F linked by a short loop
Egr-1	early growth response protein 1
EP	entopeduncular nucleus
GABA	γ-aminobutyric acid
GAD	glutamic acid decarboxylase
GiN	gigantocellular nucleus
GP	globus pallidus
GPe	external segment of the globus pallidus
GPi	internal segment of the globus pallidus
HBN	habenula
IC	inferior colliculus
IEG	immediate early genes
IHC	immunohistochemistry
IP	intraperitoneally injected
ISC	interneuron specific cell types
ISH	*in situ* hybridisation
LC	locus coeruleus
LDTg	lateral dorsal tegmental nucleus.
LM-Sg	lateralis medialis suprageniculate thalamic nucleus
MD	mediodorsal thalamic nucleus
MEA	midbrain extrapyramidal area
MgPA	magnocellular preoptic area
MLR	mesencephalic locomotor region
MPTP	1-methyl-4-phenyl-1,2,3,6-tetrathydropyridine
MRF	medial reticular formation

mRNA	messenger ribonucleic acid
MSN	medium-sized spiny neuron
MVM	medioventral medulla
NADPH	reduced form of nicotinamide adenine dinucleotide phosphate
NbMC	nucleus basalis magnocellularis
NDS	normal donkey serum
NOS	nitric oxide synthase
NPO	nucleus reticularis pontis oralis
O-LM	oriens-lacunosum moleculare
PAG	phosphate activated glutaminase
PB	phosphate buffer
PBS	phosphate buffered saline
pCREB	phosphorylated cAMP response element-binding protein
PD	Parkinson's disease
Pf	parafascicular thalamic nucleus
PFA	paraformaldehyde
PGO	ponto-genicluo-occipital
PPN	pedunculopontine nucleus
PRF	pontine reticular formation
PV	parvalbumin
PVt	paraventricular thalamic nucleus
RAS	reticular activating system
REM	rapid eye movement
RF	reticular formation
RMTg	mesopontine rostromedial tegmental nucleus
RRF	retrorubral field
Rt	reticular thalamic nucleus
RVLM	rostral ventrolateral medulla
SC	superior colliculus
Scp	superior cerebellar peduncle
SEM	standard error of the mean
SNc	substantia nigra pars compacta
SNr	substantia nigra pars reticulata
STN	subthalamic nucleus
STR	striatum or caudate putamen
VA	ventral anterior thalamic nucleus
VGluT	vesicular glutamate transporter
VIP	vasoactive intestinal peptide
VL	ventrolateral thalamic nucleus
VM	ventromedial thalamic nucleus
VTA	ventral tegmental area
ZI	zona incerta
ΔFosB	delta FBJ murine osteosarcoma viral oncogene homolog B

1. General Introduction

1.1. Opening remarks

The pedunculopontine nucleus (PPN) is located in upper brainstem and is involved in functions including locomotion, sleep and arousal. These roles are made possible by the PPNs wide-ranging interconnectivity with other structures such as the basal ganglia, thalamus, cortex and spinal cord among others. Furthermore, this complex nucleus contains a heterogeneous complement of cell types, which can be characterised by their biochemistry, physiological properties and connections with other brain regions. These cells, within the confines of the PPN, will be the focus of this thesis.

1.2. Introduction to the pedunculopontine nucleus

1.2.1. Localisation of the PPN

The first description of the human PPN was given by Jacobsohn in 1909 (Ranson, 1939) and it has subsequently been described as being confined laterally by fibres of the superior cerebellar peduncle (scp), rostrally by the substantia nigra (SN) and dorsally by the retrorubral field (Olszewski, 1982). The dorsal PPN is bounded caudally by the pontine cuneiform formation and lies adjacent to the locus coeruleus (Olszewski, 1982; Pahapill & Lozano, 2000). The stereotaxic coordinates of the human PPN have been more accurately described in recent years to aid surgical interventions (Paxinos, 1995; Zrinzo *et al.*, 2008).

The PPN has been conserved in evolution across species and is present in early mammals, fish and amphibians (Brantley & Bass, 1988; Mesulam *et al.*, 1989; Marin *et al.*, 1998; Ainge *et al.*, 2004; Grillner *et al.*, 2008). The precise boundaries of the PPN have always been difficult to define, in part because of its irregular shape, but also because of the lack of a clear anatomical landmark to define its precise limits. In the rat, the bounds of the PPN extend rostrally to the substantia nigra *pars reticulata* (SNr), caudally to the laterodorsal tegmental nucleus (LDTg) and dorsally to the brachium conjunctivum (Garcia-Rill, 1991; Garcia-Rill *et al.*, 2011) (Figure 1.1).

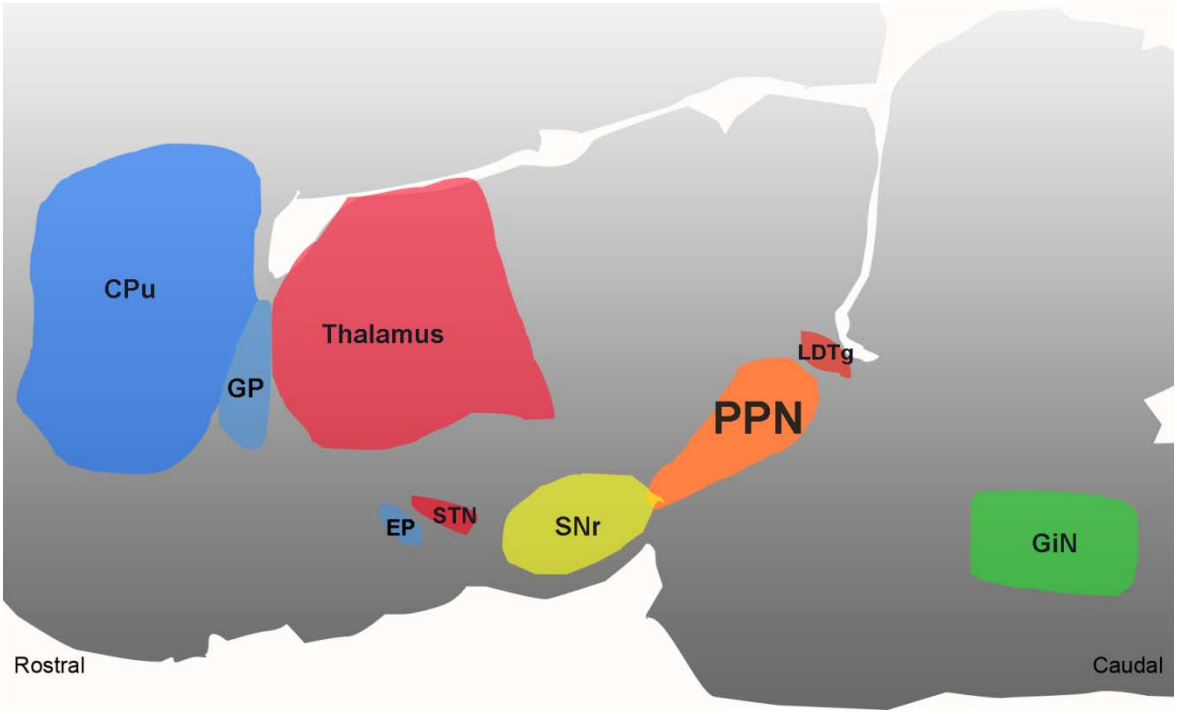


Figure 1.1. Schematic representation of the rat pedunculopontine nucleus (PPN) in relation to other structures of the brain, including the basal ganglia, in a sagittal section. The PPN (orange) is located at the top of the brainstem, with its rostral extent lying adjacent to the substantia nigra *pars reticulata* (SNr; yellow) and the caudal PPN bordering the laterodorsal tegmental nucleus (LDTg; red). Abbreviations: CPu, caudate putamen or striatum (dark blue); GP, globus pallidus (pale blue); EP, entopeduncular nucleus (pale blue); thalamus (red); STN, subthalamic nucleus (red); GiN, gigantocellular nucleus (green).

1.2.2. Subdivisions of the PPN

The PPN contains the cholinergic Ch5 group of neurons that use acetylcholine as a neurotransmitter (Mesulam *et al.*, 1983). These cholinergic neurons have been used historically to delimit the boundaries of the irregularly shaped PPN (Mesulam *et al.*, 1983; Garcia-Rill, 1986; Rye *et al.*, 1987) and are still used to this day as a measure of its limits (Winn, 2006; Mena-Segovia *et al.*, 2009).

The PPN is not a homogeneous structure in terms of its neuronal organisation. The PPN was originally divided into the *pars dissipata* (rostral) and *pars compacta* (caudal) on the basis of the density and arrangement of its cholinergic neurons (Olszewski, 1982). This subdivision resembles the organisation of the SNr and substantia nigra *pars compacta* (SNc) and structural similarities between the PPN and the SN have been suggested (Winn, 2006). Similarly, the anterior and posterior PPN can be divided by their innervation of midbrain dopaminergic neurons (Mena-Segovia *et al.*, 2008b). Moreover, behavioural studies have shown a functional dissociation of the rostral and caudal PPN (Inglis *et al.*, 2001); a restricted lesion in the rostral PPN of the rat leads to locomotor depression, but a lesion in the caudal PPN does not (Alderson *et al.*, 2008). In contrast, self-administration of nicotine in rats is altered by a lesion in the caudal, but not the rostral, PPN (Alderson *et al.*, 2006).

Another way to subdivide the PPN uses the centre of the SNr and the middle point of the base of the superior cerebellar peduncle as external anatomical landmarks to subdivide the PPN into ten segments (1-5 anterior and 6-10 posterior segments; Mena-Segovia *et al.*, 2009). These segments define functional sub-territories in the PPN that correlate with the cholinergic *pars dissipata* and *pars compacta* subdivisions (Figure 1.2; Mena-Segovia *et al.*, 2009).

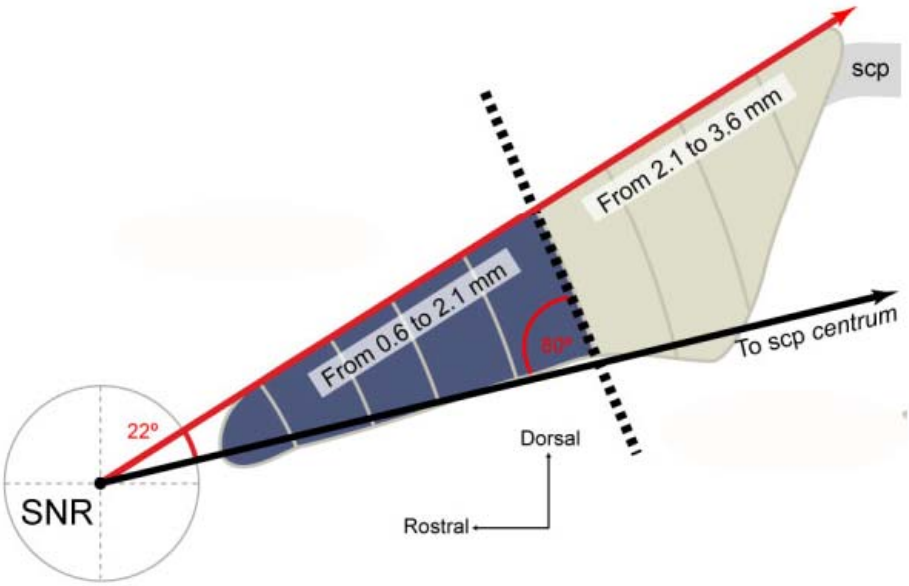


Figure 1.2. Diagram of subregions of the PPN in the rat based on two types of neurons. The anterior PPN segments containing a higher density of GABAergic neurons are shown in blue (segments 1-5) and posterior PPN segments are shown in yellow-green (segments 6-10). The two regions are separated by a line between segment 5 and 6 at 2.1 mm from the centre of the SNr (Mena-Segovia *et al.*, 2009; scp: superior cerebellar peduncle).

In addition, the distribution of distinct neuronal populations supports this rostro-caudal segregation GABA (gamma-aminobutyric acid)-ergic neurons are highly concentrated in the rostral segments of the PPN. Historically, the PPN has been subdivided into rostral, middle and caudal thirds (Rye *et al.*, 1987), or defined as including an area referred to as the midbrain extrapyramidal area (MEA); this receives a dense innervation from the basal ganglia but lies outside the cholinergic borders of the PPN (Steininger et al., 1992).

1.3. Neuronal diversity

The PPN is composed of neurons of differential size, neurochemical phenotype and connectivity. There are three major, neurochemically distinct, groups of neurons that have been identified in the PPN: cholinergic, GABAergic and glutamatergic neurons.

1.3.1. Cholinergic neurons

The cell bodies of the Ch5 group of cholinergic neurons are large (20-50 μm), with a triangular or polygonal somatic shape and 2-5 primary dendrites (Armstrong *et al.*, 1983; Sugimoto *et al.*, 1984; Rye *et al.*, 1987). They are distributed along the rostro-caudal axis of the PPN, but the neurons in the rostral PPN are more sparsely distributed than those in the caudal PPN. In addition, cholinergic neurons in the rostral PPN follow a 'layer like' arrangement in alignment with the superior cerebellar peduncle, whereas the cholinergic neurons in the caudal PPN do not (Mena-Segovia *et al.*, 2009).

The Ch5 cholinergic neurons of the PPN and the nearby Ch6 group, that constitutes the LDTg (Mesulam *et al.*, 1983), provide extensive ascending innervation to many parts of the brain, as well as descending innervation to the spinal cord and motor structures (Woolf & Butcher, 1986; Hallanger *et al.*, 1987; Semba & Fibiger, 1992). Although

cholinergic neurons of the PPN can be labelled with antibodies against choline acetyltransferase (ChAT; enzyme in the biosynthetic pathway of acetylcholine) (Eckenstein & Thoenen, 1982; Sofroniew *et al.*, 1982; Armstrong *et al.*, 1983; Bolam *et al.*, 1984; Wainer *et al.*, 1984), the majority of the cholinergic neurons in the PPN can be identified by the presence of two other markers: nitric oxide synthase (NOS) and the reduced form of nicotinamide adenine dinucleotide phosphate (NADPH) (Vincent *et al.*, 1983; Vincent *et al.*, 1986; Dun *et al.*, 1994; Leonard *et al.*, 1995).

However, it should be noted that cholinergic neurons are not the most abundant type of neuron in the PPN (Wang & Morales, 2009). The cholinergic neurons are intermingled amongst a larger number of GABAergic and glutamatergic neurons (Mena-Segovia *et al.*, 2009). These are distinct from the cholinergic neurons, as it has been shown that less than 1% of cholinergic neurons express the GABAergic marker, glutamic acid decarboxylase (GAD) messenger ribonucleic acid (mRNA) and less than 2% co-express the glutamatergic marker, vesicular glutamate transporter 2 (VGluT2) mRNA (Wang & Morales, 2009); these values are probably within the margin of experimental error.

1.3.2. GABAergic neurons

GABA is one of the major inhibitory neurotransmitters used in the brain and GABAergic neurons are widely distributed across the basal ganglia and the brainstem (Smith *et al.*, 1987; Parent *et al.*, 1995; Bolam *et al.*, 2000), including the PPN (Ford *et al.*, 1995). GABAergic neurons can be identified by their expression of GAD, the enzyme that synthesizes GABA from glutamate. There are two isoforms of this enzyme that are expressed in the brain: GAD65 and GAD67 (Erlander *et al.*, 1991), and GABAergic neurons of the PPN are seen to express one or both of these (Mena-Segovia *et al.*, 2009; Wang & Morales, 2009).

GABAergic neurons are highly abundant in the rostral PPN (which lies adjacent to the caudal SNr), but their density decreases towards the caudal PPN (Mena-Segovia et al., 2009). However, overall they are approximately twice as abundant as the cholinergic neurons in the rat PPN (Mena-Segovia *et al.*, 2009), and form a distinct neuronal population (Wang & Morales, 2009). GABAergic neurons of the PPN send axonal projections towards several nuclei of the basal ganglia (see section 1.5.1). Until now, no other neurochemical marker has been seen to be associated with these neurons (see Chapter 4).

1.3.3. Glutamatergic neurons

Glutamate is the most common excitatory amino acid neurotransmitter in the central nervous system. Glutamatergic neurons express vesicular glutamate transporters (VGluTs) that specifically transport glutamate from the cytoplasm into vesicles of the synaptic terminal. Three vesicular glutamate transporters have been identified: VGluT1 (Ni *et al.*, 1994; Ni *et al.*, 1996; Takamori *et al.*, 2000), VGluT2 (Aihara *et al.*, 2000; Fremeau *et al.*, 2001; Herzog *et al.*, 2001) and VGluT3 (Fremeau *et al.*, 2002; Gras *et al.*, 2002).

Two of these, VGluT1 and VGluT3, are not expressed in the PPN (Wang & Morales, 2009). VGluT1 mRNA is expressed strongly in subpopulations of neurons in the cerebral cortex, hippocampus, cerebellum, amygdala, olfactory bulb and retina; there is very little expression of VGluT1 mRNA in subcortical structures (Ni *et al.*, 1996; Mimura *et al.*, 2002). VGluT3 is largely expressed outside of the brain, in the liver and kidney, but within the brain its abundance and localisation is still somewhat unclear (Fremeau *et al.*, 2002; Gras *et al.*, 2002; Schafer *et al.*, 2002).

Conversely, VGluT2, is largely expressed in subcortical regions (Fremeau *et al.*, 2004; El Mestikawy *et al.*, 2011), including the diencephalon, brainstem, cerebellum and spinal cord (Aihara *et al.*, 2000; Sakata-Haga *et al.*, 2001; Hisano *et al.*, 2002; Kaneko *et al.*, 2002; Stornetta *et al.*, 2002a; Stornetta *et al.*, 2002b; Varoqui *et al.*, 2002). The expression of VGluT2 mRNA is largely complementary to VGluT1 and, with a few exceptions, its pattern of distribution is very different (Sakata-Haga *et al.*, 2001; Kaneko & Fujiyama, 2002; Mimura *et al.*, 2002; Barroso-Chinea *et al.*, 2008). VGluT2 mRNA-containing neurons are highly abundant in the PPN and rarely co-express ChAT immunoreactivity (<2%; Wang & Morales, 2009). They are distributed all along its rostro-caudal axis and, in the caudal PPN, are at least 1.5 times more abundant than the cholinergic neurons (Wang & Morales, 2009). Like GABAergic neurons of the PPN, other neurochemical markers contained by these neurons have not yet been identified (see Chapter 4).

In summary, there are at least three main neuronal types in the PPN: cholinergic, GABAergic and glutamatergic neurons, based upon the neurotransmitters expressed by each. To further characterise these neurons more information is required on which other neurochemical markers they might contain.

1.3.4. Calcium-binding proteins in the PPN

Despite fact that they may use the same transmitter, neurons that express calcium-binding proteins, in particular those expressing calbindin, calretinin and parvalbumin (PV), have been shown to have distinct functional properties in many parts of the brain. As a consequence, they have been used extensively as markers to distinguish between functionally diverse populations of neurons in the hippocampus (Acsady *et al.*, 1993; Somogyi & Klausberger, 2005), neocortex (Staiger et al., 2004), basal ganglia (Fortin &

Parent, 1996; Parent *et al.*, 1996; Airaksinen *et al.*, 1997; Alfahel-Kakunda & Silverman, 1997) and basal forebrain (Fortin & Parent, 1999; Gritti *et al.*, 2003). As calcium-binding proteins are expressed by neurons in the PPN (Dun et al., 1995), Chapters 3 and 4 of this thesis will examine the number and distribution of these neurons and, most importantly whether they are cholinergic, GABAergic or glutamatergic.

Calcium-binding proteins form part of the large super family of proteins containing EF-hand motifs (alpha helices E and F linked by a short loop) (Kretsinger & Nockolds, 1973; Camp & Wijesinghe, 2009). The EF-hand motif permits the specific and reversible binding of calcium. Calbindin and other members of this EF-hand super family have a functional role in the modulation of intracellular calcium levels by binding calcium at different kinetic rates (Nagerl et al., 2000), conferring upon them particular physiological and functional properties (Chard *et al.*, 1993; Schwaller *et al.*, 2002; Camp & Wijesinghe, 2009). It has been proposed that the presence of some calcium-binding proteins may protect neurons from degeneration in aging (Liu *et al.*, 2009), or in pathological conditions such as Parkinson's disease (German *et al.*, 1992; Mouatt-Prigent *et al.*, 1994).

1.3.4.1. Calbindin

Calbindin is a 28 kDa vitamin D-dependent calcium-binding protein (Pochet *et al.*, 1985) that is widely expressed in the brain, in regions including the hippocampus, cerebellum and basal ganglia (Celio, 1990; Sequier *et al.*, 1990; Parent *et al.*, 1996; Fortin & Parent, 1999). In the hippocampus, calbindin is a useful marker to differentiate between the two types of pyramidal cells and many types of interneurons (Acsady *et al.*, 1993; Klausberger *et al.*, 2003). The combined presence of calbindin and cholecystokinin (CCK) immunoreactivity in the same cell is used to identify Shaffer collateral-associated neurons, whereas the combination of calbindin and somatostatin immunoreactivity is used as a

marker for hippocampo-septal neurons (Somogyi & Klausberger, 2005). Immunoreactivity for calbindin has been observed in PPN neurons (Parent *et al.*, 1996) and will be discussed in Chapters 3 and 4 of this thesis.

1.3.4.2. Calretinin

Calretinin is another calcium-binding protein member of the EF-hand superfamily (Pochet *et al.*, 1985; Camp & Wijesinghe, 2009) that is widely expressed in the brain (Arai *et al.*, 1991; Resibois & Rogers, 1992; Parent *et al.*, 1996; Fortin & Parent, 1999). Calretinin is present in GABAergic and glutamatergic neurons and is a useful marker to distinguish discrete populations of neurons in several structures of the brain. In the striatum, calretinin is present within a sub-population of GABAergic interneurons that are distinct from parvalbumin and nitric oxide synthase interneurons (Bennett & Bolam, 1993). In the hippocampus, calretinin is present in non-pyramidal cells (Acsady *et al.*, 1993) and, in combination with the vasoactive intestinal peptide (VIP), is a marker for the GABAergic interneuron specific cell types (ISC) I, II and III (Somogyi & Klausberger, 2005). The enthorinal cortex (EC) receives innervation from local calretinin-positive interneurons containing VGluT2 and projection fibres from the thalamus (Wouterlood *et al.*, 2008). In the medial septum of the rat, calretinin-positive neurons are present and intermingled with ChAT-positive cholinergic neurons, but the co-expression of the two markers has never been observed (Kiss *et al.*, 1997). In the basal forebrain, the majority of the calretinin-positive neurons contain phosphate activated glutaminase (PAG); an enzyme used as a marker of glutamatergic neurons (Gritti *et al.*, 2003). Immunoreactivity against calretinin has also been found in the rat and primate PPN, mostly in non-cholinergic neurons (Parent *et al.*, 1996; Fortin & Parent, 1999). Other neurochemical markers for these neurons are yet to be determined (but see Chapter 4 for more detail).

1.3.4.3. Parvalbumin

Parvalbumin (PV) is a 12 kDa protein member of the EF-hand super family that was first isolated from skeletal muscle in mammals (Heizmann, 1984a; b). In the hippocampus, four types of GABAergic interneurons show PV immunoreactivity: axo-axonic cells, one type of basket cell, bistratified cells and oriens-lacunosum moleculare (O-LM) cells (Klausberger *et al.*, 2003; Somogyi & Klausberger, 2005). In the basal forebrain, the majority of parvalbumin-containing neurons are GABAergic (Gritti *et al.*, 2003). In the PPN, parvalbumin has been detected only in non-cholinergic neurons (Dun *et al.*, 1995). There are a large number of PV-positive fibres passing through the PPN, likely originating in the cerebellum, and to a lesser extent the SNr. These fibres make it difficult to visualise PV-positive neurons in the PPN by conventional immunohistochemical techniques.

1.4. Electrophysiological properties of PPN neurons

Many different firing properties have been observed in PPN neurons *in vivo*. (for review Jenkinson *et al.,* 2009). Among the cholinergic neurons in the PPN, two types of firing patterns have been identified: slow-firing cholinergic neurons that are associated with the cortical upstate during slow cortical oscillations and fast-firing cholinergic neurons that are correlated with the cortical downstate during slow oscillations (Mena-Segovia *et al.*, 2008a). As of yet these neurons can only be identified by their differential activities; nothing is known of their neurochemical markers that could help us to differentiate between these two types of neurons.

In the case of non-cholinergic neurons, GABAergic and glutamatergic neurons can be detected by labelling GAD65/67 or VGluT2 mRNAs respectively. A subset of putatively glutamatergic neurons (because they give rise to asymmetric synaptic contacts)

have been divided into two main subtypes based on their physiological activity: fast-firing neurons that are associated with the cortical slow oscillations (Mena-Segovia *et al.*, 2008a) and quiescent (or very slow firing) neurons whose firing is independent of the cortical activity (Ros *et al.*, 2010). These putatively glutamatergic neurons have a different axonal trajectory and pattern of innervation from those of cholinergic neurons, although some targets are shared by both types (notably, the basal ganglia). Other non-cholinergic neurons that have not been characterised in terms of their neurochemical nature include tonic firing neurons and irregular firing neurons; it is likely that at least one of these subtypes is GABAergic.

The correlation between neurochemical subtypes and electrophysiological properties recorded in *in vitro* experiments is more limited. Three types of PPN neuron have been described on the basis of their membrane properties *in vitro*; those displaying A-currents, low-threshold spikes or a mixture of the two (Leonard & Llinas, 1994; Takakusaki *et al.*, 1997; Saitoh *et al.*, 2003). These classifications of neurons do not appear to be related to their neurochemical nature or their synaptic targets. The different membrane properties, however, are likely to underlie some of the functional differences between each subtype, which could influence the effects of the PPN upon other brain regions.

1.5. Efferent connectivity of the PPN

Neurons of the PPN give rise to long axons that innervate several targets. The longest axons arise from cholinergic neurons and give rise to as many as 5 or 6 collaterals that innervate the basal ganglia, thalamus, tectum and lower brainstem, among other regions (Mena-Segovia *et al.*, 2008a). The axons of non-cholinergic neurons are more restricted in terms of length and number of collaterals. Tracer studies have produced

extensive data on the connectivity of the PPN with the cortex, basal ganglia, thalamus, tectum, forebrain, brainstem and spinal cord (for review Jenkinson *et al.,* 2009; Table 1.1; Figure 1.3).

1.5.1. PPN efferents to the basal ganglia

The basal ganglia are a collection of subcortical nuclei that are involved in motor, cognitive and mnemonic functions. The basal ganglia include the striatum, the subthalamic nucleus (STN), the globus pallidus (GP or external segment of the GP in primates; GPe), entopeduncular nucleus (EP, internal segment of the GP in primates; GPi), and the substantia nigra (SN) (Bolam *et al.*, 2000) (for details see section 1.8). Several nuclei of the basal ganglia project to the PPN and receive input from the basal ganglia in a topographical manner.

1.5.1.1. PPN efferents to the striatum

The striatum is the major input structure of the basal ganglia with 2.79 million neurons per hemisphere in the rat (Oorschot, 1996), with approximately 95% of these neurons being accounted for by one main type of neuron, the medium-sized spiny neuron (MSN) (Kemp & Powell, 1971; Kita & Kitai, 1988). The MSNs can be divided into two main types based upon their neurochemical markers and whether their axons project directly or indirectly to the output nuclei of the basal ganglia (Albin *et al.*, 1989; Alexander & Crutcher, 1990; DeLong, 1990; Bolam *et al.*, 2000). The striatum integrates inputs from the cortex, thalamus, SNc and other areas of the brain, including the PPN. Tracer studies using anterograde and retrograde markers have shown the existence of a direct projection from the PPN to the striatum in the rat (Saper & Loewy, 1982) and in primates (Nakano et al., 1990).

1.5.1.2. PPN efferents to the subthalamic nucleus

The subthalamic nucleus (STN) is the only glutamatergic structure of the basal ganglia and it contains approximately 13,600 neurons per hemisphere in the rat (Oorschot, 1996). The STN lies below the thalamus, with its dorsal extreme bordering the zona incerta (ZI). Its rostral edge borders the cerebellar peduncle (cp) and at its posterior it borders the SN. The STN is heavily connected with the cortex, GP, SN, the centromedian (CM) and parafascicular nuclei (Pf) of the thalamus and the PPN (Saper & Loewy, 1982; Edley & Graybiel, 1983; Hammond *et al.*, 1983; Canteras *et al.*, 1990; Bevan & Bolam, 1995; Hassani *et al.*, 1997; Cragg *et al.*, 2004).

It has been shown by tracer experiments in the cat, rat and in primates that the STN receives input from the PPN (Nomura *et al.*, 1980; Carpenter *et al.*, 1981; Saper & Loewy, 1982; Edley & Graybiel, 1983; Hammond *et al.*, 1983; Lavoie & Parent, 1994c). More recently, tractography studies have confirmed these findings in humans (Muthusamy et al., 2007). It has been shown that the PPN output to the STN arises from neurons located in the caudal PPN (Carpenter *et al.*, 1981; Kita & Kita, 2010). Such projections include cholinergic, GABAergic and glutamatergic neurons (Bevan & Bolam, 1995).

1.5.1.3. PPN efferents to the entopeduncular nucleus/internal globus pallidus

The entopeduncular nucleus (EP, in rat and cat, equivalent to the internal segment of the globus pallidus or GPi in primates) is a mainly GABAergic structure (Smith *et al.*, 1987) that represents an important output nucleus of the basal ganglia despite being a relatively small structure. It contains around 3,200 neurons per hemisphere in the rat and it is located rostral to the STN (Oorschot, 1996).

The EP/GPi receives input from the PPN (Saper & Loewy, 1982; Jackson & Crossman, 1983; Woolf & Butcher, 1986; Shink *et al.*, 1997). It has been observed in the rat and cat that this PPN projection has an excitatory influence on EP/GPi neurons (Scarnati *et al.*, 1988). A species-specific difference seems to exist regarding the strength of this connection; projections have been reported to be more abundant in the monkey than in the cat (Edley & Graybiel, 1983). In primates, tracer injections in the GPi give rise to a large number of retrogradely labelled PPN neurons in the rostral PPN, around 40% of which are cholinergic. In contrast, an injection restricted to the GPe produces a smaller number of labelled neurons in the PPN than an injection restricted to the GPi (Charara & Parent, 1994). Supporting this, anterograde *Phaseolus vulgaris* leucoagglutinin tracer injections in the PPN give rise to a substantially higher density of anterogradely-labelled fibres in the GPi than in the GPe (Lavoie & Parent, 1994c).

1.5.1.4. PPN efferents to the substantia nigra

The substantia nigra (SN) is divided into two main parts, the SN *pars compacta* (SNc) and SN *pars reticulata* (SNr). Together with the EP/GPi, the SNr is a major GABAergic output nucleus of the basal ganglia and the SNc supplies dopaminergic feedback to the striatum. The SNr and the SNc contain approximately 26,300 and 7,200 neurons respectively, per hemisphere in the rat (Oorschot, 1996). The SN is located caudal to the STN and rostral to the PPN. It is interconnected with several thalamic nuclei, the striatum, GPe, STN and the PPN (Woolf & Butcher, 1986; Celada *et al.*, 1999; Paladini *et al.*, 1999; Sidibé *et al.*, 2002).

The SNc and the SNr both receive input from the PPN (Saper & Loewy, 1982; Woolf & Butcher, 1986). Tracer studies in the rat and monkey have shown that SNc dopaminergic neurons receive direct glutamatergic and cholinergic input from PPN

neurons (Sugimoto & Hattori, 1984; Clarke *et al.*, 1987; Scarnati *et al.*, 1987; Gould *et al.*, 1989; Bolam *et al.*, 1991; Futami *et al.*, 1995; Oakman *et al.*, 1995; Charara *et al.*, 1996). Furthermore, the activation of the glutamatergic and cholinergic PPN neurons in the rat can elicit excitatory postsynaptic currents in dopaminergic and non-dopaminergic SN neurons *in vivo* (Scarnati *et al.*, 1984; Scarnati *et al.*, 1987; Futami *et al.*, 1995; Rohrbacher *et al.*, 2000). The neurons that project to the SN are concentrated in the rostral PPN and about 25% of these are cholinergic (Lavoie & Parent, 1994a); SN-projecting neurons of the primate PPN are also preferentially located in rostral regions (Lavoie & Parent, 1994a). Additionally, studies in the rat have shown that cholinergic and non-cholinergic neurons that innervate the SNc are preferentially located in the rostral PPN (Takakusaki *et al.*, 1996); these projections are mostly ipsilateral (Oakman *et al.*, 1995; Oakman *et al.*, 1999).

1.5.2. PPN efferents to the ventral tegmental area

The ventral tegmental area (VTA), together with the SNc, constitute the two main dopaminergic structures in the midbrain. The VTA receives substantial cholinergic innervation from the PPN; these PPN efferents have been observed in the rat and in primates (Sugimoto & Hattori, 1984; Oakman *et al.*, 1995; Charara *et al.*, 1996; Geisler & Zahm, 2005). Anterograde tracing experiments in primates have shown the existence of glutamatergic and GABAergic efferents from the PPN to the VTA (Charara et al., 1996). Studies in the rat have shown that the PPN output to the VTA arises mostly from neurons located in the caudal PPN; this projection is bilateral and involves cholinergic (Sugimoto & Hattori, 1984; Oakman *et al.*, 1995), GABAergic and glutamatergic axons (Mena-Segovia et al., 2005).

Stimulation of cortical and PPN projections to the VTA *in vitro*, can induce glutamatergic synaptic currents in VTA dopaminergic and non-dopaminergic neurons (Bonci & Malenka, 1999). More recently, it has been described that GABAergic and glutamatergic PPN inputs do not converge onto the same VTA neurons (Good & Lupica, 2009). Nicotinic acetylcholine receptors (nAChR) can also modulate this excitatory synaptic transmission (Good & Lupica, 2009). The PPN also targets the mesopontine rostromedial tegmental nucleus (RMTg), which is a GABAergic structure also known as the 'tail of the VTA' (Jhou *et al.*, 2009; Kaufling *et al.*, 2009).

1.5.3. PPN efferents to the thalamus

The thalamus is heavily innervated by the PPN, with widespread projections innervating several thalamic nuclei (Saper & Loewy, 1982; Hallanger & Wainer, 1988a) (Smith *et al.*, 1988; Steriade *et al.*, 1988; Kolmac & Mitrofanis, 1998). The stimulation of the PPN can induce c-*fos* expression in the centrolateral (CL), ventrolateral (VL) and reticular (Rt) thalamic nuclei (Ainge *et al.*, 2004), suggesting neuronal activation. The projection from the PPN to the thalamus has been reported to be topographically organised (Steriade *et al.*, 1988; Lavoie & Parent, 1994c), arising mostly from neurons located in the caudal PPN. Thalamic nuclei receive less than 10% of their PPN innervation from the rostral PPN, with the exception of the mediodorsal thalamic nucleus (MD), which receives up to 20% of its innervation from the rostral PPN; the rest of the PPN output to the thalamus arises from the caudal PPN. (Steriade et al., 1988).

A large proportion of the thalamic input provided by the PPN is cholinergic (Sugimoto & Hattori, 1984; Sofroniew *et al.*, 1985; Hallanger *et al.*, 1987; Hallanger & Wainer, 1988a; b; Takakusaki *et al.*, 1996; Oakman *et al.*, 1999; Parent & Descarries, 2008); however, a small proportion is not (Smith et al., 1988; Steriade et al., 1988). It has

been described that cholinergic and glutamatergic PPN neurons innervate the parafascicular nucleus (Pf) of the thalamus (Barroso-Chinea *et al.*, 2011). Retrograde labelling from the mediodorsal thalamic nucleus (MD) in the cat produces prominent labelling of non-cholinergic neurons in both the ipsilateral and contralateral PPN (Smith et al., 1988). The ventroanterior (VA) and the ventrolateral (VL) thalamic nuclei receive between 50 and 75% of their cholinergic afferents from the central-caudal PPN, whereas the ventromedial thalamic nucleus (VM) receives its cholinergic input mainly from the caudal PPN and the LDTg (Smith et al., 1988).

Studies in the rat have shown that the Pf receives input from the caudal PPN (Sugimoto & Hattori, 1984). The cholinergic innervation of the Pf has a higher density than the innvervation of the dorsolateral geniculate (DG) and reticular (Rt) thalamic nuclei (Parent & Descarries, 2008). Individual Pf neurons receive convergent synaptic input from the PPN and the superior colliculus (SC) (Kobayashi & Nakamura, 2003). In turn, Pf neurons that receive input from the PPN project to striatum (Erro et al., 1999), monosynaptically linking PPN axons to thalamostriatal neurons (Kobayashi et al., 2007).

Cholinergic neurons that project to the thalamus can also send collaterals to the basal forebrain (Losier & Semba, 1993), pontine reticular formation (Semba et al., 1990), superior (SC) and inferior (IC) colliculi and the basal ganglia (Mena-Segovia et al., 2008). In the cat it has been observed that glutamatergic and GABAergic neurons of the lateralis medialis-suprageniculate nuclear complex (LM-Sg) receive cholinergic input from the PPN (Hoshino et al., 1997; Hoshino et al., 2000). It has been shown in the rat that other thalamic nuclei, such as the centrolateral (CL), centromedial (CM) and paraventricular (PVt) nuclei, receive a more heterogeneous mixture of cholinergic and non-cholinergic PPN afferents (Erro et al., 1999; Krout et al., 2002).

1.5.4. PPN efferents to the tectum

The superior (SC) and inferior (IC) colliculi that form part of the tectum are innervated by the PPN; individual cholinergic neurons of the PPN project to the SC and IC (Mena-Segovia et al., 2008). The large majority of the cholinergic inputs to the IC arise from the ipsilateral PPN and, to a lesser extent, from the LDTg. These projections arise from cholinergic neurons that are located in the caudal PPN and include a subpopulation that project to both the ipsilateral and contralateral IC (guinea pig) (Motts & Schofield, 2009). Retrograde tracer studies in the rat and cat have shown that the SC receives cholinergic and non-cholinergic innervation from the PPN (Beninato & Spencer, 1986; Hall *et al.*, 1989); these afferents arise mainly from the caudal PPN (Beninato & Spencer, 1986). PPN neurons projecting to the SC, as identified by antidromic stimulation, are segregated into two groups: those that are sensitive or insensitive to physiological sensory stimuli (Krauthamer et al., 1995).

1.5.5. PPN efferents to the forebrain

In the forebrain, the magnocellular preoptic area (MgPA) and the nucleus basalis magnocellularis (NbMC) receive afferents from the PPN (Semba *et al.*, 1988; Losier & Semba, 1993). In the cat, a small group of neurons located in the rostral PPN have been observed to send collaterals that innervate the LM-Sg in addition to the SC (Hoshino et al., 2004). The posterior lateral hypothalamus receives cholinergic input from PPN neurons that are scattered throughout the rostro-caudal axis and GABAergic innervation from neurons that are concentrated in the rostral PPN; the neurochemical nature of the majority of these neurons has not been identified (Ford et al., 1995).

1.5.6. PPN efferents to the brainstem and PPN descending projections

Neurons in the PPN give rise to a dense innervation of structures in the lower brainstem, pons, medulla and spinal cord. Descending axons of juxtacellularly-labelled cholinergic PPN neurons have been observed to innervate the nucleus reticularis pontis oralis (NPO) and caudalis nuclei in the rat (Mena-Segovia *et al.*, 2008a). Both cholinergic and non-cholinergic neurons have been observed to innervate the pontine reticular formation (PRF) in the rat (Semba *et al.*, 1990; Takakusaki *et al.*, 1996) and the cat (Mitani et al., 1988).

The PPN projects to the gigantocellular nucleus (GiN) (Mitani *et al.*, 1988; Rye *et al.*, 1988; Grofova & Keane, 1991), medioventral medulla (MVM) (Skinner et al., 1990b), rostral ventrolateral medulla (RVLM) (Yasui et al., 1990), medial reticular formation (MRF), medulla oblongata (Nakamura *et al.*, 1989; Grofova & Keane, 1991) and spinal cord (Rye *et al.*, 1988; Spann & Grofova, 1989; Skinner *et al.*, 1990a). The majority of the PPN neurons projecting to the spinal cord are non-cholinergic (Skinner et al., 1990a). These descending PPN projections are considered to be directly involved in locomotion, since the stimulation of neurons in the caudal PPN leads to a prolonged activation of neurons in the NPO and changes within the flexor and extensor nerves of decorticated cats (Garcia-Rill et al., 2001).

1.5.7. Summary

To summarise section 1.5, tracer studies in the rat, cat, guinea pig and primates have shown that ascending projections that arise from the rostral PPN preferentially innervate the EP/GPi, SN and lateral hypothalamus; these projections are largely GABAergic and cholinergic. In contrast, the ascending projections that arise from the caudal PPN preferentially innervate the thalamus, STN, VTA, SC and IC; these projections are largely cholinergic and glutamatergic (Table 1.1 and Figure 1.3).

TABLE 1.1. Efferent connectivity of the pedunculopontine nucleus. Abbreviations: STN, subthalamic nucleus; EP, entopeduncular nucleus; GPi, internal segment of the globus pallidus; SN, substantia nigra; VTA, ventral tegmental area; STR, striatum; MD, mediodorsal; VA, ventral anterior; VL, ventrolateral; VM, ventromedial; Pf, parafascicular; DG, dorsal geniculate; Rt, reticular thalamic; LMSg, lateralis medialis suprageniculate; CM, centromedian; CL, centrolateral; PVt, paraventricular; IC, inferior colliculus; SC, superior colliculus; MgPA, magnocellular preoptic area; NbMC, nucleus basalis magnocellularis; RMTg, mesopontine rostromedial tegmental nucleus; PRF, pontine reticular formation; GiN, gigantocellular nucleus; MVM, medioventral medulla; MRF, medial reticular formation; NPO, nucleus reticularis pontis oralis (data from several species).

Target Brain Area	PPN region	References
Basal ganglia		
STN	Caudal	(Nomura *et al.*, 1980; Carpenter *et al.*, 1981; Saper & Loewy, 1982; Edley & Graybiel, 1983; Hammond *et al.*, 1983; Lavoie & Parent, 1994c; Bevan & Bolam, 1995; Muthusamy *et al.*, 2007; Mena-Segovia *et al.*, 2008a; Kita & Kita, 2010)
EP/GPi	Rostral	(Saper & Loewy, 1982; Gonya-Magee & Anderson, 1983; Jackson & Crossman, 1983; Woolf & Butcher, 1986; Scarnati *et al.*, 1988; Charara & Parent, 1994; Lavoie & Parent, 1994c; Shink *et al.*, 1997)
SN	Rostral	(Saper & Loewy, 1982; Scarnati *et al.*, 1984; Sugimoto & Hattori, 1984; Woolf & Butcher, 1986; Clarke *et al.*, 1987; Scarnati *et al.*, 1987; Gould *et al.*, 1989; Nakamura *et al.*, 1989; Bolam *et al.*, 1991; Lavoie & Parent, 1994c; Futami *et al.*, 1995; Oakman *et al.*, 1995; Charara *et al.*, 1996; Takakusaki *et al.*, 1996; Oakman *et al.*, 1999; Mena-Segovia *et al.*, 2008a)
VTA	Caudal	(Sugimoto & Hattori, 1984; Oakman *et al.*, 1995; Charara *et al.*, 1996; Geisler & Zahm, 2005; Mena-Segovia *et al.*, 2005; Good & Lupica, 2009)
STR		(Saper & Loewy, 1982; Nakano *et al.*, 1990)
Thalamus		
MD	Caudal	(Steriade *et al.*, 1988; Lavoie & Parent, 1994c)
VA	Caudal	(Smith et al., 1988)
VL	Caudal	(Smith et al., 1988)
VM	Caudal	(Smith et al., 1988)
Pf	Caudal	(Sugimoto & Hattori, 1984; Kobayashi & Nakamura, 2003; Kobayashi *et al.*, 2007; Mena-Segovia *et al.*, 2008a; Parent & Descarries, 2008)
DG	Caudal	(Parent & Descarries, 2008)
Rt	Caudal	(Parent & Descarries, 2008)
LMSG	Caudal	(Hoshino et al., 1997; Hoshino et al., 2000)
CM/CL/PVt	Caudal	(Steriade *et al.*, 1990a; Erro *et al.*, 1999; Krout *et al.*, 2002; Mena-Segovia *et al.*, 2008a)
Tectum		
IC	Caudal	(Mena-Segovia *et al.*, 2008a; Motts & Schofield, 2009)
SC	Caudal	(Beninato & Spencer, 1986; Hall *et al.*, 1989; Krauthamer *et al.*, 1995; Mena-Segovia *et al.*, 2008a)
Forebrain		
MgPA		(Semba & Fibiger, 1992; Losier & Semba, 1993)
NbMC		(Semba & Fibiger, 1992)
Hypothalamus	Rostral	(Woolf & Butcher, 1986; Hallanger *et al.*, 1987; Ford *et al.*, 1995)
LM-Sg	Rostral	(Hoshino et al., 2004)
RMTg		(Jhou et al., 2009)
Brainstem		
PRF	Caudal	(Mitani *et al.*, 1988; Semba *et al.*, 1990; Takakusaki *et al.*, 1996)
GiN	Caudal	(Mitani *et al.*, 1988; Rye *et al.*, 1988; Grofova & Keane, 1991) (Skinner et al., 1990b)
MVM	Caudal	(Nakamura *et al.*, 1989; Grofova & Keane, 1991)
MRF	Caudal	(Garcia-Rill *et al.*, 2001; Mena-Segovia *et al.*, 2008a)
NPO	Caudal	
Spinal Cord	Caudal	(Rye *et al.*, 1988; Spann & Grofova, 1989; Skinner *et al.*, 1990a)

1.6. Afferent connectivity of the PPN

The PPN receives heterogeneous input arising from diverse areas of the brain, although information is not as abundant or detailed as it is for PPN efferent connectivity. Nevertheless, it is known that neurons in the PPN receive afferents from structures including the cortex, thalamus, hypothalamus, pons, cerebellum, medulla, spinal cord, and basal ganglia (Saper & Loewy., 1982; Semba & Fibiger, 1992; Table 1.2; Figure 1.3).

1.6.1. PPN afferents from the basal ganglia

1.6.1.1. PPN afferents from the subthalamic nucleus

The PPN has been shown to receive a direct input from the STN as shown in the rat (Jackson & Crossman, 1981; Kita & Kitai, 1987), cat and primates (Nauta & Cole, 1978). In addition to the anatomical evidence, electrophysiological experiments have shown that these inputs are excitatory (Granata & Kitai, 1989). Furthermore, the STN can modulate PPN activity indirectly through the SNr; this pathway has an inhibitory effect upon PPN neurons (Hammond *et al.*, 1983; Florio *et al.*, 2007).

1.6.1.2. PPN afferents from the entopeduncular nucleus/internal globus pallidus

Tracer studies in rats and primates have shown that neurons of the EP/GPi send axonal projections that innervate PPN neurons (Semba & Fibiger, 1992; Shink *et al.*, 1997). GPi afferents preferentially target NADPH diaphorase-negative (likely non-cholinergic) neurons in the rostral PPN (Shink *et al.*, 1997), establishing symmetric synapses with proximal dendrites. GPi afferents to the PPN arise from the caudal GPi, in contrast to the rostral GPi that mainly projects to the STN (Moriizumi & Hattori, 1992) and striatum (Bevan *et al.*, 1998). GPi projection neurons can be segregated into two types

based upon their target selectivity. Type I neurons, which are abundant in the centre of the GPi, give rise to axonal branches that innervate the PPN, whereas type II neurons innervate neurons of the lateral habenula (HBN) (Parent et al., 2001).

1.6.1.3. PPN afferents from the substantia nigra *pars* reticulata

The PPN also receives afferents from the SNr (Nakamura *et al.*, 1989; Spann & Grofova, 1991; Semba & Fibiger, 1992); these inputs are inhibitory (Noda & Oka, 1984; Scarnati *et al.*, 1987; Granata & Kitai, 1991) and mediated by GABA (Saitoh et al., 2003). It is not yet clear which PPN neurons are the targets of these afferents, but electron microscopy studies have shown that SNr afferents to the PPN preferentially establish synaptic contacts with non-cholinergic neurons located in the rostral PPN, some of which have been identified as glutamatergic (Spann & Grofova, 1991; Grofova & Zhou, 1998).

1.6.2. PPN afferents from the cerebral cortex

The primate PPN receives a direct input from the cerebral cortex arising from distinct regions of the frontal lobe that are involved in motor control; these convergent inputs target the dorsal and caudal PPN (Matsumura et al., 2000). Similar afferents have been observed in the rat, in this case arising from the medial prefrontal cortex (Sesack et al., 1989), however, they seem to be less abundant than those seen in primates (Semba & Fibiger, 1992). In addition, cholinergic PPN neurons have been shown to receive afferents from the primary auditory cortex in the guinea pig (Schofield & Motts, 2009).

1.6.3. PPN afferents from other brain regions

Studies in the rat show that the PPN also receives afferents from the HBN (Semba & Fibiger, 1992), ZI (Semba & Fibiger, 1992; Kolmac *et al.*, 1998), VTA (Semba & Fibiger, 1992), RMTg (Jhou et al., 2009), SC and IC (Woolf & Butcher, 1986; Redgrave *et*

al., 1987; Semba & Fibiger, 1992; Steininger *et al.*, 1992). Primate studies have shown projections to the PPN from the ventral striatum (Haber et al., 1990) and deep cerebellar nuclei (Hazrati & Parent, 1992), and a dopaminergic innervation, likely arising from the mesencephalon (Rolland et al., 2009).

In the brainstem, tracer studies in the rat have shown that the rostral and caudal portions of the dorsal raphé (DR) innervate the PPN (Vertes, 1991), where they preferentially target non-cholinergic neurons in caudal regions (Steininger et al., 1997). The PPN also receives inputs from the locus coeruleus (LC) (Jones & Yang, 1985), LDTg (Satoh & Fibiger, 1986; Cornwall *et al.*, 1990; Semba & Fibiger, 1992) and the contralateral PPN (Semba & Fibiger, 1992).

1.6.4. Summary

To summarise, tracer studies have shown that the basal ganglia output nuclei (EP/GPi and SNr) preferentially innervate the rostral PPN, whereas neurochemically unidentified cortical and DR afferents preferentially innervate the caudal PPN. For many other afferents of the PPN it is unknown whether they target rostral or caudal regions (Table 1.2 and Figure 1.3).

Origin	Target PPN region	Reference
Cerebral cortex		
FL	Caudal	(Semba & Fibiger, 1992; Matsumura *et al.*, 2000)
PAC		(Schofield and Motts, 2009)
MPC		(Sesack et al., 1989)
Cerebellum		
DCN		(Hazrati & Parent, 1992)
Basal ganglia		
STN		(Nauta & Cole, 1978; Jackson & Crossman, 1981; Hammond *et al.*, 1983; Kita & Kitai, 1987; Granata & Kitai, 1989; Semba & Fibiger, 1992; Florio *et al.*, 2007)
EP/GPi	Rostral	(Smith *et al.*, 1990; Moriizumi & Hattori, 1992; Semba & Fibiger, 1992; Shink *et al.*, 1997; Parent *et al.*, 2001)
SN	Rostral	(Noda & Oka, 1986; Scarnati *et al.*, 1987; Nakamura *et al.*, 1989; Granata & Kitai, 1991; Spann & Grofova, 1991; Semba & Fibiger, 1992; Saitoh *et al.*, 2003)
VTA		(Haber *et al.*, 1990; Semba & Fibiger, 1992)
STR		(Semba & Fibiger, 1992)
Tectum		
SC		(Woolf & Butcher, 1986; Redgrave *et al.*, 1987; Semba & Fibiger, 1992; Steininger *et al.*, 1992)
Brainstem		
LTDg		(Satoh & Fibiger, 1986; Cornwall *et al.*, 1990; Semba & Fibiger, 1992)
Contralateral PPN		(Semba & Fibiger, 1992)
Other		
LC		(Jones & Yang, 1985)
Habenula		(Semba & Fibiger, 1992)
RMTg		(Jhou et al., 2009)
ZI		(Satoh & Fibiger, 1986; Semba & Fibiger, 1992; Kolmac *et al.*, 1998)
DR	Caudal	(Vertes, 1991; Steininger *et al.*, 1997)

TABLE 1.2. Afferent connectivity of the pedunculopontine nucleus. Abbreviations: FL, frontal lobe; PAC, primary auditory cortex; MPC, medial prefrontal cortex; DCN, deep cerebellar nuclei; STN, subthalamic nucleus; EP, entopeduncular nucleus; GPi, internal segment of the globus pallidus; SN, substantia nigra; VTA, ventral tegmental area; STR, striatum; SC, superior colliculus; LDTg, laterodorsal tegmental nucleus; PPN, pedunculopontine nucleus; LC, locus coeruleus; RMTg, mesopontine rostromedial tegmental nucleus; ZI, zona incerta; DR, dorsal raphé (data from several species).

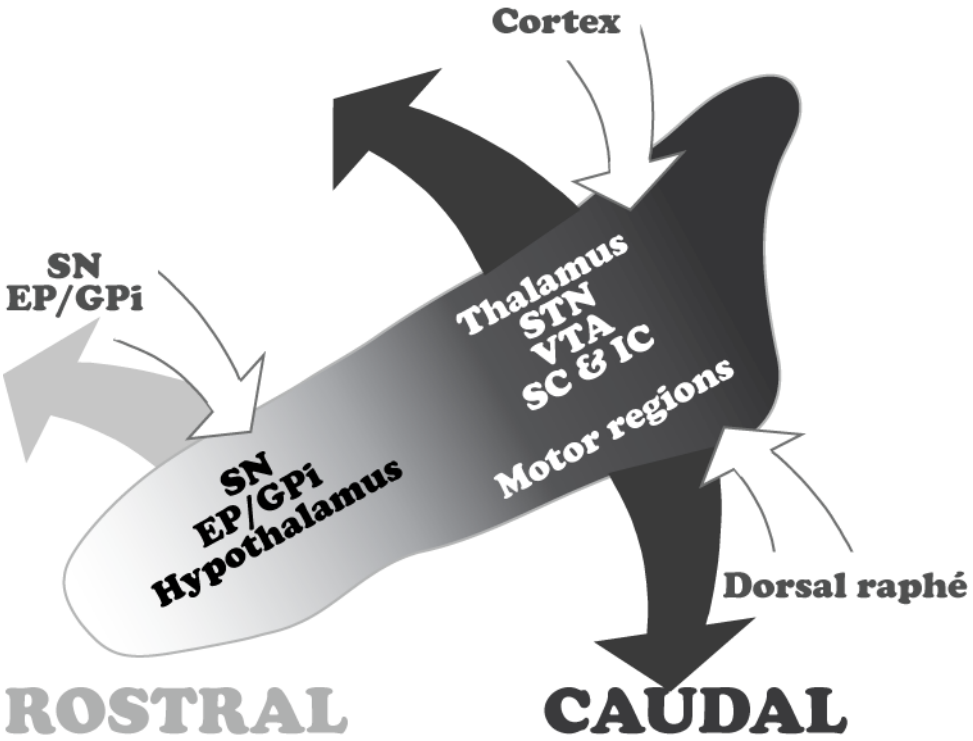


Figure 1.3. Summary of the topographical organisation of the connectivity in the PPN

The rostral PPN, which is predominantly GABAergic, maintains interconnections with the GABAergic output nuclei of the basal ganglia. In contrast, the caudal PPN (where cholinergic and glutamatergic neurons are more abundant than GABAergic neurons) receives input from the cortex and dorsal raphé and projects to the thalamus, cortex, STN and locomotor regions. Only major PPN inputs and outputs are shown in this scheme. Abbreviations: EP, entopeduncular nucleus; GPi, internal segment of the globus pallidus; IC, inferior colliculus; SC, superior colliculus; SN, substantia nigra; STN, subthalamic nucleus; VTA, ventral tegmental area (Mena-Segovia *et al.*, 2009).

1.7. Functional roles of the PPN

Classically, the PPN has been considered part of the ascending activating system (Garcia-Rill, 1991; Vincent, 2000). However, recent evidence from several studies suggests that the role of the PPN is integrative, rather than simply relaying information, due to the complexity of its internal organisation and its high level of connectivity with other regions of the brain and spinal cord (Inglis & Winn, 1995; Takakusaki *et al.*, 2004; Mena-Segovia *et al.*, 2005; Winn, 2008). The PPN is also part of the mesencephalic locomotor region (MLR) and is involved in locomotion (Skinner & Garcia-Rill, 1984; Garcia-Rill *et al.*, 1987). One of the main characteristics of PPN neurons is their long-range axonal projections, reaching numerous targets across the brain, including the cortex, basal ganglia, brainstem, distant forebrain structures (Woolf & Butcher, 1986; Hallanger & Wainer, 1988a) and the spinal cord (Rye *et al.*, 1988; Spann & Grofova, 1989). In addition, most of the structures that receive a PPN input also send axonal projections to feed back information to the PPN (Haber *et al.*, 1990; Semba & Fibiger, 1992).

1.7.1. Locomotion

Early studies have shown that the PPN plays a role in locomotion. The PPN is part of the MLR (Garcia-Rill *et al.*, 1987) and the stimulation of this region and related regions (including the cuneiform nucleus) in decerebrate cats can induce locomotion (Skinner & Garcia-Rill, 1984). The electrical stimulation of the PPN can induce prolonged activation of pontine reticular neurons and can subsequently induce locomotion (Garcia-Rill, 1986; Garcia-Rill *et al.*, 2001). Distinct types of PPN neuron display rhythmic activity in relation to locomotion (Garcia-Rill & Skinner, 1988). Extracellular recordings in the PPN of decerebrate cats revealed that neurons fire differentially during locomotion. Two main types of neurons were recorded; the ‘on-type’ showed a tonic firing frequency during

locomotion and the 'off-type' decreased its firing rate as locomotion increased (Garcia-Rill & Skinner, 1988).

It has been proposed that the locomotion induced by the stimulation of the PPN is likely to act through the reticulospinal system. Axons from the MLR, which includes the PPN, innervate reticulospinal neurons in the MVM, GiN and magnocellular tegmental nucleus (Steeves & Jordan, 1984; Garcia-Rill & Skinner, 1987b). The PPN innervates approximately one half of MVM neurons (which can elicit locomotion if electrically or chemically stimulated), and over a third of these project to the spinal cord (Garcia-Rill & Skinner, 1987b; a; Kinjo *et al.*, 1990; Reese *et al.*, 1995). Because of these descending projections, and its prominent ascending projections to the thalamus and basal ganglia, the PPN holds a key position in the modulation of gait initiation and posture (Reese *et al.*, 1995; Pahapill & Lozano, 2000; Winn, 2006).

1.7.2. REM sleep and sleep-wake cycles

The electrical stimulation of the PPN can have diverse effects, not always linked to locomotion, depending on the stimulation protocol used (Garcia-Rill *et al.*, 2001). For example, some protocols can induce the release of acetylcholine by PPN neurons in the PRF, leading to respiratory depression (Lydic & Baghdoyan, 1993), whereas others can induce the suppression of muscular tone (Leonard & Lydic, 1997). Excitation of cholinergic PPN neurons can induce REM-like sleep, which is characterised by low voltage fast activity and muscle atonia (Baghdoyan *et al.*, 1987; Greene *et al.*, 1989; Yamamoto *et al.*, 1990; Jones, 1991; Datta & Siwek, 1997; Leonard & Lydic, 1997). The firing rates of PPN neurons increase in REM sleep when compared to slow wave sleep (Sakai *et al.*, 1990; Steriade *et al.*, 1990a; Steriade *et al.*, 1996; Garcia-Rill *et al.*, 2001), and single unit activity of these neurons also appears to be associated with REM sleep-related events, namely ponto-geniculo-occipital (PGO) spikes (el Mansari *et al.*, 1989;

1990; Steriade *et al.*, 1990b). Destroying cholinergic neurons of the mesopontine region (which includes the PPN), with kainic acid neurotoxic lesions, results in a loss of REM sleep and muscle atonia (Jones & Webster, 1988; Webster & Jones, 1988; Jones, 2005).

1.8. The basal ganglia

The PPN and the basal ganglia share a very close relationship (see sections 1.5 and 1.6) and might be considered to be parts of the same group rather than independent entities (Mena-Segovia *et al.*, 2004a). In order to understand the implications of such a close relationship, it is necessary to understand how nuclei of the basal ganglia are connected, between themselves and the rest of the brain, and the functional consequences of these connections. This has been studied extensively in physiological conditions, as well as in certain pathologies, such as Parkinson's disease (Albin *et al.*, 1989; Bolam *et al.*, 2000).

The basal ganglia are, "...a group of interconnected subcortical nuclei spanning the telencephalon, diencephalon and midbrain" (Albin *et al.*, 1989). They are involved in a wide variety of processes including association, movement, cognition, reward and mnemonic function (Graybiel *et al.*, 1994; Graybiel, 1998; Bolam *et al.*, 2000). They are classically divided into the striatum (or caudate-putamen), the globus pallidus (GP in the rat, or external segment of the globus pallidus in primates; GPe), the entopeduncular nucleus (EP in the rat, or internal segment of the globus pallidus in primates; GPi), the subthalamic nucleus (STN) and the substantia nigra *pars compacta* (SNc) and *pars reticulata* (SNr) (Albin *et al.*, 1989; Bolam *et al.*, 2000).

The basal ganglia receive two main excitatory inputs, from the cortex and the thalamus. The main recipient of these inputs is the striatum, and to a lesser extent, the STN. The inhibitory medium-sized spiny neurons (MSNs) of the striatum innervate neurons of the basal ganglia output nuclei (SNr and EP/GPi) either directly, with small

collaterals passing to the GPe, or indirectly, via connections through the GPe and STN. Inhibitory neurons of the basal ganglia output nuclei innervate subcortical structures including the superior colliculus (SC), reticular formation (RF), habenula (HBN) and PPN. The thalamus is also a target of the basal ganglia output nuclei and neurons of the thalamus in turn innervate the cortex. Cortical outputs to the brainstem and spinal cord can influence motor activity, whereas cortical outputs to the striatum and STN complete a feedback loop to regulate basal ganglia activity.

Dopaminergic neurons of the SNc also receive input from the direct and indirect output pathways of the striatum and modulate this output via their extensive axonal projections to striatal regions. Cortical and thalamic neurons also project to ventral regions of the striatum (nucleus accumbens core and shell); these neurons mainly project to the ventral pallidum and also receive synaptic input from neurons of the VTA. The connectivity of the basal ganglia is described schematically in Figure 1.4 (Bolam *et al.*, 2009).

1.9. Parkinson's disease

Parkinson's disease is a neurodegenerative disorder, first described by James Parkinson in 1817, that shows symptoms of resting tremor, bradykinesia and rigidity of posture and gait (Bergman & Deuschl, 2002). It is a progressive neurodegenerative disorder with an incidence of 1% of the population over the age of 60. The neuropathology of the disease is characterised by the progressive loss of dopaminergic neurons of the SNc and the increased presence of proteinaceous cytoplasmic inclusions called Lewy bodies (Braak *et al.*, 2001; Braak *et al.*, 2004). These cytoplasmic inclusions are aggregations mainly composed of insoluble α-synuclein, a small protein of 140 amino acids that, in its soluble form, is present in many nerve cells.

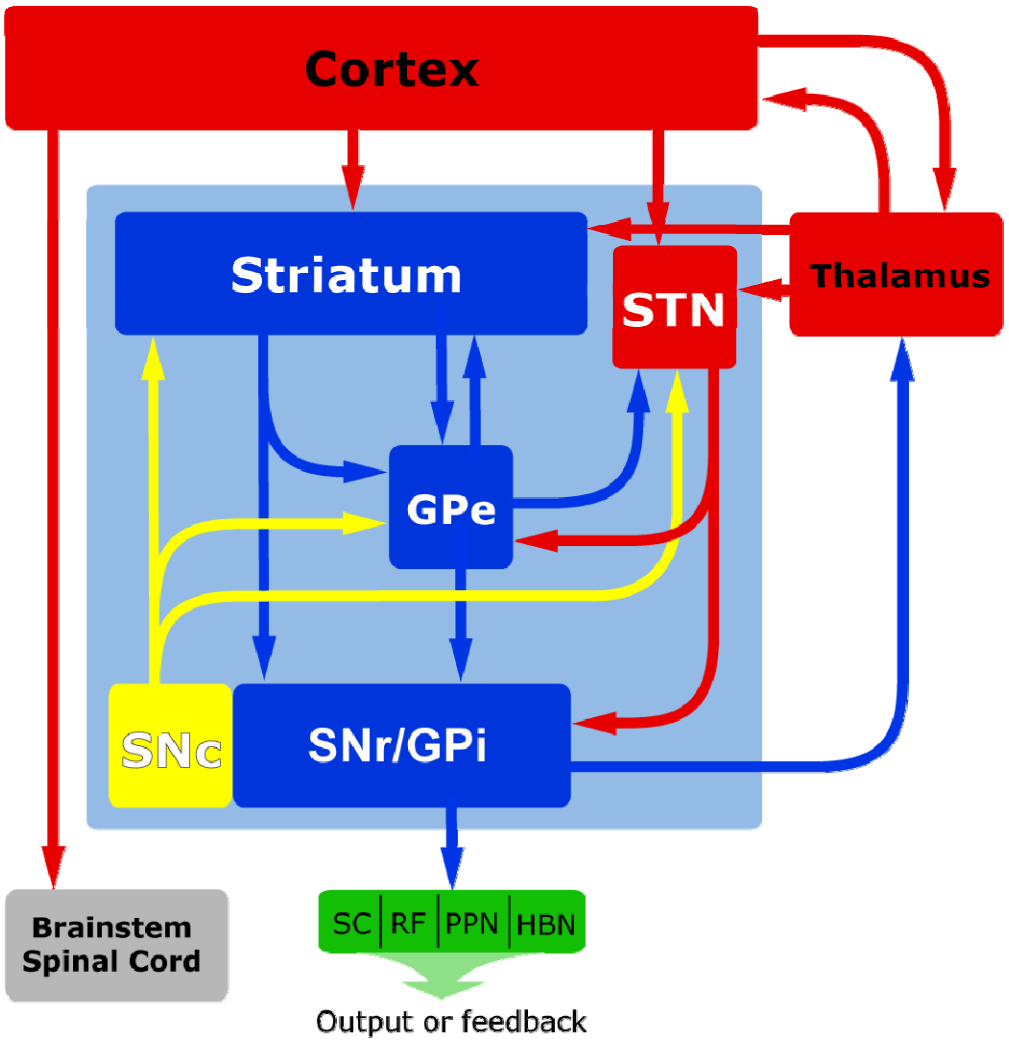


Figure 1.4. Schematic diagram of the dorsal divisions of basal ganglia connectivity (Bolam *et al.*, 2009). The excitatory cortical and thalamic inputs are indicated in red. The basal ganglia are contained in the pale blue box. Cortical and thalamic neurons send major axonal projections to the striatum and relatively minor projections to the subthalamic nucleus (STN). The inhibitory (dark blue) medium-sized spiny neurons (MSNs) of the striatum innervate neurons of the basal ganglia output nuclei, the substantia nigra *pars reticulata* (SNr) and the entopeduncular nucleus/internal segment of the globus pallidus (EP/GPi) either directly or indirectly via neurons of the external segment of the globus pallidus (GPe) and STN. Neurons of the SNr and EP/GPi send inhibitory projections to subcortical structures (in green), including the superior colliculus (SC), reticular formation (RF), habenula (HBN) and the pedunculopontine (PPN). SNr and EP/GPi neurons also innervate the thalamus, which sends projections to the cortex (that in turn innervates the brainstem and spinal cord), striatum and STN. Dopaminergic neurons of substantia nigra *pars compacta* (SNc; in yellow) also receive input from the direct/indirect output pathways of the striatum. Their axons feed information back to the striatum, GPe and STN, and serve to modulate basal ganglia output.

1.9.1. Parkinson's disease progression

In the early stages of Parkinson's disease, Lewy bodies are found in structures such as the medulla oblongata and pontine formation (Braak *et al.*, 2004). Lewy bodies were first described in 1913 as "globular inclusions of cytoplasmic condensations.....in the pigmented ganglion cells of the substantia nigra in Parkinson's disease" (Bethlem & Den Hartog Jager, 1960; Den & Bethlem, 1960) and mainly consist of misfolded α-synuclein aggregates (Wakabayashi *et al.*, 1992; Duda *et al.*, 2000; Jensen & Gai, 2001).

Parkinson's disease can be divided into three pre-symptomatic stages followed by three symptomatic stages (Braak *et al.*, 2003a; Braak *et al.*, 2003b; Braak *et al.*, 2004). In the pre-symptomatic stages, Lewy bodies are first observed in cells of the enteric nervous system (stage 1); they are then seen in the medullary raphé nuclei, gigantocellular nucleus and locus coeruleus (stage 2), followed by the SNc, amygdala, hippocampus, entorhinal regions and magnocellular nuclei of the basal forebrain (stage 3). As the disease progresses to its symptomatic stages, greater neuronal loss occurs in the SNc and other subcortical structures. Lewy bodies are then seen in the cortex, by which time a full range of symptoms are evident, including dementia.

The SNc is one of the more severely affected brain structures in Parkinson's disease, and cell loss in this structure occurs in a progressive manner (Fearnley & Lees, 1991; Damier *et al.*, 1999b); cell loss is more dramatic within the calbindin-poor nigrosomes than in the calbindin-rich matrix (Damier *et al.*, 1999a; b). The major consequence of the progressive loss of dopaminergic SNc neurons is a long term reduction in the dopamine levels of the striatum; this can lead to rearrangements of corticostriatal and thalamostriatal connectivity.

Dopaminergic neurons of the SNc are highly susceptible in Parkinson's disease, however, those of the retrorubral field (RRF) and VTA survive longer in comparison. The axon of a single SNc dopaminergic neuron forms an extensive network of collaterals in the rat striatum that can form roughly 300,000 synapses (Matsuda *et al.*, 2009; Moss, 2009). In contrast, dopaminergic VTA neurons provide a much more limited projection to the striatum, innervating approximately 21,000 neurons. Because of their large axonal arbours, SNc dopaminergic neurons are subject to a heavy energetic burden and are therefore more susceptible to death in Parkinson's disease (Drs Pissadaki and Bolam, personal communication). In addition to α-synuclein aggregation, Lewy bodies and energetic stress, there are other factors implicated in the pathogenesis of Parkinson's disease, such as oxidative stress, mitochondrial complex I dysfunction and ubiquitin-proteasome system defects (Betarbet *et al.*, 2005; Panov *et al.*, 2005; Pallanck & Greenamyre, 2006).

1.9.2. Parkinson's disease models

Several animal models have been used to understand the pathology of Parkinson's disease; these include the 1-methyl-4-phenyl-1,2,3,6-tetrathydropyridine (MPTP)-treated primate, the 6-hydroxydopamine (6-OHDA) lesioned rat, the rotenone- or paraquat-treated rat as well as several transgenic animals that incorporate α-synuclein pathologies (Betarbet *et al.*, 2002). One of the most studied models of Parkinson's disease is the 6-OHDA lesioned rat. It does not reproduce all the symptoms observed in Parkinson's disease patients, but is widely used to mimic the acute loss of dopamine.

Injecting the neurotoxin 6-OHDA, intracranially into the substantia nigra, nigrostriatal fibre tract or striatum will lesion catecholaminergic neurons of the nigrostriatal pathway (dopaminergic neurons and a small proportion of noradrenergic neurons) leading to reduced dopamine levels in the striatum (Ungerstedt, 1968; Sachs &

Jonsson, 1975; Perese *et al.*, 1989; Przedborski *et al.*, 1995). Unilateral injections of 6-OHDA allow the degree of the lesion to be assessed by an injection of amphetamine or apomorphine (at 2-3 weeks post-lesion) and subsequent evaluation of asymmetric turning behaviour. Amphetamine induces dopamine release and apomorphine activates dopamine receptors, and both result in contralateral turning behaviour if the lesion is complete (Perese *et al.*, 1989).

1.9.3. PPN and Parkinson's disease

Locomotion and gait initiation problems, as well as bradykinesia, are major impediments for Parkinson's disease patients (Morris *et al.*, 1994; Morris *et al.*, 1996). However, the neuropathological mechanisms behind those alterations are not well understood. Several studies link the activity of PPN neurons with locomotion (Garcia-Rill, 1986; Garcia-Rill *et al.*, 1990; Masdeu *et al.*, 1994). Previous studies have shown that, in addition to the damage in the SN, the PPN also deteriorates in Parkinson's disease. Post-mortem examination of Parkinson's disease patients has shown that up to 40% of cholinergic and non-cholinergic neurons can be lost in the PPN (Hirsch *et al.*, 1987; Herrero *et al.*, 1993). Furthermore, it has been proposed that the degree of cholinergic neuronal loss in the PPN is linked to the severity of disease symptoms (Zweig *et al.*, 1989). Surgical interventions, such as lesioning or stimulation, have therefore been applied to the PPN to treat some of these symptoms in Parkinson's disease patients (Lozano, 2001; Benabid, 2003; Kringelbach *et al.*, 2007; Stefani *et al.*, 2007; Jenkinson *et al.*, 2009).

1.9.4. Deep brain stimulation of the PPN

Deep brain stimulation (DBS) has been used since the 1990s to treat tremor and other symptoms of Parkinson's disease. The best candidates for DBS are idiopathic Parkinson's disease patients with motor symptoms and dyskinesias induced by L-DOPA;

the most effective drug treatment for Parkinson's disease (Benabid, 2003). However, the best targets and stimulation protocols used to attenuate distinct symptoms is widely debated (Stefani *et al.*, 2007). Early studies in different models showed that the thalamus was a good target for surgical intervention, but more recently it has been demonstrated that the STN and PPN are better targets to treat specific symptoms of the disease (Nandi *et al.*, 2002a; Benabid, 2003; Jenkinson *et al.*, 2005; Lozano & Snyder, 2008).

In MPTP-treated primates, low frequency deep brain stimulation of the PPN was shown to attenuate symptoms of Parkinson's disease such as akinesia (Jenkinson *et al.*, 2005; Nandi *et al.*, 2008). It was shown to reduce these symptoms to similar levels as L-DOPA treatment, and when combined with L-DOPA treatment, it served better than L-DOPA alone (Jenkinson *et al.*, 2005). In untreated control animals, low frequency stimulation causes hyperkinesia, whereas high frequency stimulation decreases movement; this might explain why low frequency stimulation of the PPN in MPTP-treated primates appears to improve symptoms such as akinesia (Nandi *et al.*, 2002c; Jenkinson *et al.*, 2004; Jenkinson *et al.*, 2006; Kringelbach *et al.*, 2007; Jenkinson *et al.*, 2009).

In Parkinson's disease patients, stimulation in the PPN can improve some motor symptoms and prevent falls (Mazzone *et al.*, 2005; Hamani *et al.*, 2007; Lozano & Snyder, 2008; Pierantozzi *et al.*, 2008; Moro *et al.*, 2010). Low frequency stimulation (20-25 Hz) in the PPN of patients, both on and off L-DOPA medication, can improve gait dysfunction and postural instability (Plaha & Gill, 2005). Delineating the neuroarchitecture and functional domains of the PPN is essential for improving the efficacy of deep brain stimulation for Parkinson's disease patients (Starr *et al.*, 1998; Benabid, 2003; Stefani *et al.*, 2007). For example, the efferent connectivity of the rostral PPN greatly differs from that of the caudal PPN (see section 1.5), and therefore stimulating different regions of the PPN might substantially change the effects seen (Alderson *et al.*, 2008).

1.10. Aims of the Thesis

To understand how the PPN is able to drive and/or modulate functions as diverse as locomotion and REM sleep, and to understand what happens in the PPN in conditions such as Parkinson's disease, it is crucial to examine its anatomy, internal organisation and connectivity with the rest of the brain. However, little is known of which neuronal subtypes are present in the PPN, how abundant they are and how they are distributed.

To provide new insights into the anatomy of the rat PPN, the first aim of this thesis is to quantify the number of neurons containing two of the most abundant calcium-binding proteins in the brain: calbindin and calretinin. These results, including the analyses of the rostro-caudal distribution of these neurons, are shown in Chapter 3. The second aim of the thesis is to define the neurotransmitter phenotypes of calbindin- and calretinin-positive neurons (cholinergic, GABAergic or glutamatergic) of the PPN; these results, and the analysis of their rostro-caudal distributions, are shown in Chapter 4.

The third aim of the thesis is to evaluate the ascending and descending efferents of the PPN to the subthalamic and gigantocellular nuclei, respectively. These structures were chosen because their connectivity with the PPN has implications in motor control and Parkinson's disease therapies, such as DBS. Quantification of PPN neurons projecting to these structures, their rostro-caudal distributions and neurochemical characterisation are reported in Chapter 5. Activity of these neurons, in control and 6-OHDA lesioned animals, will also be assessed by evaluating their expression of the immediate early gene Egr1.

Together, these investigations should provide essential information regarding the number, distribution and neurochemistry of PPN neurons, as well as furthering our knowledge of their connectivity with rest of the brain and their activity in health and disease.

2. Materials and methods

2.1. Introduction

This chapter will describe the methods for the thesis, first examining those techniques used in Chapter 3, before detailing any extra techniques used in Chapters 4 and 5. A summary of methods will be included in each results chapter, but for a full description of each technique this methods chapter should be referred to. Where similar processes are used in more than one chapter, any subtle differences will be noted as and when they arise.

2.2. Chapter 3 methods

2.2.1. Perfusion, fixation and sectioning of brain tissue

All animal procedures used in this study were carried out in accordance with the Animals (Scientific Procedures) Act, 1986 (UK) or the NIDA IRP local Animal Care and Use Committee. Sprague-Dawley rats (225–300 g) were used for immunohistochemical analyses. They were deeply anaesthetised using a mixture of ketamine (30 mg/kg, intraperitoneally injected (IP); Ketaset, Willow Francis, Crawley, UK) and xylazine (3 mg/kg, IP; Rompun, Bayer, Germany) and intracardially perfused with 0.1 M phosphate-buffered saline (PBS) followed by 4% paraformaldehyde (PFA) in 0.1 M phosphate buffer (PB; pH 7.4) as fixative. Brains were removed and post-fixed in the same fixative for 30-90 min at room temperature. Sagittal sections (50 μm thick) of the brainstem were then cut using a vibratome (Leica Microsystems, UK), collected in six series and stored in PBS containing 0.05% sodium azide.

2.2.2. Immunoperoxidase reactions

Two of the six series collected for immunohistochemical analyses and containing the PPN (n=6 rats) were double-immunolabelled to reveal each of the following combinations: calbindin and choline acetyltransferase (ChAT) or calretinin and ChAT. For permanent peroxidase reactions, free-floating serial sections were blocked for 1 h in normal donkey serum (NDS; Jackson Immunoresearch Laboratories Inc., West Grove, PA;

10% in 0.3% Triton X-100 in PBS) then incubated overnight at 4 °C, with either an antibody raised against calbindin in mouse or with an antibody raised against calretinin in rabbit (Swant, Marly, Switzerland; 1:5000 dilutions in 1% NDS, 0.3% Triton X-100 in PBS; see Table 3.1). In the next step, sections were washed in PBS and incubated with the appropriate biotinylated secondary antibody; horse anti-mouse for calbindin or horse anti-rabbit for calretinin (Vector laboratories Inc., Burlingame, CA, USA; 1:500 dilutions in 1% NDS, 0.3% Triton X-100 in PBS; see Table 3.1). The calbindin or calretinin immunolabelling was revealed by incubation of the tissue in Vector-SG substrate solution for 3-5 min at room temperature, according to the manufacturers' instructions (Vector-SG peroxidase substrate kit: SK-4700; Vector laboratories Inc.).

After several PBS washes, sections were incubated with an antibody against ChAT raised in goat (Chemicon, Temecula, CA, USA; 1:500 dilution in 1% NDS, 0.3% Triton X-100 in PBS; see Table 3.1). The next day, sections were washed in PBS and incubated overnight with a biotinylated horse anti-goat secondary antibody (Vector Laboratories Inc.; 1:500 dilution in 1% NDS, 0.3% Triton X-100 in PBS; see Table 3.1). After PBS washes, the sections were incubated for 4-7 h at room temperature or overnight at 4°C in avidin-biotin horseradish peroxidase complex (ABC elite; Vector Laboratories Inc.; prepared according to the manufacturers' instructions: three drops of solution A and three drops of solution B in 5 ml PBS). Immunolabelling for ChAT was then revealed by pre-incubation for 15 min in 1 ml of diaminobenzidine (DAB; Sigma, St. Louis, MO, USA; 0.025% w/v in 0.05 M Tris buffer, pH 7.4), and then in the same solution initiating the reaction by adding 20 µl of hydrogen peroxide solution (H_2O_2; Sigma; 1% in dH_2O) for 5-10 min. Sections were then washed in PBS, mounted on gelatin-coated slides, dried and dehydrated through increasing concentrations of alcohol and xylene and mounted in resin (XAM, BDH Chemicals). The sections were typically 14 µm thick once processed.

2.2.3. Image acquisition and identification of immunopositive neurons

Light microscopic images of peroxidase immunolabelled neurons were captured with a DVC camera (Digital Video Camera Company, Suite M-500, Austin, TX, USA) attached to an Eclipse 80i microscope (Nikon, Kingston Upon Thames, Surrey, UK) with Neurolucida software (Micro Bright Field Inc., Colchester, VT, USA). A neuron was considered immunopositive if its cytoplasm and proximal dendrites were stained brown, the typical colour of the DAB peroxidase reaction product, or black-blue by the Vector-SG reaction product. The blue-black stained Vector-SG neurons were easily differentiated from the brown stained DAB neurons, and where neurons were double-positive for both reaction products the two were easily identifiable (see analysis of double-positive neurons in Chapter 4).

2.2.4. Measurement and comparison of somatic diameter

Somatic diameter measurements were carried out using Stereo Investigator software (version 8; MicroBrightField Inc. Magdeburg, Germany), an Eclipse 80i microscope (Nikon) with a computer-controlled motorized stage (LUDL Electronic Products, Hawthorne, NY, USA) and a Lucivid module projecting the computer display into the drawing tube of the microscope. To determine the average somatic diameter of neurons, lines dividing round-shaped neurons by half or measuring the widest diameter of multipolar neurons were drawn under a 63× oil immersion objective (n=100 calbindin- and calretinin-positive neurons each). The neurons used for this analysis were chosen randomly in the rostral and caudal PPN using the Stereo Investigator software. No correction was made for shrinkage of the tissue.

To determine whether the somatic diameters of calbindin- and calretinin-positive neurons were normally distributed, their diameters were plotted on a histogram and a normality test was carried out (Shapiro-Wilk). The calbindin-positive neurons failed the

test (W = 0.896; P < 0.001) indicating that the data varied significantly from the pattern expected for a normal distribution. The calretinin-positive neurons passed the test (W= 0.984; P = 0.26) and a non-linear regression was used to adjust the data to a Gaussian-normal distribution. To determine the difference in somatic diameter between the calbindin- and calretinin-positive neurons a Mann-Whitney Rank Sum Test was used.

2.2.5. Segmentation of the PPN for stereological analysis

The rostro-caudal distribution of the peroxidase labelled calbindin- and calretinin-positive neurons in the PPN was analysed using a stereological method, based upon the subdivision of the PPN into equally-spaced segments, as described previously (Mena-Segovia et al., 2009). Using the centre of the SNr, concentric circles at 300 μm intervals were drawn outwards to cover the entire extent of the PPN; two segments covered the SNr, then up to ten segments covered the PPN up to its caudal extremity (Figure 2.1). The limits of the PPN were defined by the cholinergic (ChAT-positive) neurons, with segment S1 being the most rostral and closest to the SNr and segment S10 being the most caudal.

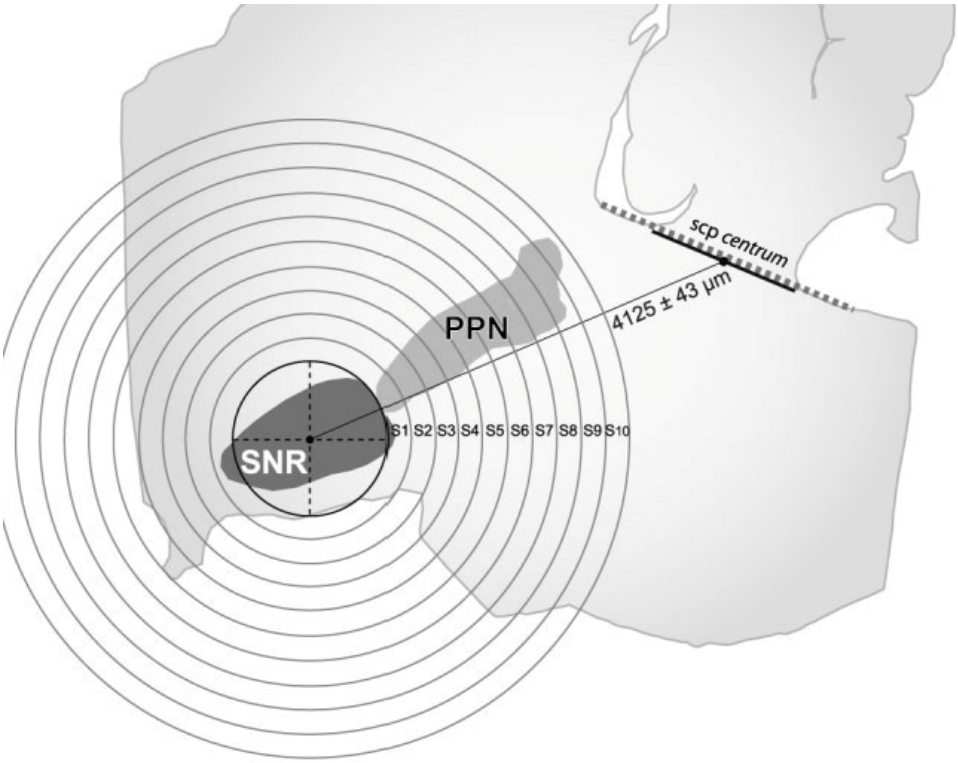


Figure 2.1. Schematic representation of the rat PPN subdivided into segments of 300 µm. Using the centre of the substantia nigra *pars reticulata* (SNr) as the starting point, serial concentric circles at intervals of 300 µm were drawn. The entire PPN was usually contained in 10 segments. Segment S1 contains the part of the PPN that is closest to the SNr, whereas segment S10 is closest to the superior cerebellar peduncle (scp; Mena-Segovia *et al*., 2009).

2.2.6. Stereological estimation of total cell numbers and densities

Stereological sampling was used to estimate the total number of calbindin- and calretinin-positive neurons in the PPN (*n*= 6). All the medio-lateral levels of the PPN were cut and collected in six series; two of these series were analysed. Thus, the total number of counted neurons was multiplied by three to estimate their total number in the PPN. Each PPN segment was drawn as a contour using a 4× objective and Stereo Investigator software. Frames used to count neurons were 75 × 75 µm in the XY plane, and in the Z plane sections were approximately 14 µm. Guard zones of 2 µm at the top and bottom of the sections were left unused to avoid cutting artefacts that occur at the surface of the tissue. A calbindin- or calretinin-positive neuron was counted in the stereological analysis if the top surface of the cell was below the 2 µm guard zone. Therefore, to estimate the total number of positive neurons in each segment, the following formula was used:

$$\text{Estimated total number of neurons} = \text{Total neurons counted} \times \frac{1}{\textit{fraction of height of section sampled}} \times \frac{1}{\textit{fraction of sections sampled}}$$

To estimate the total numbers of calbindin- and calretinin-positive neurons in the PPN, the numbers of each for all segments were totalled and expressed as a mean of six animals (± standard error of the mean; SEM). The total numbers of neurons counted per segment were also averaged across animals to give a mean (± SEM) to allow the distributions of these neurons along the rostro-caudal axis of the PPN to be compared. Cell densities of each segment were calculated by dividing the number of neurons within a segment by its volume. These densities were then averaged over the six animals used (± SEM).

2.2.7. Statistical analyses of cell numbers and densities

Estimated total numbers of calbindin- and calretinin-positive neurons were compared using a Student's t-test. To assess if the distributions of calbindin- and calretinin-positive neurons across the segments of the PPN were uniform, a one way ANOVA test was used. To determine differences between specific PPN segments a Bonferroni t-test was used. If the data failed to pass the normality test required for ANOVA, a Kruskal-Wallis (one way ANOVA on ranks) test was used to test if the differences between median values per segment were greater than would be expected by chance. The Dunn's t-test was used for all pairwise comparisons following a rank-based ANOVA (Kruskal-Wallis), as unlike the Bonferroni t-test, this method is suitable for when group sizes are unequal. In some cases, negative results should be interpreted cautiously when the power of the one way ANOVA test or a Kruskal-Wallis test was below the desired power; which makes it more difficult to detect differences that exist, usually due to a low *n* number.

2.3. Chapter 4 methods

2.3.1. Analysis of double-immunoperoxidase labelling

Using tissue double-immunolabelled for calbindin or calretinin and ChAT (as described in section 2.2.2), the proportions of calbindin- and calretinin-positive neurons that were also immunopositive for ChAT were determined. The immunolabelling reaction products for each of these (Vector SG and DAB peroxidase) were easily distinguishable from each other (as further described in Chapter 4).

2.3.2. *In situ* hybridisation

For *in situ* hybridisation reactions, 5 Sprague-Dawley rats (200-300 g) were deeply anaesthetised with chloral hydrate (300 mg/kg) and intracardially perfused with 4% PFA (in 0.1 M PB, pH 7.3) for fixation. The brains were removed and post-fixed for 2 h at 4°C

and then stored at -80°C until cryosections of 18 µm thickness were collected in 8 series. These sections were processed first for *in situ* hybridisation and second for immunoperoxidase labelling, to reveal in each case two markers in the same tissue (see Table 4.1).

In situ hybridisation experiments were carried out under the supervision of Dr. Marisela Morales in her laboratory at the NIH National Institute on Drug Abuse, Intramural Research Program, Biomedical Research Center in Baltimore, USA. All the RNAase free tissue and radioactive riboprobes were provided by this laboratory. *In situ* hybridisations for rats 1 and 2 were carried out by members of the Morales laboratory, whereas the remainder of the experiments were carried out by myself under the supervision of Dr. Morales.

In situ hybridisation was performed as described previously (Wang & Morales, 2008; 2009). Series of sections were incubated for 10 min in Triton X-100 (0.5% in PB), washed in PB, incubated with 0.2 M HCl for 10 min, washed in PB again and then acetylated in acetic anhydride (0.25% in 0.1 M triethanolamine, pH 8.0) for 10 min. Sections were briefly washed in PB, post-fixed for 10 min in 4% PFA, rinsed in PB and then hybridised for 16 h at 55°C in hybridisation buffer (50% formamide; 10% dextran sulfate; 5× Denhardt's solution; 0.62 M NaCl; 50 mM dithiothreitol; 10 mM EDTA; 20 mM PIPES, pH 6.8; 0.2% sodium dodecyl sulfate; 250 µg／ml salmon sperm DNA; 250 µg／ml tRNA).

The hybridisation buffer contained 40 × 10^7 counts per minute (cpm)/ml of the [^{35}S]- and [^{33}P]-labelled, single-stranded, antisense riboprobes for either ChAT (nucleotides 271–2247, accession no. 017464), VGluT2 (nucleotides 1704–2437; accession no. NM_053427), GAD65 (nucleotides 1–1758; accession no. NM_012563) and GAD67 (nucleotides 1–1782; accession no. NM_017007), calbindin (nucleotides 26-1731;

accession no. NM_031984.2) or calretinin (nucleotides 29-1547; accession no. BC087603.1).

The plasmid containing VGluT2 was generously provided by Dr Robert H. Edwards (University of California, San Francisco, CA, USA) and the plasmids containing GAD65 and GAD67 were generously provided by Dr Allan Tobin (University of California, Los Angeles, CA, USA). Plasmids for calbindin and calretinin were provided by Dr. Marisela Morales. After the hybridisation, the sections were treated with 4 μg/ml RNAase A at 37°C for 1 h (to remove any remaining single stranded RNA), washed in formamide (50% in 1× standard sodium citrate) for 1 h at 55°C, followed by a wash in 0.1× standard sodium citrate for 1 h at 68°C.

2.3.3. Immunoperoxidase labelling (subsequent to *in situ* hybridisation)

After *in situ* hybridisation for GAD65/67 or VGluT2, sections were immunolabelled to reveal calbindin or calretinin, and after *in situ* hybridisation for calbindin or calretinin, sections were immunolabelled to reveal ChAT (see Table 4.1 for combinations). They were rinsed in PB six times for 10 min each before being blocked in bovine serum albumin (BSA; 4%; in 0.3% Triton X-100 in PB) for 1 h. Primary antibodies for calbindin (1:1000; raised in rabbit; Swant), calretinin (1:500; raised in rabbit; Swant) or ChAT (1:500; raised in goat; Sigma) were added to the sections in 4% BSA (in 0.3% Triton X-100 in PB) and incubated overnight at 4°C.

Next day, sections were rinsed several times in PB and incubated in a secondary biotinylated antibody for 1 h (1:200; horse anti-rabbit or horse anti-goat; in 4% BSA, 0.3% Triton X-100 in PB). The sections were then rinsed in PB and incubated for 1 h in ABC (Vector Laboratories Inc.; as per the manufacturers' instructions: two drops of solution A and two drops of solution B in 10 ml PB). Immunolabelling was then revealed by a pre-

incubation in DAB for 15 min (Sigma; 0.025% w/v in 0.05 M Tris buffer, pH 7.4), followed by the addition of 20 µl H_2O_2 (Sigma; 1% in dH_2O). Sections were then rinsed in PBS three times and dehydrated through increasing concentrations of alcohol. Finally, slides were dipped in Ilford K.5 nuclear tract emulsion (Polysciences Inc., Warrington, PA, USA; 1:1 dilution in dH_2O) and exposed in the dark (at 4°C for 4 weeks) prior to development. Although the sections were 18 µm in thickness when cut they were 6-8 µm thick after processing.

2.3.4. Quantification of *in situ* hybridisation and immunoperoxidase labelling

Cell counting was carried out using Stereo Investigator software, an Eclipse 80i microscope with a computer-controlled motorized stage and a Lucivid module, projecting the computer display into the drawing tube of the microscope. Counting frames for the sections were 135 µm × 93 µm in the XY plane, but no guard zones (see section 2.2.6) in the Z plane were used because the lack of penetration of the silver granules in the tissue. A 100× 1.4 NA oil-immersion objective was used for all cell counts for low depth of field.

For the sections processed for *in situ* hybridisation and immunoperoxidase labelling, the quantification of the co-expression of different markers was determined as follows:

1) Neurons showing a dense accumulation of black-silver granules, higher than the background, and following the shape of the cell soma and principal dendrites, were considered *in situ* hybridisation-positive and counted.
2) Neurons showing the DAB-brown precipitate in their soma and principal dendrites were considered immunopositive and counted.
3) Neurons showing both forms of labelling were considered double-positive.

Using these numbers, the proportions of calbindin- and calretinin-positive neurons that were positive for markers of GABAergic (GAD65/67), glutamatergic (VGluT2) or cholinergic (ChAT) neurons were determined. Numbers of double-positive neurons found in each segment of the PPN were assessed and plotted on histograms to describe their distribution (see section 2.2.5). Contours of the PPN were established using sections labelled by *in situ* hybridisation for ChAT (Table 4.1).

Unlike before, densities for these segments were calculated in only two dimensions (densities described per mm^2) as the autoradiography used to detect the riboprobes is greatly affected by the thickness of the tissue and riboprobe-containing neurons located at the bottom of the section (closest to the slide) are unlikely to have a sufficient enough effect as to result in the formation of silver granules on the surface of the tissue. Beyond a distance of 5 μm it is difficult to get complete labelling of all riboprobes in the tissue (Dr Marisela Morales, personal communication). This problem can be overcome by using thin sections, but the sections in this study were approximately 5-8 μm in thickness after processing, meaning that those neurons located towards the bottom of the section might appear unlabelled whilst actually containing the radioactive riboprobes (i.e. false negatives; see technical considerations, section 6.2.1).

2.3.5. Triple immunofluorescent labelling

The immunofluorescent labelling of ChAT, calbindin and calretinin was performed in sections where the PPN was largest in its medio-lateral axis (*n*=3). The brains of three rats were perfuse-fixed and sectioned, as described in section 2.2.1. These sections were then washed three times in PBS and blocked for 1 h (in 10% NDS in PBS), before primary antibodies were added in a blocking solution (1% NDS in PBS; see Table 4.2) and incubated overnight at 4°C. Next day, sections were washed in PBS (three times), then incubated overnight in secondary antibodies (in 1% NDS in PBS; 4°C). The day after,

sections were washed in PBS (three times), mounted with Vectashield mounting medium (Vector laboratories Inc.) and stored in the dark at 4°C until examined. Control reactions were performed by omitting each of the primary antibodies in turn. The immunofluorescence of the remaining two markers was assessed, which revealed a complete absence of fluorescence for the omitted antibody.

Confocal microscope images were obtained with a scanning microscope (LSM510 NLO; Zeiss, Welwyn Garden City, UK). Stacks of 20 images were taken through the Z-axis using a 40× oil objective (Plan-Neofluar: Zeiss) and a frame of 325.8 µm × 325.8 µm × 1 µm (X,Y and Z, respectively). The filters used were: Ch1, LP 650; Ch2, LP 505; Ch3, LP 560. The laser wavelengths were 633 nm, 543 nm and 488 nm, respectively. The brightness and contrast of the images were subsequently adjusted in Photoshop (Adobe Systems Inc., Mountain View, CA, USA).

2.4. Chapter 5 methods

2.4.1. Tracer injections in the STN and GiN

To identify PPN neurons with ascending or descending projections, fluorescently labelled red and green retrobeads (Lumafluor, Inc) were injected into the subthalamic nucleus (STN) or gigantocellular nucleus (GiN) respectively. Anaesthesia was induced using 4% isofluorane in O_2 and maintained during surgery using an average of 2% isofluorane (Iso, Schering-Plough Ltd., Welwyn Garden City, UK). The animals were placed in a stereotaxic frame (David Kopf Instruments, Tujunga, CA, USA), a small craniotomy was made above the STN (3.7 mm posterior to Bregma, 2.6 mm lateral to Bregma and 7.6 mm ventral to the dura) and 100 nl of red retrobeads were injected in the STN (1 µl syringe, 70 mm long; SGE, World Precision Instruments, Stevenage, UK). Following withdrawal of the syringe, a second small craniotomy was made above the GiN (10.5 mm posterior to Bregma, 0.9 mm lateral to Bregma and 9.5 mm ventral to the dura),

into which 150 nl of green retrobeads were injected. The syringe was left in place for 5 min before and after the injections and then withdrawn. After suturing the wound, the animals were removed from the stereotaxic frame and kept under observation until they recovered from the anaesthesia.

2.4.2. Processing tissue for tracer injections

Two to three weeks after the tracer injections, the animals were anaesthetised and transcardially perfused with fixative, and 50 μm sections collected in six series and stored in sodium azide (0.05% in PBS; as described in section 2.1.1). Sections, lateral and medial to the PPN (containing the STN and the GiN, respectively), were collected to localise the sites of the tracer injections. These sections were mounted with Vectashield mounting medium (Vector Laboratories Inc.) and analysed under the fluorescent microscope (Zeiss LSM-710, ApoTome structured illumination system, Colibri LED fluorescence illumination source). Only animals with the tracer injection largely restricted to the STN and GiN were used in the study (see Chapter 5 summary of methods for more detail).

2.4.3. Immunofluorescent labelling of calbindin, calretinin and ChAT in STN- and GiN-projecting neurons

Sections of tracer-injected rat brains containing the PPN, were double-immunolabelled for calbindin and ChAT or calretinin and ChAT (one series of sections for each; $n = 3$). Sections were washed three times in PBS, blocked for 1 h (in 10% NDS in PBS), before primary antibodies were added (in 1% NDS in PBS; see Table 5.1) and incubated overnight at 4°C. Next day, sections were washed in PBS and secondary antibodies were added (in 1% NDS in PBS; at 4°C overnight; see Table 5.1). Sections were then washed in PBS, mounted with Vectashield mounting medium (Vector laboratories Inc.) and stored in the dark at 4°C until used. Control reactions were performed as before (see section 2.3.5).

2.4.4. Analysis of immunofluorescent and retrograde labelled PPN neurons

Retrobead labelling had a distinctive granular pattern in the cytoplasm and primary dendrites, leaving the nucleus unlabelled. Immunolabelling for calbindin-, calretinin- and ChAT-positive neurons was clearly distinguishable from either red or green retrobead labelling (STN- and GiN-projecting neurons, respectively). This allowed the quantification of STN- and GiN-projecting neurons that were positive for calbindin, calretinin and ChAT using Image J software (publicly available).

Immunofluorescent and retrogradely labelled neurons were analysed by capturing images of the entire PPN through X, Y and Z planes. This was done using a Zeiss LSM-710 fluorescent microscope (20× 0.8 NA dry objective lens) with an ApoTome-structured illumination system and using Colibri LED fluorescence as illumination source. Multi-channel stacks of images were taken in the Z plane, each separated by approximately 3 μm using a digital camera (Axiocam HRm) in combination with acquisition software (Axiovision 4.8.1; Zeiss). For each Z plane level, squares of tissue were captured in the X and Y axes, each overlapping slightly with adjacent squares, to create an image of the whole PPN (Figure 2.2 A).

Following the same method, low magnification images were captured (using a 5× 0.16 NA dry objective) to include the entire PPN as well as the SNr. Using the centre of the SNr as a reference point, concentric circles (330 μm apart) were drawn to delimit segments of the PPN (see section 2.2.5) to allow the distributions of labelled neurons to be analysed using Image J software (Figure 2.2 B). The distances between concentric circles were modified from previous analyses (section 2.2.5) as non-dehydrated sections shrank 10-13% less than dehydrated sections. This was confirmed by measurements taken between the centre of the SNr and the scp (approximately 1.9 mm lateral to Bregma; using Stereo Investigator software). In dehydrated sections this distance was 4125 μm ± 43 μm

(*n*=6; see Figure 2.1, Mena-Segovia *et al*., 2009); in non-dehydrated sections this distance was 4659.4 ± 16.8 μm (mean ± SEM; *n*=3).

2.4.5. 6-hydroxydopamine lesions

Unilateral 6-hydroxydopamine (6-OHDA) lesions were carried out in 30 Sprague-Dawley rats (200-250 g; see Table 5.3). Anaesthesia was induced using 4% isofluorane in O_2 and maintained during surgery using an average of 2% isofluorane (Iso, Schering-Plough Ltd.). The animals were placed in a stereotaxic frame (David Kopf Instruments) and IP injected with desipramine (25 mg/kg in 0.9 % NaCl in dH_2O; Sigma) 20 min prior to 6-OHDA injections to minimise the uptake of 6-OHDA by noradrenergic neurons (Schwarting & Huston, 1996b).

A small craniotomy was made in the right hemisphere of the brain (4.5 mm posterior to Bregma, 1.3 mm lateral to Bregma and 7.9 mm ventral to the dura) and 3 μl of a 6-OHDA solution (3 mg/ml of 6-OHDA hydrochloride salt; dissolved immediately before use in an ice-cold solution of 0.9% NaCl and 0.02% ascorbic acid in dH_2O; Sigma) was injected (10 μl syringe; Hamilton 701RN; HA-763501; Jaytee Biosciences Ltd., Herne Bay, Kent, UK). Injections were carried out with the aid of a micropump at a rate of 0.5 μl/min. The syringe was left in place for 5 min before and after the injections and then slowly withdrawn.

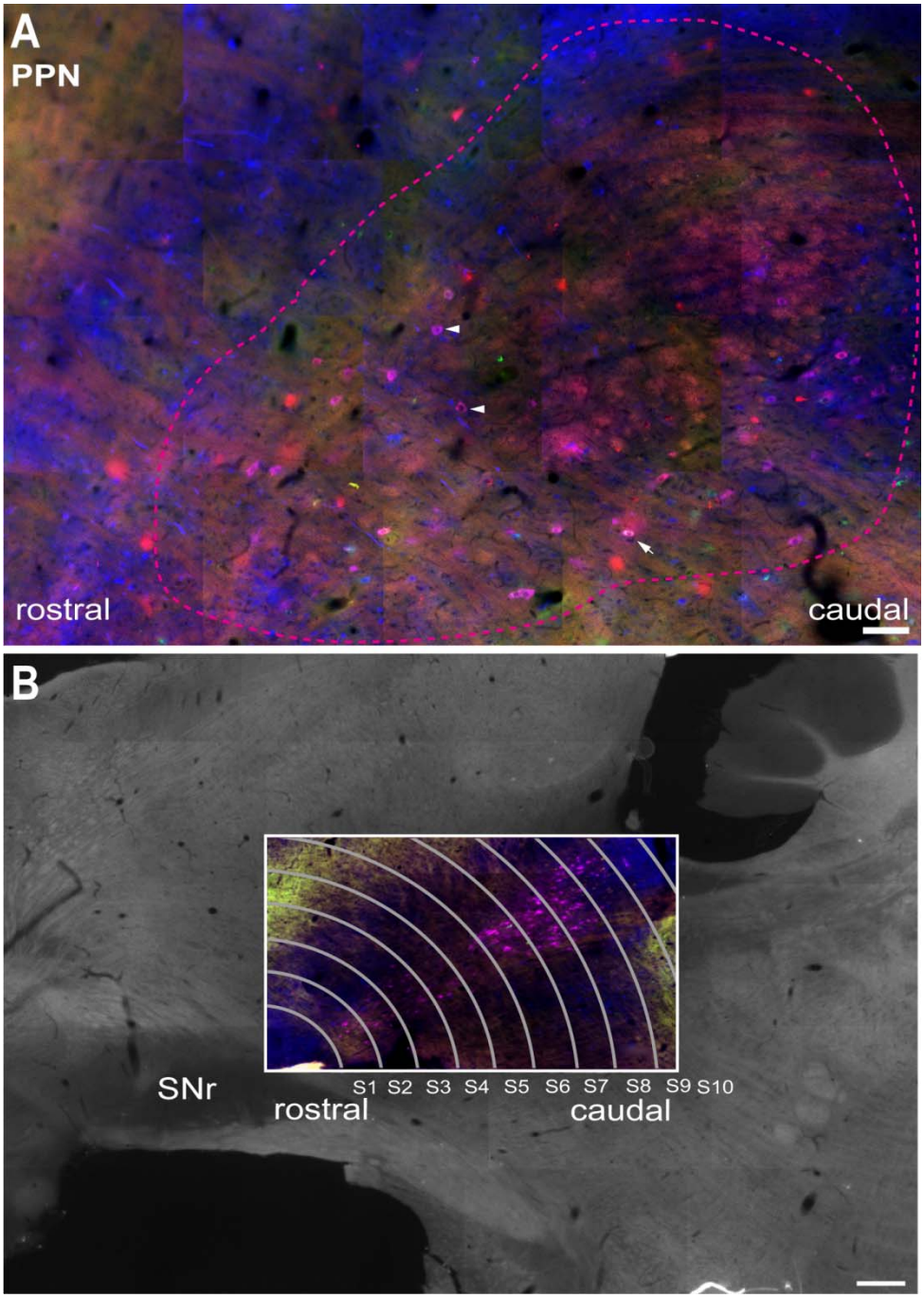


Figure 2.2. A, Montage of fluorescent images in one Z plane, showing ChAT (magenta, examples indicated by arrowheads) and calretinin (blue) labelling in the PPN (dotted lines, as determined by cholinergic neurons), together with STN- and GiN-projecting neurons (red and green retrobeads, respectively). A cholinergic neuron projecting to both the STN and GiN is indicated by an arrow. B, A high magnification multi-channel image of the PPN (defined by ChAT labelling, magenta; see rectangle) overlying a low magnification image of a sagittal rat brain section, with a schematic representation of the PPN segments used to analyse neuronal distribution. Scale bar for A: 500 µm. Scale bar for B: 330 µm.

After suturing the wound, animals were removed from the stereotaxic frame and kept under observation until they recovered from the anaesthesia. Post-surgery recoveries and levels of stress were evaluated in the animals and scored daily until they fully recovered (3-4 days). In some cases, additional food supplements were provided to alleviate the initial weight lost following the lesion.

2.4.6. Behavioural evaluation of 6-OHDA lesioned animals

The extent of the 6-OHDA lesion was assessed 14-15 days after the injection by challenge with a subcutaneous injection of apomorphine, a dopamine agonist, (0.05 mg/kg; 0.9 % NaCl, Sigma) (Hudson *et al.*, 1993; Schwarting & Huston, 1996a). Apomorphine injection should induce a strong response from the lesioned side of the brain, as dopamine receptors are upregulated in the dopamine-depleted striatum of this hemisphere. The degrees to which the animals rotated in the contralateral direction (in 20 min; Hudson *et al.*, 1993) in response to apomorphine were used to assess the extent of the lesion; lesioned rats rotated 80 times or more, partially lesioned rats rotated 40-79 times and non-lesioned rats rotated less than 40 times. In some cases the animals did not turn or move at all; instead they froze or displayed compulsive, repetitive grooming behaviour. In these cases, animals were re-tested with apomorphine two to three days later (see Table 5.3).

After these tests were performed, 19 of 30 animals were confirmed to be lesioned, 3 had only a partial lesion and 8 showed no sign of a lesion at all. Animals with partial lesions or no lesions were not used for the study and were humanely killed following Schedule I procedure, in accordance with the Animals (Scientific Procedures) Act, 1986 (UK).

2.4.7. Tracer injections in control and 6-OHDA lesioned animals

One to two days after 6-OHDA lesions were confirmed, 19 lesioned animals and 6 control animals were injected with retrograde tracers (to reveal the PPN neurons projecting

to the STN and GiN) as previously described (section 2.4.1). Two weeks after tracer injections, the brains of these animals were perfuse-fixed and sectioned for immunolabelling of the immediate early gene Egr1 (as described in section 2.2.1, between 6 and 8 pm to minimise the effect of the sleep-wake cycle on Egr1 expression; Mena-Segovia et al., 2004b). Sections containing the PPN were collected in six series and stored in PBS containing sodium azide (0.05%) until used.

Sections containing the STN or GiN were also collected and examined under the fluorescence microscope to evaluate the location of the injection sites. Additionally, sections containing the STN were immunolabelled to reveal FoxP2; this marker labels neurons of the STN and not surrounding areas, making it a useful tool to visualise STN boundaries (Dr. Peter Magill, personal communication).

The sections were rinsed in PBS (3 times, 10 min each) and blocked for 1 h in NDS (10% in PBS), before adding an anti-FoxP2 primary antibody (raised in rabbit; Sigma; 1:500 dilution in 1% NDS, 0.03% Triton X-100 in PBS) and incubated overnight at 4°C. Next day, sections were washed in PBS then incubated overnight at 4°C in a secondary antibody (donkey anti-rabbit-Alexa488; Jackson Immunoresearch Laboratories Inc.; 1:1000 dilution in 1% NDS in PBS). They were then washed 3 times in PBS, mounted onto slides with Vectashield mounting medium (Vector laboratories Inc.) and stored in the dark at 4°C until examined. Control reactions were performed by omitting the primary antibody, which resulted in a complete absence of fluorescence. Three control and three 6-OHDA lesioned animals had injections largely restricted to the STN and GiN (see Chapter 5, Figure 5.1) and were thus used to evaluate the expression of Egr1.

2.4.8. Egr1 immunolabelling in tracer-injected, control and lesioned animals

Brain sections from control and 6-OHDA lesioned animals, with accurate tracer injections in the STN and GiN, were immunolabelled to reveal Egr1 and ChAT (to define

the boundaries of the PPN). Sections containing the PPN (1 of the 6 series) were rinsed in PBS (3 times, 10 min each) and blocked for 1 h in NDS (10% in PBS), before adding primary antibodies (anti-Egr1, raised in rabbit, Santa Cruz, Heidelberg, Germany, 1:2500; anti-ChAT, raised in goat, Chemicon, 1:500; in 1% NDS in PBS, incubated overnight at 4°C). Next day, sections were washed in PBS then incubated overnight at 4°C in secondary antibodies (donkey anti-rabbit-Cy5, 1:250; donkey anti-goat-AMCA, 1:100; Jackson Immunoresearch Laboratories Inc.; in 1% NDS in PBS). They were then washed 3 times in PBS, mounted onto slides with Vectashield mounting medium (Vector Laboratories Inc.) and stored in the dark at 4°C until examined. Control reactions were performed by omitting each of the primary antibodies in turn, which revealed a complete absence of fluorescence for the omitted antibody.

Analyses were performed as before (see section 2.4.4), but with a Zeiss fluorescent microscope attached to a Hamamatsu digital video camera and Stereo Investigator software. Z-plane stacks of images were acquired at intervals of 4 μm rather than 3 μm and the use of low magnification images to define the segments of the PPN was not necessary. Stereo Investigator software was able to define these segments, using the high magnification (20×) images, once the centre of the SNr and the boundaries of the PPN were specified.

The numbers and proportions of STN-, GiN- and double-projecting neurons immunopositive for Egr1 were quantified for the segments of the PPN of control and 6-OHDA lesioned animals. Immunolabelling for Egr1 (Cy5-defined as blue) was easily distinguishable from STN (Cy3-red) or GiN (Alexa488-green) retrobead labelling. Additionally, Egr1 immunolabelling was restricted to the nucleus, whereas retrobead labelling was restricted to the cytoplasm.

3. Calbindin- and calretinin-positive neurons in the PPN

3.1. Introduction

Neurons that express calcium-binding proteins have been shown to have distinct functional properties despite the fact that they may use the same neurotransmitter (Gulyas *et al.*, 1991). As a consequence they have been extensively used as markers to distinguish between populations of neurons in the hippocampus (Acsady *et al.*, 1993; Somogyi & Klausberger, 2005), neocortex (Staiger et al., 2004), basal ganglia (Parent et al., 1996), basal forebrain (Gritti *et al.*, 2003) and PPN (Dun et al., 1995). Some of these calcium-binding proteins form the large super family of EF-hand proteins, which contain an amino acid motif permitting the specific and reversible binding of calcium ions (Kretsinger & Nockolds, 1973; Camp & Wijesinghe, 2009). Because of this, it has been proposed that some members of this super family may have a functional role in the modulation of intracellular calcium (Nagerl et al., 2000).

The calcium-binding proteins calbindin, calretinin (Pochet et al., 1985) and parvalbumin (Dun *et al.*, 1995) are all members of the EF-hand family, but modulate intracellular calcium levels in subtly different ways (Chard *et al.*, 1993; Schwaller *et al.*, 2002; Camp & Wijesinghe, 2009). For instance, proteins containing a different number of calcium-binding motifs have been shown to bind calcium at different kinetic rates (Schwaller *et al.*, 2002). Parvalbumin binds calcium at a high kinetic rate and is usually associated with fast firing neurons, whereas calbindin and calretinin bind calcium at lower affinities and neurons containing them show a more diverse range in their electrophysiological properties (Schwaller *et al.*, 2002).

Previous studies have reported the presence of calbindin- and calretinin-positive neurons in the PPN, and at lower numbers, parvalbumin-positive neurons (Dun *et al.*, 1995; Parent *et al.*, 1996), but their total numbers and distribution are not yet known. As

calbindin- and calretinin-positive neurons account for the vast majority of neurons containing calcium-binding proteins in the rat PPN, the aim of this chapter will be to quantify their total numbers and to characterise their distribution. This assessment of the calcium-binding protein complement of PPN neurons will allow a greater appreciation of their physiological characteristics and will, in turn, contribute to our understanding of how the PPN functions.

3.2. Summary of methods

To determine the presence and distribution of the calcium-binding proteins calbindin and calretinin in PPN neurons, immunohistochemical peroxidase reactions were carried out. Six Sprague-Dawley rats were deeply anaesthetised (ketamine/xylazine mixture) and intracardially perfused with fixative. Brains were removed and cut in 50 μm thick sagittal sections. Brainstem sections containing the PPN were collected in series of six and stored in PBS with 0.05% sodium azide until used (see Methods Chapter 2.2.1).

Brain sections were double-immunolabelled to reveal either calbindin and ChAT or calretinin and ChAT (see Table 3.1); for each reaction two of the six series collected were used. These were revealed with peroxidase reactions, using DAB and Vector SG as chromogens, to label ChAT and calbindin or calretinin respectively (see Methods Chapter 2.2.2 and Table 3.1). Neurons displaying the typical brown colour of the DAB peroxidase reaction product were considered to be ChAT-immunopositive and were used to delimit the borders of the PPN. Neurons showing the blue-black reaction product formed by the Vector SG were considered to be calbindin- or calretinin-immunopositive (see Methods Chapter 2.2.3).

	Primary antibody	Species of Origin	Dilution	Manufacturer	Secondary Antibody	Dilution	Manufacturer	ABC	Chromogen
1a	calbindin	Mouse	1:5000	Swant	Biotin horse anti-mouse	1:500	Vector	ABC elite	Vector-SG
1b	ChAT	Goat	1:500	Chemicon	Biotin horse anti-goat	1:500	Vector	ABC elite	DAB
2a	calretinin	rabbit	1:5000	Swant	Biotin horse anti-rabbit	1:200	Vector	ABC elite	Vector-SG
2b	ChAT	goat	1:500	Chemicon	Biotin horse anti-goat	1:500	Vector	ABC elite	DAB

Table 3.1. Combinations of antibodies used to double-immunoperoxidase label sections to reveal calbindin and ChAT (1) or calretinin and ChAT (2).

3.3. Results

3.3.1. Morphology of calbindin- and calretinin-positive neurons

Calbindin- and calretinin-immunopositive cell bodies, dendrites and axonal processes were observed, intermingled with cholinergic neurons, throughout the rat PPN and this immunolabelling was clearly distinguishable from background levels (Figure 3.1). Similar to previous reports, calbindin- and calretinin-positive neurons were also observed in other areas of the brain, including the hippocampus, forebrain, cerebellum and cortex (Baimbridge *et al.*, 1992; Parent *et al.*, 1996; Gritti *et al.*, 2003).

The calbindin-positive neurons in the PPN had rounded cell bodies that appeared bipolar or multipolar in shape (Figure 3.1, A and C). The average diameter of their cell bodies was 14.5 ± 3.5 μm (± SD; n = 100 neurons; see Methods Chapter 2.2.4) and the majority of these neurons were of a small size (75% were less than 15.8 μm in diameter). However, a few conspicuously larger calbindin-positive neurons were also observed, with a somatic size between 21.6 μm and 27.9 μm (Figure 3.2, A). Consequently, the diameters of calbindin-positive neurons did not follow a normal distribution when plotted on a frequency histogram (Figure 3.2, C; Shapiro-Wilk test, $P < 0.001$).

Despite also being bipolar or multipolar, calretinin-positive neurons were more irregular in shape than calbindin-positive neurons (Figure 3.1, B and D) and displayed a wider range of somatic sizes, with an average somatic diameter of 15.5 ± 4.4 μm (± SD; n = 100 neurons). These diameters followed a normal distribution (Shapiro-Wilk test, $P = 0.264$; Figure 3.2, B and D) and were significantly larger than calbindin-positive neurons (Mann-Whitney Rank sum test; $U = 4147$; $P = 0.037$).

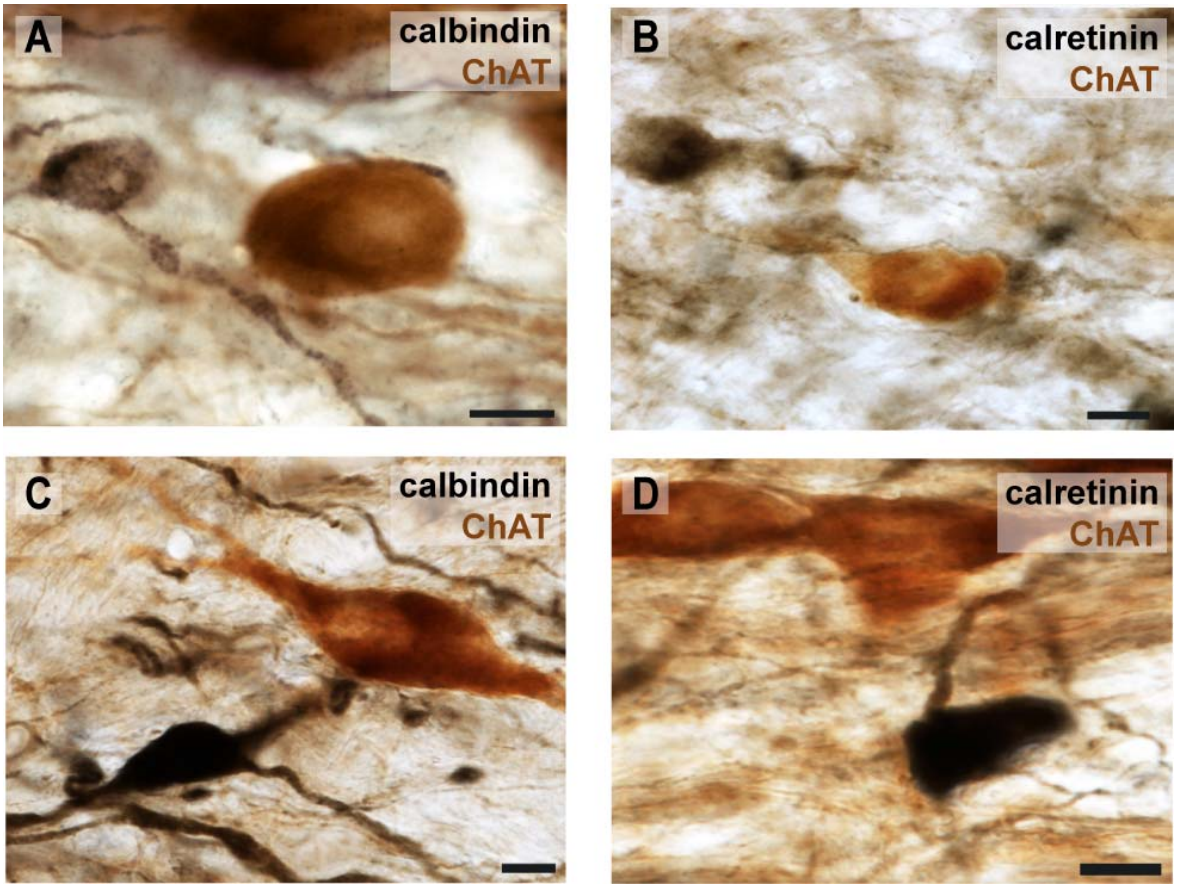


Figure 3.1. Calbindin- and calretinin-positive neurons are present in the PPN

Light micrographs of PPN sections double-immunohistochemically labelled to reveal ChAT with the brown DAB precipitate and, with the blue-black precipitate, either calbindin- (A and C) or calretinin-positive neurons (B and D). Scale bars: 10 µm.

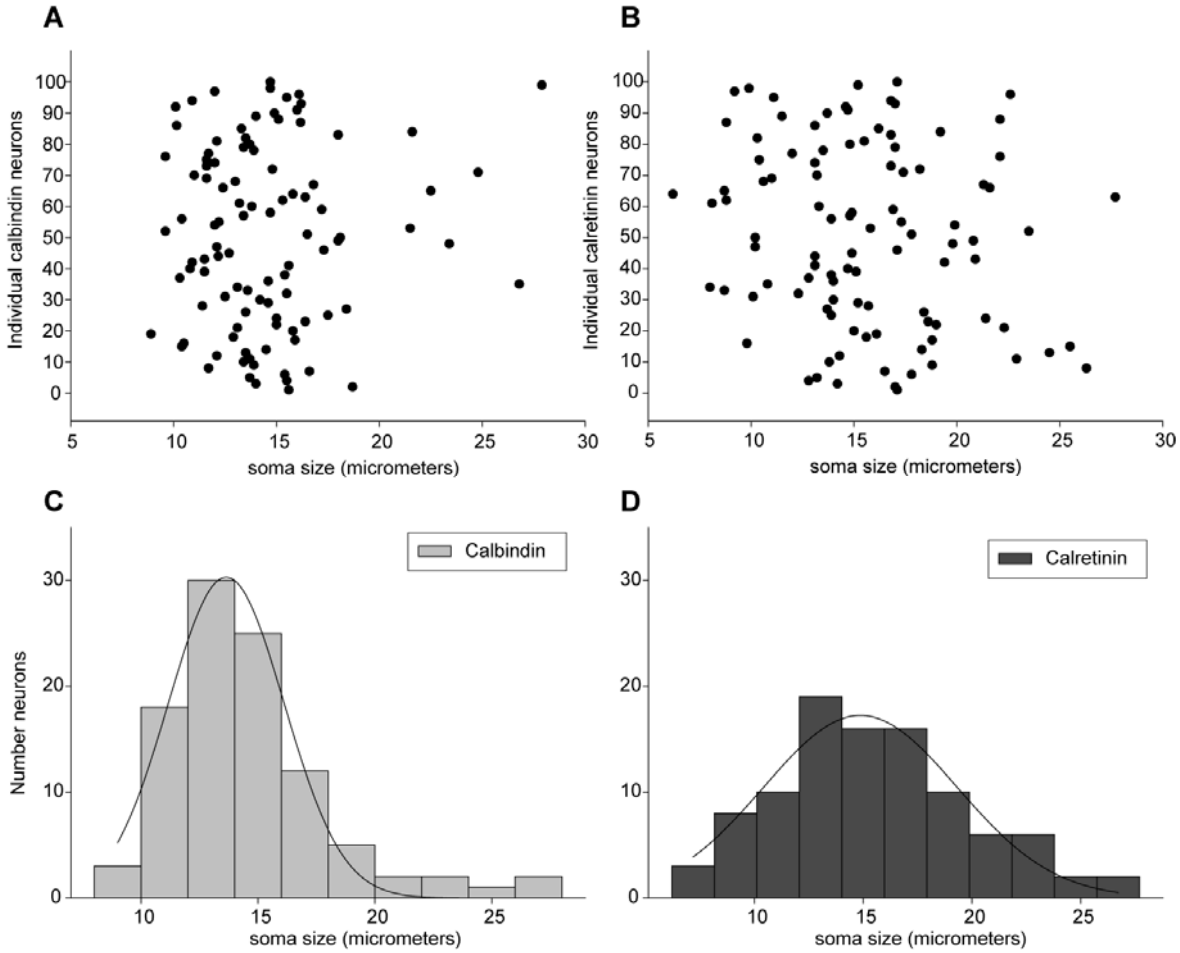


Figure 3.2. Distribution of the somatic sizes of calbindin- and calretinin-positive neurons in the PPN

Scatter plots of somatic sizes of calbindin- (A) and calretinin-positive neurons (B) in the PPN and their corresponding frequency histograms used to assess the normality of their distributions (C and D, respectively).

3.3.2. Estimated total number of calbindin- and calretinin-positive neurons

A stereological approach was used to estimate the total number of calbindin- and calretinin-positive neurons in the PPN (using one in every three 50 μm sections collected; *n*=6 animals; see Methods Chapter 2.2.6). The estimated total number of calbindin-positive neurons in the PPN (one hemisphere) was 2,318 ± 388; whereas the estimated total number of calretinin-positive neurons was 2,452 ± 408 (mean ± SEM). The difference between them was not significantly different (Student's t-test, $t_{(10)} = -0.23$, $P = 0.816$).

3.3.3. Distribution of calbindin- and calretinin-positive neurons in the PPN

Calbindin- and calretinin-positive neurons were seen to be intermingled with cholinergic neurons and distributed across the whole rostro-caudal extent of the PPN (Figure 3.3). These neurons did not show a layer-like arrangement, as the cholinergic neurons do, but were instead sparsely distributed. In addition, calbindin- and calretinin-positive neurons were also observed outside the PPN borders (as defined by the cholinergic neurons) in regions corresponding to the SNr, LDTg and cuneiform formation.

Calbindin- and calretinin-positive neurons appeared to be less abundant in the rostral PPN (Figure 3.3, A and C) in comparison to the caudal PPN (Figure 3.3, B and D respectively). In order to quantitatively evaluate this observation, the distributions of calbindin- and calretinin-positive neurons along the rostro-caudal axis of the PPN were analysed using a stereological approach (Mena-Segovia et al., 2009). This method is based upon the subdivision of the PPN into ten equally-sized segments (for details see Methods Chapter 2.2.5). By using the centre of the substantia nigra *pars reticulata* (SNr) as the starting point, concentric circles of increasing radii (300 μm apart) were drawn to divide the PPN into ten segments (S1-S10); S1 being the most rostral and S10 being the most caudal.

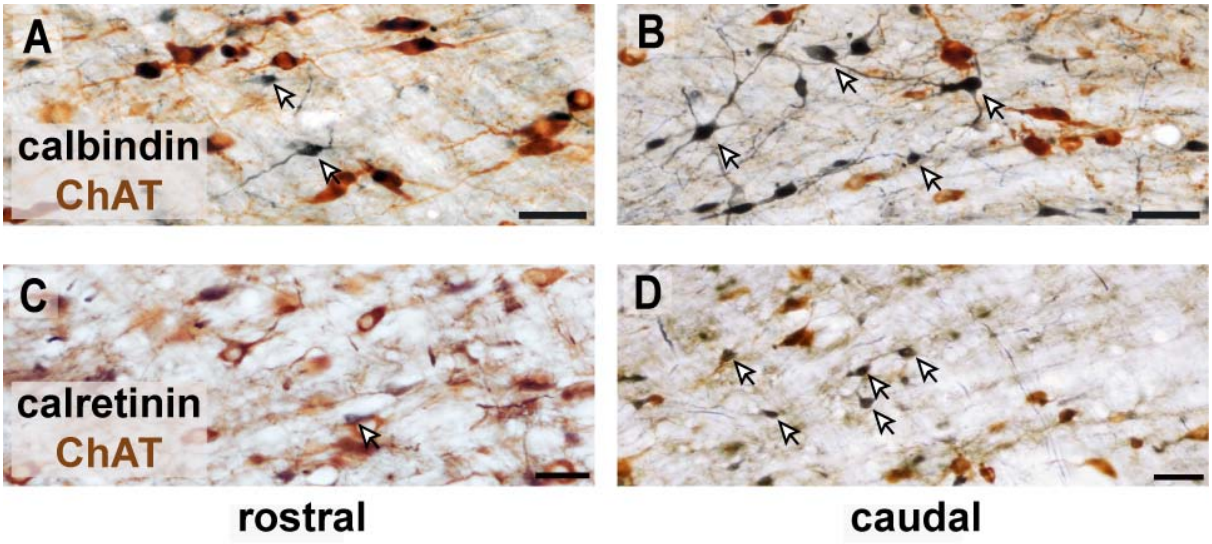


Figure 3.3. Calbindin- and calretinin-positive neurons in the rostral and the caudal PPN

Light micrographs of sections double-immunolabelled (arrows) for ChAT (brown DAB precipitate) and calbindin or calretinin (dark-blue Vector SG precipitate). Scale bars: 50µm.

The estimated total numbers of calbindin- and calretinin-positive neurons were calculated per segment of the PPN (see Methods Chapter 2.2.6) and histograms showing the totals for each segment were plotted (Figure 3.4). To compare the numbers of neurons in each segment, ANOVA on ranks (Kruskal-Wallis) was used because the data failed to pass the normality test required for one way ANOVA. The analysis revealed significant differences in the distributions of calbindin- and calretinin-positive neurons across PPN segments (Kruskal-Wallis; $H_{(9)} = 37.78$ for calbindin and $H_{(9)} = 35.45$ for calretinin; $P < 0.001$; Figure 3.4 A and B; $n = 6$). A pairwise multiple comparison between segments indicated that calbindin-positive neurons were more abundant in segments S6 and S7 than in segment S1 ($P < 0.001$; Dunn's method; Figure 3.4 A). In contrast, calretinin-positive neurons were seen to be more abundant in segment S6 than in either segments S1 or S10, more abundant in segment S5 than in segments S1 or S10 and more abundant in segment S4 than in segment S10 ($P < 0.05$; Dunn's method; Figure 3.4 B).

3.3.4. Density analysis of calbindin- and calretinin-positive neurons

The estimated total number of calbindin- and calretinin-positive neurons was larger in the segments where the area of the PPN was also larger. To test whether the total number of neurons in each segment was affected by the volume of the segment, cell densities (neurons/mm^3) were calculated (total number of neurons/volume of segment; Figure 3.5). The distribution of calbindin-positive neuron densities across the segments was not uniform (ANOVA on ranks; Kruskal-Wallis; $H_{(9)} = 19.51$; $P = 0.021$). However, a pairwise multiple comparison did not show differences between specific segments ($P > 0.05$; Dunn's method; Figure 3.5 A). Calretinin-positive neurons, however, were found to be uniformly distributed along the rostro-caudal axis of the PPN ($F_{(9,42)} = 1.75$; $P = 0.108$; one way ANOVA; Figure 3.5 B), lacking the variability seen for calbindin-positive neurons.

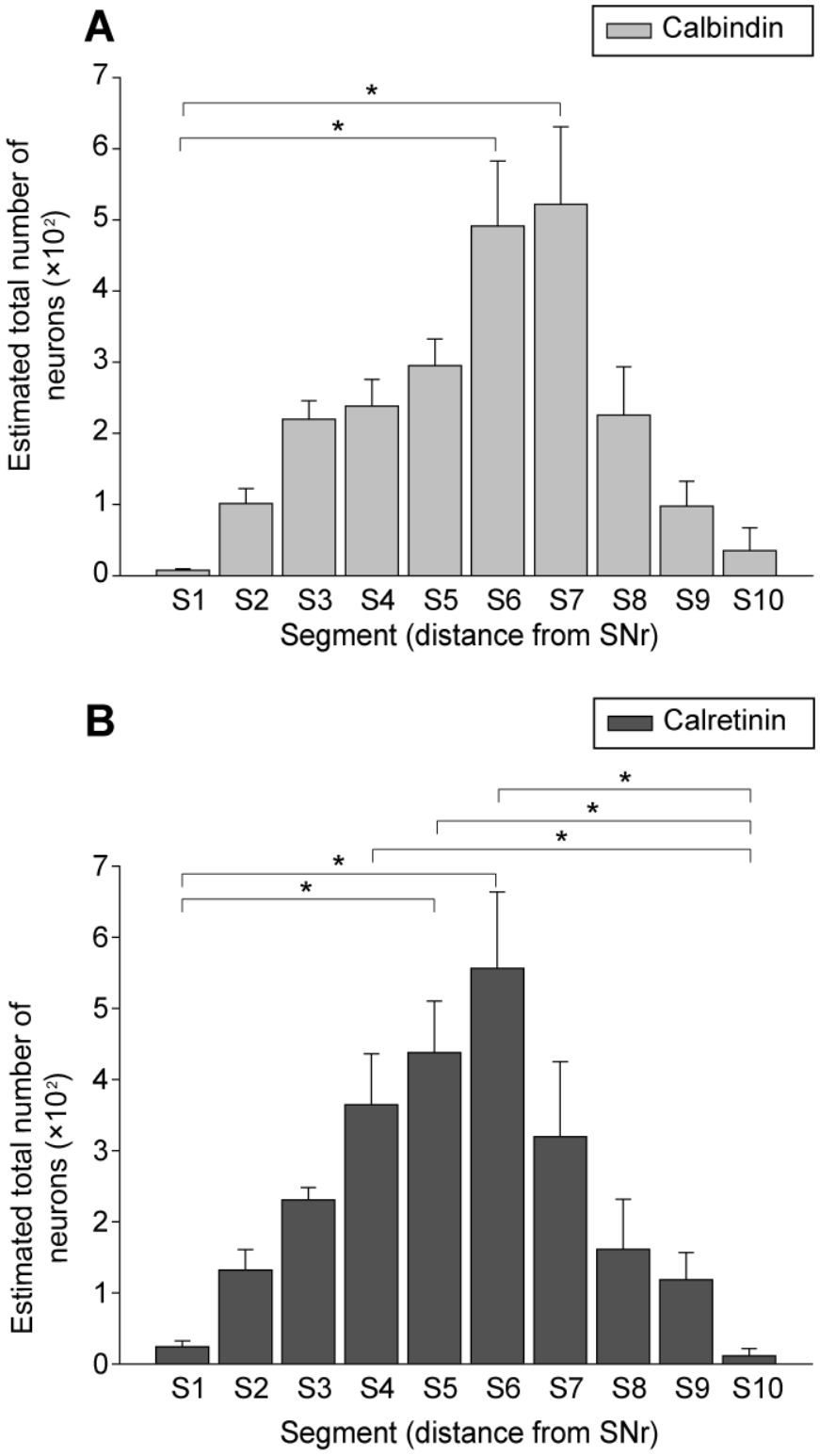


Figure 3.4. Distributions of calbindin- and calretinin-positive neurons across segments of the PPN

Histograms showing the estimated total number of calbindin- (**A**) and calretinin-positive (**B**) neurons ($\times 10^2$) in segments S1-S10 of the PPN (n = 6; columns represent the mean total number per segment; error bars indicate SEM; * indicates statistically different pairwise comparisons between segments; $P < 0.001$).

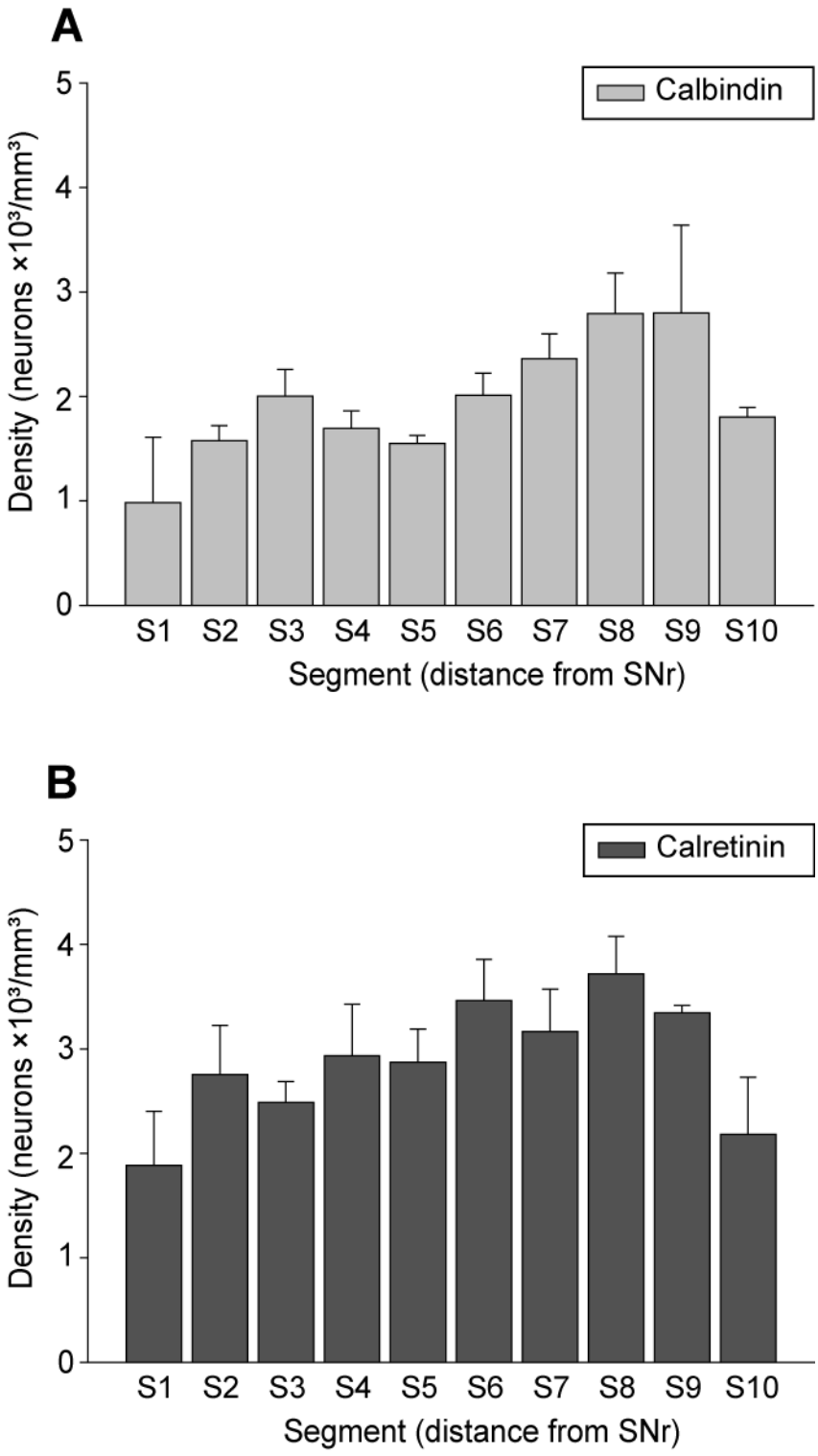


Figure 3.5. Densities of calbindin- and calretinin-positive neurons across segments of the PPN

Histograms of the densities of calbindin- (**A**) and calretinin-positive (**B**) neurons ($\times 10^3/mm^3$) for segments S1-S10 of the PPN (n = 6; columns represent the mean cell density; error bars indicate SEM).

3.4. Discussion

To understand the role of the PPN it is first necessary to understand its basic anatomy, starting with the neuronal subtypes it contains. The three main subtypes of PPN neuron are the cholinergic, GABAergic and glutamatergic neurons, based on the neurotransmitters they utilise, but neurons containing calcium-binding proteins are also present in the PPN. Calbindin and calretinin are two of the most abundant calcium-binding proteins in the brain and appear to be present in substantial numbers of neurons in the PPN, suggesting a significant role for them in PPN physiology (Dun *et al.*, 1995; Fortin & Parent, 1999). In other areas of the brain, neurons that express these calcium-binding proteins express different receptors or neuropeptides, display differential axonal target selectivity and often have different electrophysiological properties (Parent *et al.*, 1996; Gritti *et al.*, 2003; Somogyi & Klausberger, 2005).

Calbindin- and calretinin-positive neurons in the PPN were found to be relatively small in size (average diameters 14.5 ± 3.5 and 15.5 ± 4.4 μm respectively), however, a larger type of calbindin-positive neuron was also seen (ranging from 21.6 to 27.9 μm diameter). The majority of the cholinergic neurons have a large soma size (20-30 μm in diameter; Armstrong *et al.,* 1983), thus it is unlikely that the calbindin- and calretinin-positive neurons represent a prominent subpopulation of the cholinergic neurons. It is possible therefore that calbindin- and calretinin-positive neurons have a GABAergic or glutamatergic nature, as these neurons are generally smaller than cholinergic neurons.

In comparison to the other neuronal subtypes of the PPN, the numbers of calbindin- and calretinin-positive neurons (2,318 ± 388 and 2,452 ± 408, respectively; mean ± SEM) were roughly half the number of GABAergic neurons (6,571 ± 818; mean ± SEM), but similar to the number of cholinergic neurons (2,942 ± 122 mean ± SEM; Mena-Segovia

et al., 2009). It is not possible to compare these numbers with the numbers of any other neuronal subtype of the PPN as their estimated total numbers are as yet unknown.

When the total numbers of neurons were analysed for their distribution across the PPN, peaks were observed towards its centre (along the rostro-caudal axis); in segments S6 and S7 for calbindin-positive neurons and in segments S4-S6 for calretinin-positive neurons. These central PPN segments were also the largest in volume, thus it was likely that this increase in total cell number was due to the increase in volume. In order to ascertain whether this was the case, cell densities were calculated for each of the segments. This showed that the peaks seen in total cell number were as a direct consequence of the increase in volume. Despite no differences being found between individual segments, calbindin-positive neurons did not display uniform density across the PPN, whereas calretinin-positive neurons did. Cholinergic neurons display a uniform density distribution, similar to calretinin-positive neurons, whereas GABAergic neurons are more densely concentrated in segments S1-S5 than in segments S6-S10 (Mena-Segovia *et al.*, 2009). This suggests that if the small-sized calbindin- or calretinin-positive neurons are GABAergic, they do not make up the entire complement of GABAergic PPN neurons.

Adding to the data on cholinergic and GABAergic PPN neurons, this chapter has shown that calbindin- and calretinin-positive neurons are present in significant numbers within the rat PPN. The possibility of an overlap between the calbindin- and calretinin-positive neurons and the other three subtypes is a distinct possibility. Due to the differences in size between the cholinergic and either calbindin- or calretinin-positive neurons, it is unlikely that their populations overlap. In contrast, GABAergic neurons containing calbindin or calretinin have been widely described in the brain and, in addition, glutamatergic neurons have been shown to express them in the brainstem (Gritti *et al.*, 2003). The extent to which this occurs in the PPN will be the topic of the next chapter.

4. Subpopulations of calbindin and calretinin neurons in the PPN contain cholinergic, GABAergic and glutamatergic markers

4.1. Introduction

Results in Chapter 3 indicated the presence of two large populations of PPN neurons containing calbindin and calretinin. It is likely that these overlap with the populations of PPN neurons defined by the neurotransmitter that they use; cholinergic, GABAergic and glutamatergic neurons. The aim of this chapter is to evaluate the proportions of calbindin- and calretinin-positive neurons that express cholinergic, GABAergic and glutamatergic markers.

Cholinergic neurons are abundant in the PPN (2,942 ± 122 mean ± SEM; Mena-Segovia *et al.,* 2009), and they are easily identified by immunolabelling against choline acetyltransferase (ChAT). GABAergic neurons are twice as abundant as the cholinergic neurons (6,571 ± 818; mean ± SEM; Mena-Segovia *et al.,* 2009) and can be identified by the expression of the enzyme that synthesises γ-aminobutyric acid (GABA); glutamic acid descarboxylase (GAD), of which there are two principal isoforms, GAD65 and GAD67 (Erlander *et al.*, 1991). Glutamatergic neurons are roughly 1.5 times more abundant than cholinergic neurons in the caudal PPN (Wang & Morales, 2009), and express vesicular glutamate transporter 2 (VGluT2), one of the three subtypes of VGluTs identified so far.

In this chapter, immunohistochemical labelling of cholinergic neurons (ChAT) will be combined with immunohistochemical labelling of calbindin- or calretinin-positive neurons to assess the degree to which the populations overlap. Additionally, *in situ* hybridisation will be used to label either calbindin- or calretinin-positive neurons alongside immunohistochemical labelling of cholinergic neurons, in order to support the purely immunohistochemical approach. In contrast to cholinergic neurons, GABAergic and glutamatergic neurons in the PPN are technically difficult to label using purely

immunohistochemical methods. Therefore, only *in situ* hybridisation will be used to label these populations together with immunohistochemical labelling for calbindin or calretinin.

4.2. Summary of methods

To evaluate the degree of co-expression of calbindin and/or calretinin with ChAT in PPN neurons, permanent peroxidase immunohistochemical reactions for calbindin and ChAT or calretinin and ChAT were carried out. Sprague-Dawley rats were deeply anaesthetised (ketamine/xylazine mixture) and intracardially perfused with fixative. Brains were removed and cut in 50 μm thick sagittal sections. The brainstem sections containing the PPN were collected in series of six and stored in PBS with 0.05% sodium azide until used (see Methods Chapter 2.2.1).

Brain sections were double-immunolabelled to reveal each of the following combinations: calbindin and ChAT (n = 2 animals), or calretinin and ChAT (n = 4 animals). For each combination two of the six series collected were used. The immunolabelling was revealed by a combination of peroxidase reactions using DAB and Vector SG as chromogens. Neurons stained by the brown DAB peroxidase reaction product showed ChAT-immunopositive neurons and were used to delimit the borders of the PPN. Neurons labelled by the blue-black reaction product (formed by the Vector SG) were considered to be calbindin- or calretinin-immunopositive. The numbers of neurons single-labelled for calbindin or calretinin, or double-labelled for calbindin or calretinin with ChAT, were then quantified (see Methods Chapter 2.3.1 and Table 3.1).

In situ hybridisation (to reveal calbindin or calretinin) was also used, in conjunction with immunohistochemistry to reveal ChAT, to further assess the co-expression of these markers. To obtain the tissue for *in situ* hybridisation, Sprague-Dawley rats were deeply anaesthetised (chloral hydrate 300 mg/kg), and intracardially perfused with fixative. Their brains were removed and stored at -80°C until used. Cryosections of 18 μm thickness,

containing the PPN, were collected in eight series under RNAase free conditions (see Methods Chapter 2.3.2 and Table 4.1). One of these series was treated for *in situ* hybridisation with radioactive riboprobes to reveal calbindin mRNA or calretinin mRNA. The sections were then immunolabelled to reveal ChAT (see Methods Chapter 2.3.3 and Table 4.1) before double-positive neurons were quantified (see Methods Chapter 2.3.4).

Rat	ISH or IHC	Series							
		1	2	3	4	5	6	7	8
1	ISH	GAD	VGluT2	CB	CR				
	IHC	CB	CB	ChAT	ChAT				
2	ISH	GAD	VGluT2	CB	CR				
	IHC	CB	CB	ChAT	ChAT				
3	ISH	GAD	VGluT2			GAD	VGluT2	ChAT	
	IHC	CB	CB			CR	CR	CR	
4	ISH					GAD	VGluT2	ChAT	
	IHC					CR	CR	CR	
5	ISH					GAD	VGluT2	ChAT	
	IHC					CR	CR	CR	

Table 4.1. Combinations of *in situ* hybridisation (ISH) and immunohistochemistry (IHC) used to reveal GABAergic (GAD65/67-positive), glutamatergic (VGluT2-positive) or cholinergic (ChAT-positive) neurons and calbindin- or calretinin-positive neurons (CB and CR, respectively) in the PPN of 5 rats.

Triple immunofluorescent labelling was used to determine the degree of co-expression of calbindin, calretinin and ChAT in PPN neurons. This was carried out in sections containing the PPN at three different medio-lateral levels (n=3; see Methods Chapter 2.3.5 and Table 4.2). The numbers of neurons single-, double- or triple-immunolabelled for each of the markers were then quantified.

Primary antibody	Species of origin	Dilution	Manufacturer	Fluorophore	Secondary antibody	Dilution	Manufacturer
calbindin	mouse	1:5000	Swant	Cy5	donkey anti-mouse	1:250	Jackson
calretinin	rabbit	1:5000	Swant	Alexa-488	donkey anti-rabbit	1:1000	Jackson
ChAT	goat	1:500	Chemicon	Cy3	donkey anti-goat	1:400	Jackson

Table 4.2. Combinations of primary and secondary antibodies used for triple-immunofluorescent labelling.

To investigate whether calbindin- and calretinin-positive neurons of the PPN express GABAergic or glutamatergic markers, permanent peroxidase immunohistochemical reactions for calbindin and calretinin were carried out in combination with *in situ* hybridisation labelling for GAD65/67 mRNA or VGluT2 mRNA. Under RNAase free conditions, one of the series previously collected was used to reveal each of the following combinations: calbindin and GAD65/67 mRNA, calbindin and VGluT2 mRNA, calretinin and GAD65/67 mRNA, calretinin and VGluT2 mRNA. The numbers of neurons single-labelled for calbindin or calretinin, or double-labelled for either GAD65/67 or VGluT2 with calbindin or calretinin, were then quantified (see Methods Chapter 2.3.4).

4.3. Results

These results will first detail the proportions of calbindin- or calretinin-positive PPN neurons that are cholinergic (ChAT-positive) and non-cholinergic (ChAT-negative). Next, the numbers and distributions of GABAergic and glutamatergic PPN neurons will be described, in relation to the segments of the PPN (see Chapter 3). Finally, the proportions and distributions of calbindin- or calretinin-positive neurons that contain markers for GABAergic (GAD65/67) or glutamatergic (VGluT2) neurons will be described.

4.3.1. Few calbindin-positive neurons contain the cholinergic marker ChAT

Calbindin- and calretinin-positive neurons of the PPN are present in similar numbers to the cholinergic neurons and they follow a similar distribution along its rostro-caudal axis (see Chapter 3). Thus, it is possible that there is overlap between these populations of neurons and several approaches were used to determine whether this was the case.

When double-immunolabelling experiments were performed to reveal the cholinergic marker ChAT alongside calbindin (in 1 of 3 sections across the PPN), it was found that of the 1127 calbindin-positive neurons examined only two were positive for ChAT (0.18%; $n = 2$; animal 1 = 1/832; animal 2 = 1/295). If this figure is extrapolated to the full volume of the PPN, using the stereological methods previously described (Methods Chapter 2.7), this equates to an average of 4.2 double-immunolabelled neurons, from a total of 2,360.4 calbindin-positive neurons (0.18%; $n = 2$; animal 1 = 4.2/3,481.8; animal 2 = 4.2/1,239.0). This suggests that there is very little overlap between these populations, but to ensure double-immunolabelled profiles were not missed as a result of a technical error, another method was used; *in situ* hybridisation labelling of calbindin mRNA together with immunolabelling for ChAT (Figure 4.1 A and C).

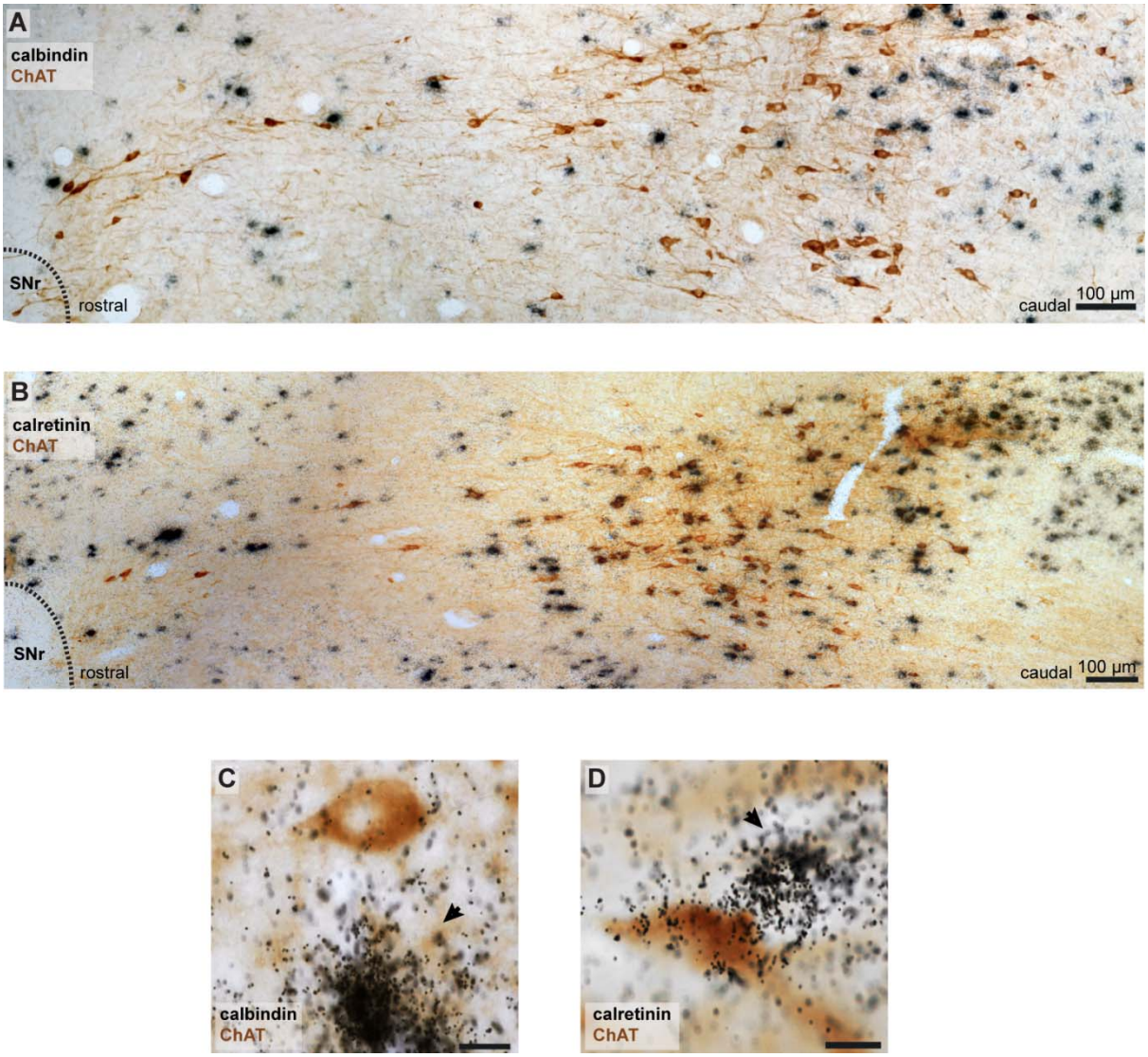


Figure 4.1. Calbindin- and calretinin-positive neurons in the PPN revealed by *in situ* hybridisation

Light micrographs of brainstem sections containing the PPN along its rostro-caudal axis (A and B). *In situ* hybridisation labelling revealing calbindin (A, C; labelled neuron indicated by arrow in C) or calretinin (B, D; labelled neuron indicated by arrow in D) is shown by silver-black granules. Immunoperoxidase labelling revealing ChAT-positive cholinergic neurons (brown precipitate) was used to delimit the boundaries of the PPN. Scale bars for panels A and B: 100 µm; C and D: 10 µm.

Using this method, double-labelling was observed in 33 neurons (n = 2; 4 neurons in animal 1; 29 neurons in animal 2; 1 in 8 series of sections analysed; Figure 4.2 A), suggesting that more double-positive neurons are present in the PPN than shown by the double-immunolabelling method. The numbers of double-positive neurons were quantified for each segment of the PPN and their densities calculated per mm^2 (as determined by the *in situ* hybridisation technique; see Methods Chapter 2.3.4). These double-positive neurons were sparsely distributed along the rostro-caudal axis of the PPN (Figure 4.2, C; white bars), however, statistical comparisons between segments were not possible because the quantification was done in only two animals.

4.3.2. A small proportion of calretinin-positive neurons are cholinergic

In contrast to calbindin-positive neurons, a larger proportion of calretinin-positive neurons were immunopositive for ChAT in the PPN; 292 of 2242 calretinin-positive neurons across four animals (13%; 72.5 ± 25.0, mean ± SEM; n = 4). Extrapolated out to the full volume of the PPN as before, this equates to an average of 306.6 ± 104.3 double-immunolabelled neurons, from a total of 2354.1 ± 637.9 calretinin-positive neurons, in the PPN (n = 4; mean ± SEM). To further confirm this data, a combination of *in situ* hybridisation labelling for calretinin mRNA with peroxidase immunolabelling for ChAT was carried out in two animals (Figure 4.1, B and D). The total number of double-positive neurons seen across a 1 in 8 series of PPN sections in the two animals examined was 242 (animal 1 = 83; animal 2 = 159; Figure 4.2, B), again suggesting that a greater number of double-positive neurons can be detected with the *in situ* hybridisation method. Furthermore, when densities were taken into account for PPN segments, calretinin mRNA/ChAT double-positive neurons were sparsely distributed along the rostro-caudal axis (Figure 4.2, C; gray bars), however, statistical comparisons between segments were not possible because the quantification was done in only two animals.

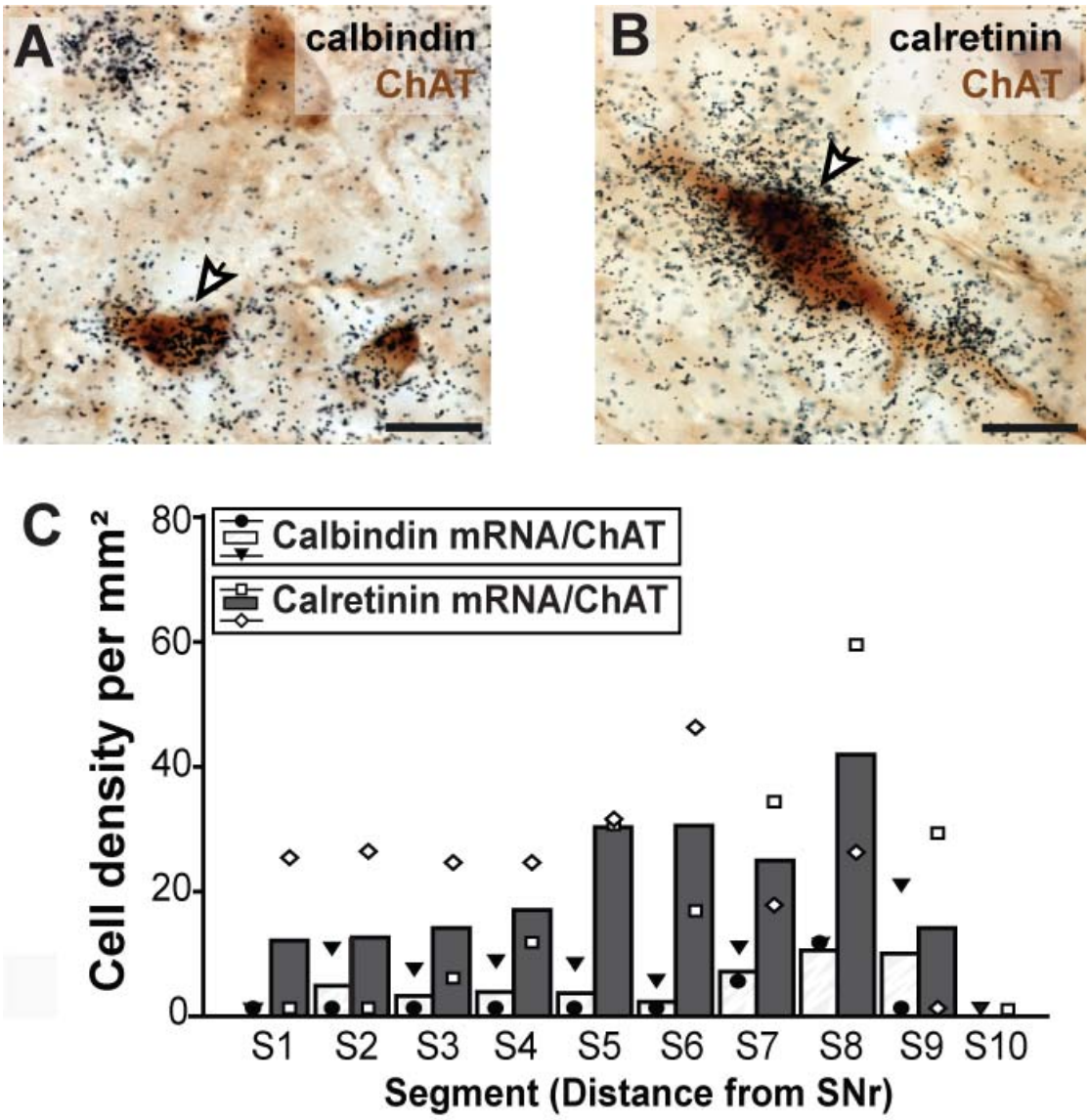


Figure 4.2. Neurons of the PPN double-labelled for ChAT and either calbindin or calretinin

A and, B.-Light micrographs of PPN sections showing double-labelled neurons for calbindin mRNA and ChAT immunoreactivity (A, arrow) or calretinin mRNA and ChAT immunoreactivity (B; arrow). Immunoperoxidase labelling revealing ChAT is shown in brown and *in situ* hybridisation labelling revealing calbindin or calretinin is shown in silver-black granules. Scale bars: 10µm. C.- Histogram showing the distributions of double-labelled neurons (calbindin mRNA/ChAT, white bars; calretinin mRNA/ChAT, grey bars) along the rostro-caudal axis of the PPN. Data is expressed as the density of neurons per mm^2 (n = 2; bars show the mean values and symbols indicate the individual values for each animal).

4.3.3. Triple-immunofluorescent labelling of calbindin, calretinin and ChAT

Co-expression of ChAT, calbindin and calretinin in the same neurons of the PPN was examined using triple-immunofluorescent labelling and analysed under the confocal microscope. In each of the three animals, image stacks of the PPN were acquired (20 images of 1 μm per stack) and all the single-, double- and triple-immunopositive neurons were counted (see Methods Chapter 2.3.5 for further information).

In the three animals examined there were an average of 138.0 ± 24.8 calbindin-positive neurons (mean ± SEM); 105.0 ± 17 (76.1%) showed no other markers, none were immunoreactive for ChAT and 33.0 ± 11.1 (23.9%) were also calretinin-positive. For the same three animals, 132.7 ± 25.8 calretinin-positive neurons were observed; 92.7 ± 22.2 (69.8%) showed no other markers, 7.0 ± 1.7 (5.3%) were ChAT-positive, and 33.0 ± 11.1 (24.9%) were also immunoreactive for calbindin. This confirms what was seen with immunoperoxidase reactions, in that very few or no calbindin-positive neurons were ChAT-positive (immunoperoxidase 0.18%, immunofluorescence 0%). Likewise, a small proportion of calretinin-positive neurons were seen to express ChAT using this method (immunoperoxidase, 13%; immunofluorescence, 5.3%).

Notably, a large number of neurons co-expressed both calbindin and calretinin; 23.9% of calbindin-positive neurons were immunoreactive for calretinin, and 24.9% of calretinin-positive neurons were immunoreactive for calbindin (Figure 4.3; $n = 3$). These calbindin/calretinin-double positive neurons were observed throughout the length of the PPN, but due to the small scanning window of confocal images, neurons could not be split into segments for distribution analysis.

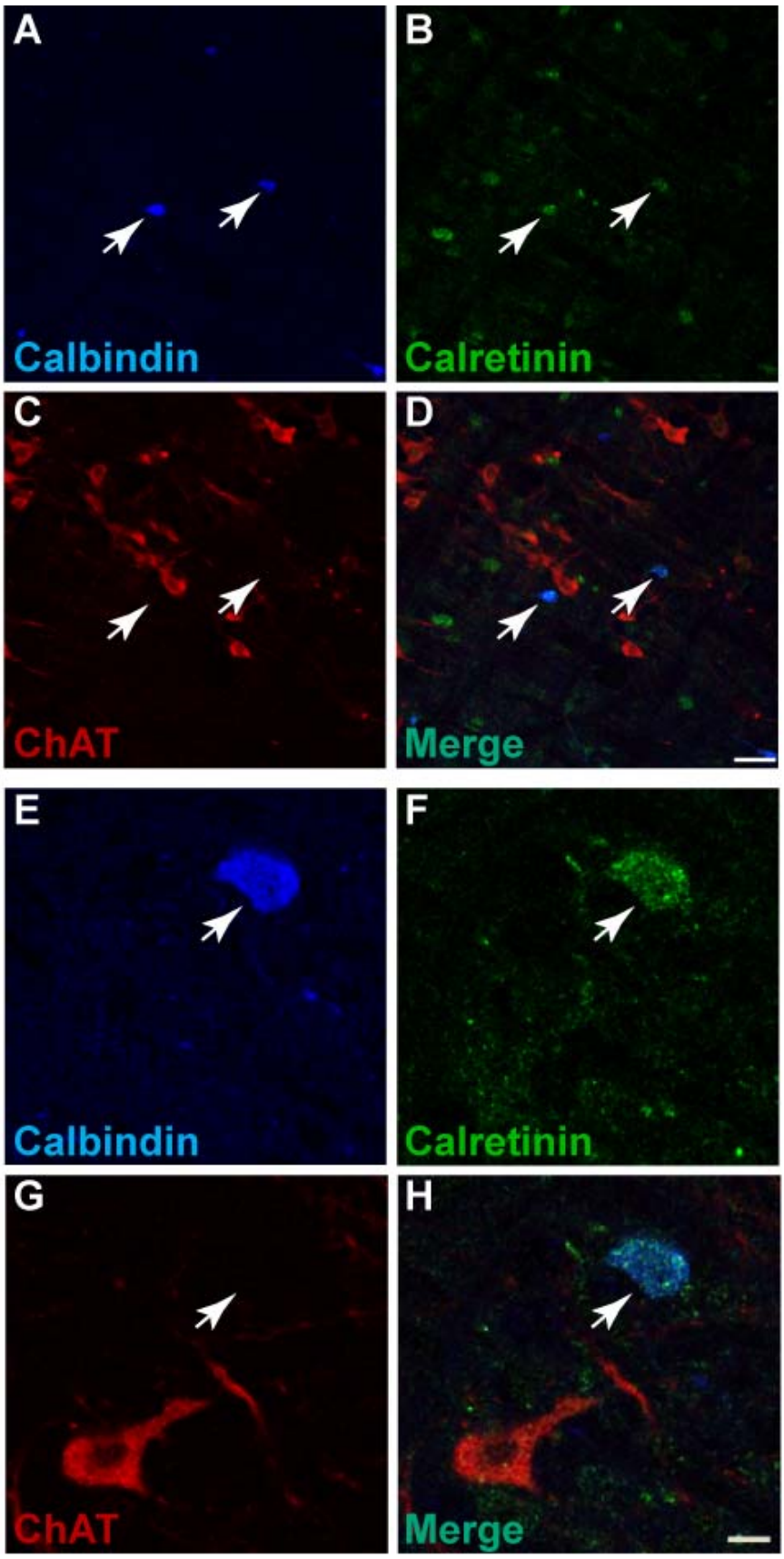


Figure 4.3. Calbindin and calretinin are co-expressed in the non-cholinergic neurons of the PPN

Confocal images showing triple immunofluorescent labelling for calbindin (blue), calretinin (green), and ChAT (red) in the PPN (D and H showing merged images of all three). Panels A-D show low magnification images displaying two neurons that are immunopositive for both calbindin and calretinin but not ChAT and panels E-H show high magnification images of one of these neurons. Scale bar for panels A-D: 50 µm; E-H: 10 µm.

4.3.4. GABAergic and glutamatergic neurons of the PPN

A small proportion of calbindin- and calretinin-positive neurons are cholinergic, which leaves a large number of these neurons that do not use acetylcholine as a neurotransmitter. So what neurotransmitter could these neurons be using? There are roughly 6,500 GABAergic neurons in the PPN, about 2,900 cholinergic neurons (Mena-Segovia *et al.*, 2009) and the number of glutamatergic neurons has been proposed to be of a similar magnitude to the GABAergic neurons (Wang & Morales, 2009). For this reason immunolabelling of calbindin or calretinin was combined with *in situ* hybridisation for either GAD65/67 or VGluT2 mRNA (GABAergic and glutamatergic markers respectively; see Methods Chapter 2.3.2 and 2.3.3; $n = 2$). The distributions of GABAergic and glutamatergic neurons in the PPN will be described, before their co-expression of either calbindin or calretinin, and distributions of these co-expressing neurons, is analysed.

Consistent with previous reports (Mena-Segovia *et al.*, 2009; Wang & Morales, 2009), neurons expressing GAD65/67 mRNA were observed in all segments along the rostro-caudal axis of the PPN and seemed to be more abundant in rostral regions (Figure 4.4 A). This was more noticeable once the areas of each segment were taken into account (density of neurons per mm^2; Figure 4.4 C).

Wang and Morales (2009) have shown that a large number of neurons containing VGluT2 mRNA are present in the PPN, but in contrast to the GABAergic neurons, these neurons were seen to be more abundant in the caudal PPN. By quantifying the number of glutamatergic neurons per segment of the PPN it was possible to confirm their observations (Figure 4.4 B). Furthermore, when densities of glutamatergic neurons were calculated for each segment, those segments towards the caudal PPN appeared to contain higher densities (Figure 4.4 D).

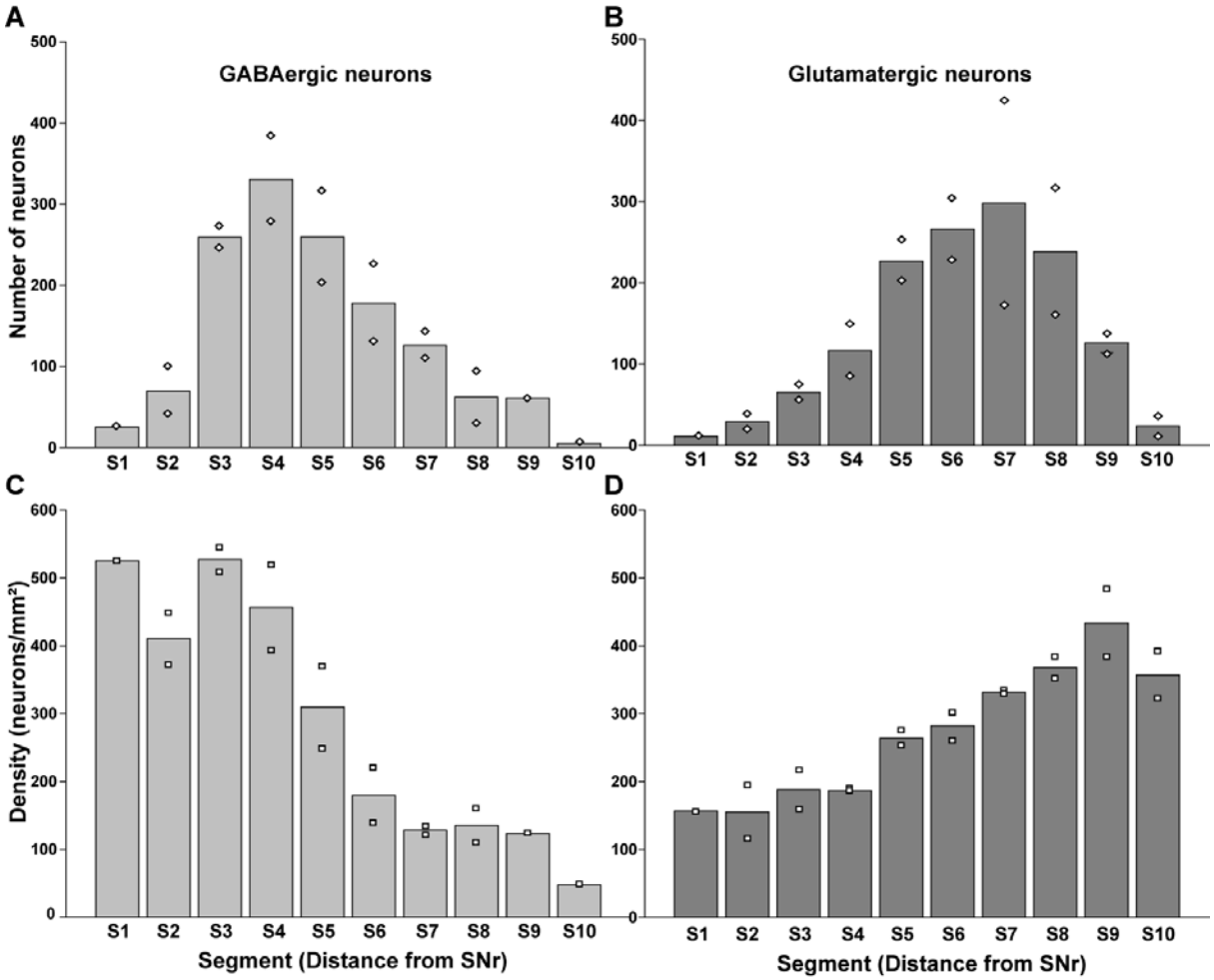


Figure 4.4. GABAergic neurons are more concentrated in the rostral PPN whereas glutamatergic neurons are more concentrated in the caudal PPN

Histograms of the distributions of GABAergic and glutamatergic neurons in the PPN. Total number of GABAergic (A) and glutamatergic (B) neurons per segment of the PPN. Densities of GABAergic (C) and glutamatergic (D) neurons (per mm^2) per segment of the PPN (bars represent mean values; symbols represent the individual values for each animal; $n = 2$).

4.3.5. Distribution of calbindin-positive neurons containing GAD65/67 or VGluT2 mRNA

In adjacent sections of the same three animals, calbindin-positive neurons (immunoperoxidase labelled) were quantified and examined for their co-expression of either GAD65/67 or VGluT2 mRNA (revealed by *in situ* hybridisation; see Methods Chapter 2.3.2 and 2.3.3). This quantification revealed that of all the calbindin-positive neurons (643.3 ± 122.1; mean ± SEM; *n*=3), there were 248.7 ± 56.6 that were also positive for GAD65/67, and thus GABAergic (38.7%; Figure 4.5 A, column 1). In adjacent sections, the proportion of calbindin-positive neurons (608.0 ± 129.4; mean ± SEM; *n*=3) that were also positive for VGluT2, and thus glutamatergic, was 66.9% (406.7 ± 81.6 calbindin/VGluT2-positive). No statistically significant differences were detected between the proportions of calbindin-positive neurons containing GAD65/67 mRNA and those containing VGluT2 mRNA (t-test; $t_{(4)} = -1.591$ $P = 0.187$; Figure 4.5 A, column 2).

Calbindin- and GAD65/67 mRNA-double positive neurons were identified (Figure 4.6 A) and counted for each segment of the PPN (Figure 4.6 C; *n*=3). A one way ANOVA revealed that the distribution of these neurons was not uniform ($F_{(9,17)} = 3.21$; $P = 0.018$), however, a pairwise multiple comparison was unable to identify differences between specific segments (Bonferroni; $P > 0.05$). To assess whether this non-uniform distribution was a product of the volume of each segment, the densities per segment were plotted (Figure 4.6 E). This demonstrated that when volume was taken into account the distribution of double-positive neurons across the segments was indeed non uniform (one way ANOVA; $F_{(9,17)} = 3.46$; $P = 0.013$). Additionally, the density of double-positive neurons was higher in segment S3 when compared to segments S6, S7, S9 and S10 (Tukey; $P < 0.05$).

Calbindin- and VGluT2 mRNA-double positive neurons were identified, as for the calbindin- and GAD65/67-double positive neurons above, and counted per segment of the PPN in order to analyse their distribution (Figure 4.6 B). This was found to be non-uniform across the PPN segments ($H_{(9)} = 20.02$; $P = 0.018$; ANOVA on ranks, Kruskal-Wallis was used because the data did not fit a normal distribution; Figure 4.6 D), however, no differences between specific segments were detected (Dunn; $P > 0.05$). Additionally, the density of calbindin- and VGluT2 mRNA-double positive neurons was found to be non-uniform (one way ANOVA; $F_{(9,18)} = 5.51$; $P = 0.001$; Figure 4.6 F). Moreover, the densities of these neurons were seen to be higher for segments S9 and S10 when individually compared to segments S1, S2, S3, S4, S5 and S6 (Tukey; $P < 0.05$).

4.3.6. Distribution of calretinin-positive neurons containing GAD65/67 or VGluT2 mRNA

Similar to the calbindin-positive neurons, calretinin-positive neurons were immunoperoxidase labelled, quantified and then examined for their co-expression of either GAD65/67 or VGluT2 mRNA (revealed by *in situ* hybridisation; see Methods Chapter 2.3.2 and 2.3.3). Of all the calretinin-positive neurons (857.3 ± 52.4; mean ± SEM; *n*=3), 238 ± 16.2 were also GAD65/67 mRNA-positive (27.8%; Figure 4.5 B, column 3). As for calbindin-positive neurons, the proportion of calretinin-positive neurons (869.3 ± 55.9; mean ± SEM; *n*=3) that were also VGluT2 mRNA-positive was much higher (73.8%; 641.3 ± 64.7 calretinin/VGluT2-positive; t-test; $t_{(4)} = -6.08$; $P = 0.004$; Figure 4.5 B, column 4).

The distribution of calretinin- and GAD65/67 mRNA-double positive neurons (Figure 4.7 A) was analysed per segment of the PPN and found to be non-uniform (one way ANOVA; $F_{(9,20)} = 12.91$; $P < 0.001$; Figure 4.7 C). These neurons were more

abundant in segment S3 than in segment S10 and more abundant in segment S4 than in either segment S1, S8 or S10 (Bonferroni; $P < 0.05$). Additionally, they were more abundant in segment S5 than in either segment S1, S8, S9 or S10 and more abundant in segment S6 or S7 than in either segment S1, S2, S8, S9 or S10 (Bonferroni; $P < 0.05$). The densities of these neurons were compared across PPN segments, but an ANOVA on ranks test indicated no differences between segments (Kruskal-Wallis; $H_{(9)} = 14.65$; $P = 0.101$; Figure 4.7 E).

Next, the numbers and distribution of calretinin- and VGluT2 mRNA-double positive neurons (Figure 4.7 B) were analysed per segment of the PPN (Figure 4.7 D), revealing a non-uniform distribution (one way ANOVA; $F_{(9,20)} = 28.31$; $P < 0.001$;). In particular, segments S5, S6 and S7 contained more neurons individually than either of segments S1, S2, S3, S8, S9 and S10, with segments S6 and S7 also containing more neurons than in segment S4 (Bonferroni; $P < 0.05$). Additionally, the densities of these neurons across PPN segments were found to be distributed in a non-uniform manner (one way ANOVA; $F_{(9,20)} = 3.85$; $P = 0.006$; Figure 4.7 F), with segment S10 displaying a higher density than segment S2 (Tukey; $P < 0.05$).

In summary, after observing that nearly all calbindin- and calretinin-positive neurons of the PPN are non-cholinergic, it was found that many contained markers for GABAergic and glutamatergic neurons. In both cases, calbindin- and calretinin-positive neurons showed a higher proportion of neurons containing the glutamatergic marker, VGluT2 (67% and 74% respectively), when compared to the proportions of neurons containing the GABAergic markers, GAD65/67 (39% and 28% respectively). These double-labelled neurons did not follow a uniform distribution along the rostro-caudal axis of the PPN, when either total number or density was examined. Interestingly, it was seen that many calbindin-positive neurons contained calretinin (24%) and vice versa (25%).

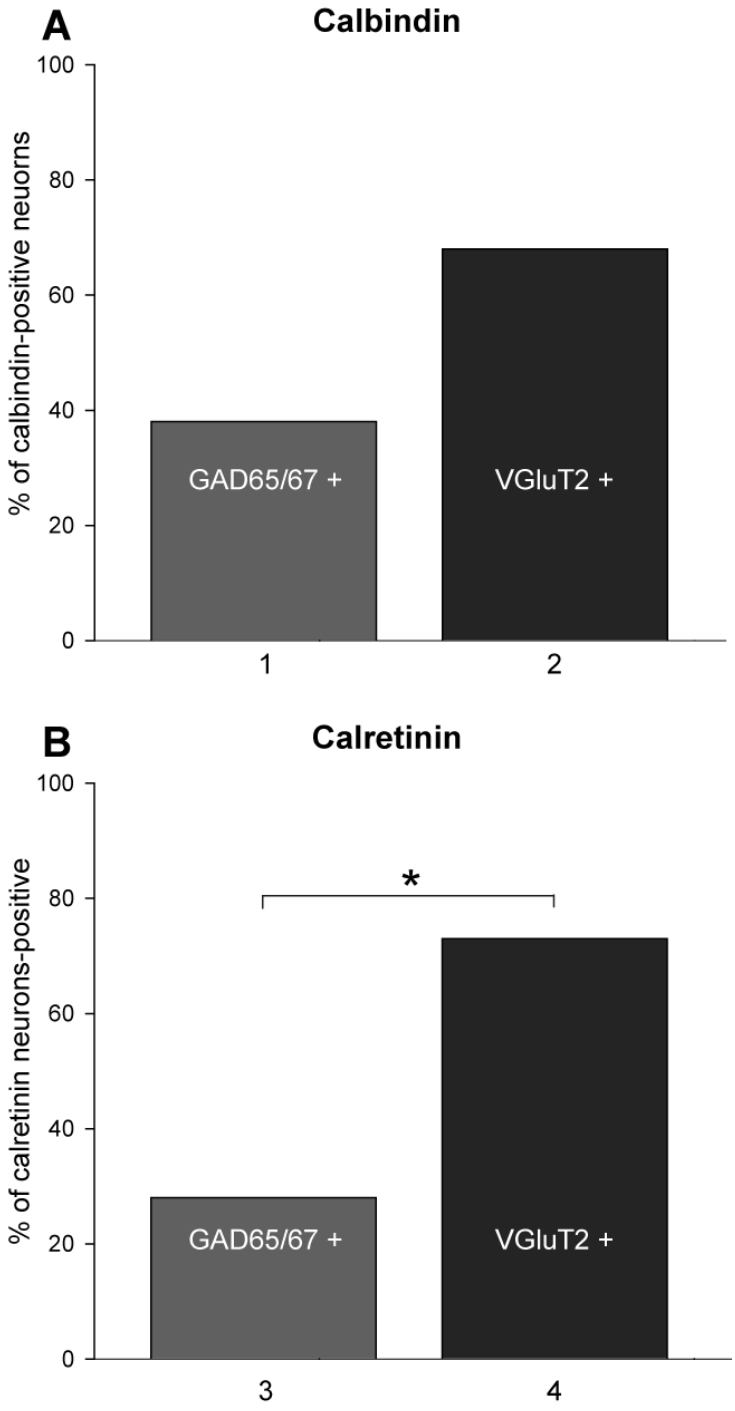


Figure 4.5. Calbindin- and calretinin-positive neurons in the PPN contain markers of GABAergic and glutamatergic neurons

Histograms showing the percentage of calbindin- (A) or calretinin-positive neurons (B) in the PPN, that expressed GAD65/67 mRNA (grey; columns 1 and 3) or VGluT2 mRNA (black; columns 2 and 4; * denotes a statistical significant difference between groups; P = 0.004; *n* = 3).

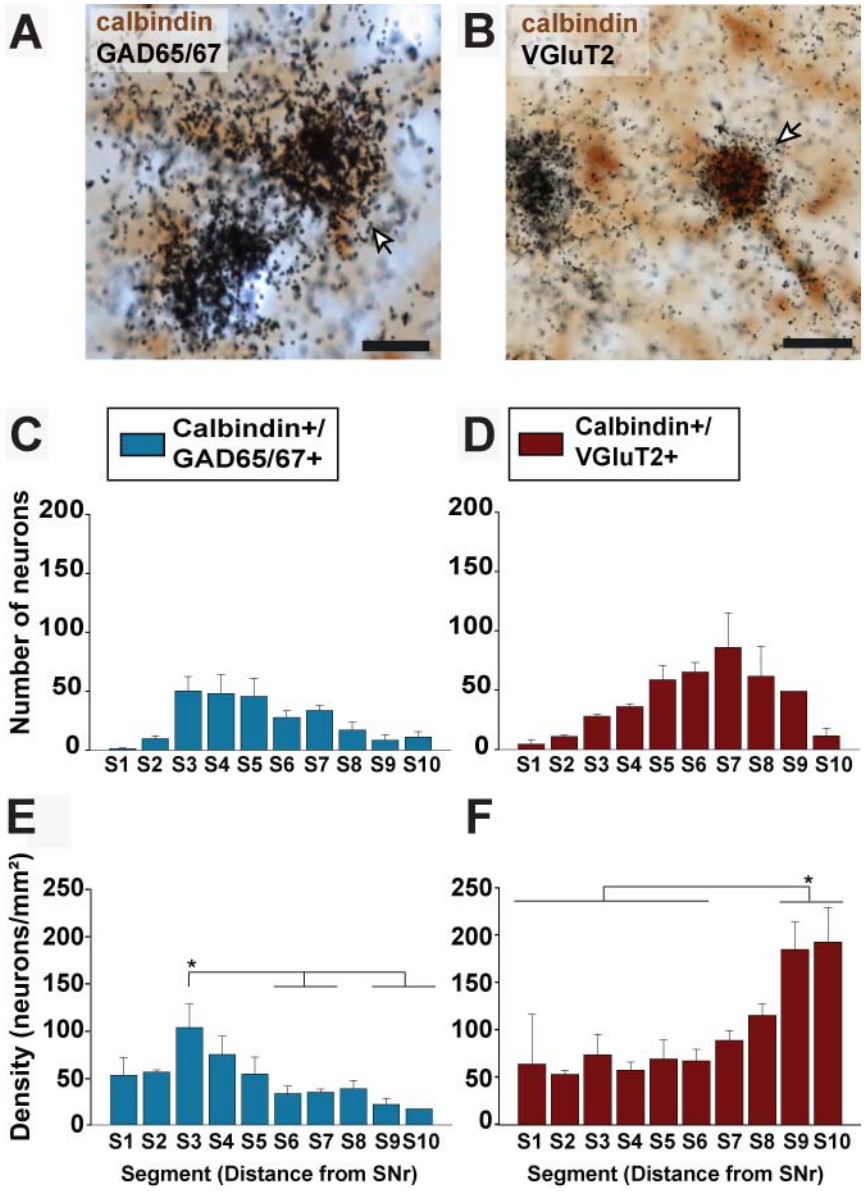


Figure 4.6. Calbindin-positive neurons in the PPN that contain GAD65/67 or VGluT2 mRNA are non-uniformly distributed along its rostro-caudal axis

A and B.- Light micrographs of PPN sections immunolabelled for calbindin (brown DAB precipitate) and labelled by *in situ* hybridisation to reveal GAD65/67 mRNA (A, dense accumulation of black-silver granules) or VGluT2 mRNA (B). The neurons indicated by arrows express both markers. Distribution of double-positive neurons (C, calbindin and GAD65/67 mRNA in blue; D, calbindin and VGluT2 mRNA in red), or cell density per mm^2 (E and F) are shown for each segment of the PPN along its rostro-caudal axis (*n* = 3; columns indicate mean values; error bars indicate SEM; * denotes a statistically significant difference between individual segments). Scale bar: 10 µm.

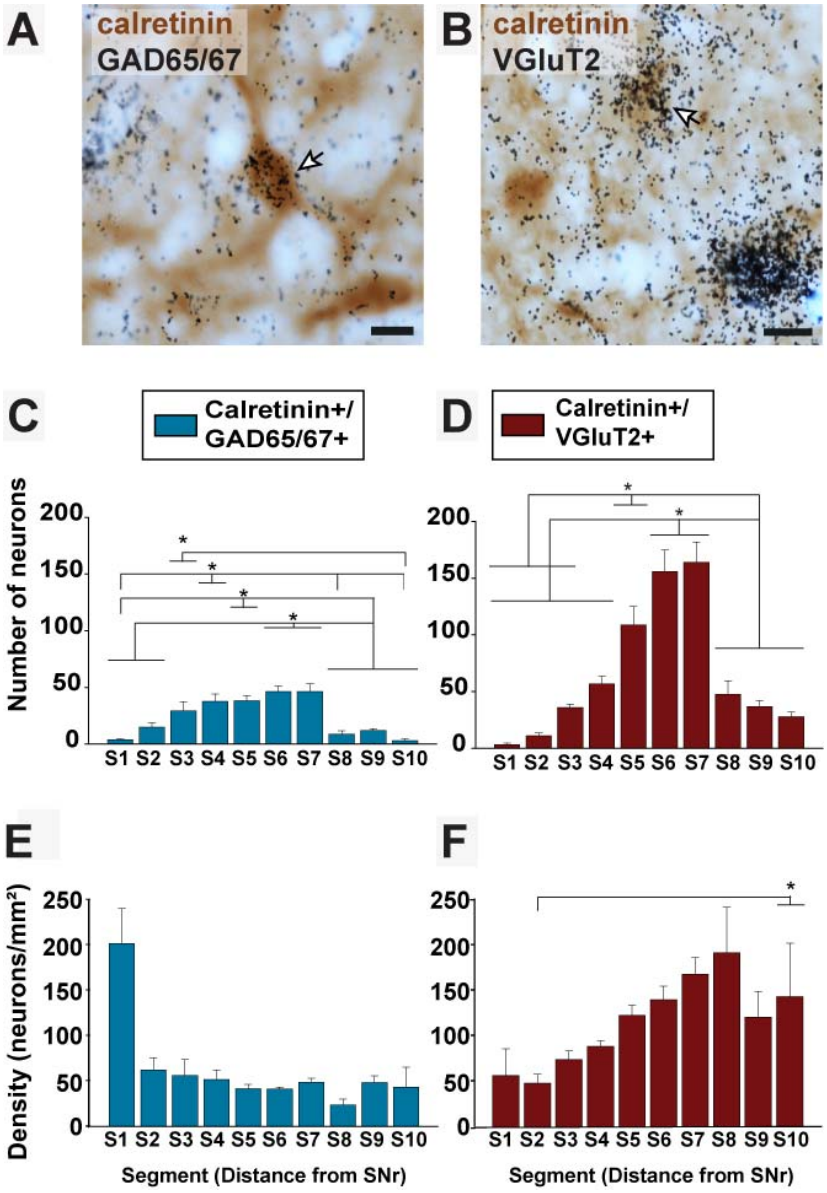


Figure 4.7. Calretinin-positive neurons in the PPN that contain GAD65/67 or VGluT2 mRNA are non-uniformly distributed along its rostro-caudal axis

A and B.- Light micrographs of PPN sections immunolabelled for calretinin (brown DAB precipitate) and labelled by *in situ* hybridisation to reveal GAD65/67 mRNA (A, dense accumulation of black-silver granules) or VGluT2 mRNA (B). The neurons indicated by arrows express both markers. Distribution of double-positive neurons (C, calretinin with GAD65/67 mRNA in blue; D, calretinin with VGluT2 mRNA in red), or cell density per mm^2 (E and F) are shown for each segment of the PPN along its rostro-caudal axis (*n* = 3; columns indicate mean values; error bars indicate SEM; * denotes a statistically significant difference between individual segments). Scale bar: 10 µm.

4.6. Discussion

The aim of this chapter was to characterise the neurotransmitters expressed by calbindin- and calretinin-positive neurons in the PPN. It was found that very few of these neurons contained the marker for cholinergic neurons (ChAT), whereas about a third of them contained mRNA for the GABAergic marker GAD65/67, and over two thirds contained mRNA for the glutamatergic marker VGluT2. Moreover, the distributions of these neurons along the rostro-caudal axis of the PPN were seen to be non-uniform. This opens the possibility that there may exist in the PPN subtypes of neurons with distinct electrophysiological properties and connectivity due to their co-expression of certain calcium-binding proteins and neurotransmitters.

4.6.1. Few calbindin- and calretinin-positive neurons in the PPN are cholinergic

Stereological analysis of sections that were double-immunolabelled for calbindin and ChAT indicated that less than 1% of the calbindin-positive neurons in the PPN were cholinergic, and subsequent immunofluorescent labelling showed that no neurons positive for calbindin were also positive for ChAT. This indicates that calbindin and ChAT rarely co-localise within the same neuron of the rat PPN, a phenomenon also seen in the PPN of primates (Cote & Parent, 1992). Slightly more calretinin-positive neurons were ChAT-positive, with 13% seen to be ChAT-positive in double-immunolabelling experiments and 5% seen when immunofluorescent labelling was used. These results are in agreement with reports concerning the primate PPN, where a similar proportion of calretinin- positive neurons were seen to express ChAT (8%; Fortin & Parent, 1999). Although these represent a small proportion of neurons, it could be the case that ChAT-positive calretinin neurons possess specific electrophysiological properties vital to the physiological functions of the PPN.

4.6.2. Calbindin- and calretinin-positive neurons of the PPN express GABAergic or glutamatergic markers

The calbindin- and calretinin-positive neurons represented only a minority of the cholinergic neurons in the PPN, leaving the possibility that they might use another neurotransmitter. GABAergic and glutamatergic neurons of the PPN are more abundant than cholinergic neurons (Mena-Segovia *et al.,* 2009; Wang & Morales, 2009). When analysed, about a third of the calbindin- and calretinin-positive neurons were GABAergic (39% and 28% respectively), and about two thirds glutamatergic (67% and 74% respectively). Because these quantifications were performed on adjacent sets of brainstem sections labelled for GAD65/67 mRNA or VGluT2 mRNA, double-labelling of these markers could not be assessed.

Additionally, the possibility of triple-positive, calbindin or calretinin neurons containing both GAD65/67 and VGluT2 mRNA cannot be excluded using this method. However, previous studies have shown that GABAergic and glutamatergic markers rarely co-localise in the same PPN neurons (< 1%; Wang & Morales, 2009). It is very possible that calbindin and calretinin could exist in the same neuron, alongside GAD65/67 and/or VGluT2 mRNA. Immunofluorescent labelling showed that 24% of calbindin-positive neurons also contained calretinin and 25% of calretinin-positive neurons contained calbindin; none of these double labelled neurons were cholinergic.

4.6.3. Calbindin- and calretinin-positive neurons of the rostral and caudal PPN

This study has shown that calbindin-positive neurons and calretinin-positive neurons in the PPN can both express either GABAergic or glutamatergic phenotypes. These four types of PPN neuron appear to be concentrated in either the rostral or caudal

PPN, depending upon their expression of either GAD65/67 mRNA (rostral) or VGluT2 mRNA (caudal), respectively. The significance of these distributions is that neurons of the rostral and caudal PPN innervate, and are innervated by, different regions of the brain (see Introduction Chapter, 1.5 and 1.6). For instance, the rostral PPN has been shown to innervate the EP/GPi, SNr and SNc (Charara & Parent, 1994; Lavoie & Parent, 1994b; Oakman *et al.*, 1995; Takakusaki *et al.*, 1996), whereas the caudal PPN innervates the STN, VTA, SC, thalamus, brainstem and spinal cord (Carpenter *et al.*, 1981; Sugimoto & Hattori, 1984; Mitani *et al.*, 1988; Rye *et al.*, 1988; Smith *et al.*, 1988; Steriade *et al.*, 1988; Spann & Grofova, 1989; Skinner *et al.*, 1990a; Skinner *et al.*, 1990b; Oakman *et al.*, 1995; Mena-Segovia *et al.*, 2008a; Motts & Schofield, 2009; Kita & Kita, 2010). Afferents to the rostral PPN include projections from the EP/GPi and SNr (Spann & Grofova, 1991; Shink *et al.*, 1997; Grofova & Zhou, 1998), whereas neurons of the caudal PPN are contacted by projections from the DR and the frontal lobe of the cortex (Steininger *et al.*, 1997; Matsumura *et al.*, 2000).

Such differences in the efferent and afferent connectivity of the PPN, between rostral and caudal regions, highlight the importance of understanding the additional phenotypes of neurons in these regions, as neurons containing calbindin or calretinin can possess differential electrophysiological properties (Schwaller *et al.*, 2002). In Chapter 5, the projections of these calbindin- and calretinin-positive neurons will be examined further, alongside a more thorough description of the connectivity and activation of PPN neurons in physiological and pathophysiological conditions.

5. Connectivity of the PPN with the subthalamic and gigantocellular nuclei

5.1. Introduction

The ascending projections of PPN neurons to the subthalamic nucleus (STN) and their descending projections to the gigantocellular nucleus (GiN) are vital for motor control. The ascending projections to the STN are particularly relevant as deep brain stimulation (DBS), of both the STN and PPN, has been shown to attenuate motor symptoms of Parkinson's disease (Lozano, 2001; Benabid, 2003; Jenkinson *et al.*, 2005; Stefani *et al.*, 2007). The descending projections to the GiN target neurons that in turn target the spinal cord (Garcia-Rill & Skinner, 1987b). These projections to the GiN are important because they represent the first connection in the pathway between the PPN and the spinal cord, which is important for locomotor activity (Garcia-Rill, 1986; Garcia-Rill *et al.*, 1987; Reese *et al.*, 1995; Garcia-Rill *et al.*, 2001). Retrograde tracer injections in the STN and GiN will be used to quantify the proportions of PPN neurons projecting to either nucleus, or both nuclei, and immunofluorescent labelling will be used to determine the proportion of these that are calbindin-, calretinin- or ChAT-positive.

The importance of the connection between the PPN and STN is starkly evident in animal models of Parkinson's disease (6-OHDA lesioned rats or MPTP-treated monkeys). There is evidence that the PPN may be over-inhibited in Parkinson's disease patients and in MPTP-treated monkeys (Mitchell *et al.,* 1989; Jenkinson *et al.*, 2004; Kringelbach *et al.*, 2007; Nandi *et al.*, 2008), however, in 6-OHDA lesioned rats, the effects on the PPN are still debated (Aravamuthan *et al.*, 2008; Jenkinson *et al.*, 2009). Some studies suggest that the activity of the PPN is increased in this model (Carlson *et al.*, 1999; Breit *et al.*, 2001), and this hyperactivity can be reversed by a lesion in the STN (Breit *et al.*, 2005). Furthermore, lesions of the PPN can reverse the hyperactivity of STN neurons, which is also seen in this model (Breit *et al.*, 2006). To assess the changes in neuronal activity seen in the PPN of lesioned animals, and how this might relate to their projections, the

expression of the immediate early gene Egr1 (marker of neuronal activation; see summary of methods that follows) will be evaluated in PPN neurons projecting to the STN, GiN or both nuclei.

5.2. Summary of methods

5.2.1. Neurochemical phenotypes of STN- and GiN-projecting PPN neurons

Fluorescently-labelled retrograde tracers were injected in the STN and GiN of Sprague-Dawley rats (n = 6). The animals were anaesthetised with isofluorane and, under stereotaxic control, Cy3- and Alexa488-retrobeads (red and green, respectively; Lumafluor) were injected in the STN and GiN, respectively (Methods Chapter 2.4.1). After two to three weeks of recovery, the animals were deeply anaesthetised with a ketamine/xylazine mixture and transcardially perfuse-fixed. Brains were removed and cut in 50 μm thick sagittal sections and those containing the PPN were collected in six series, before being stored in sodium azide (0.05% in PBS) until used (Methods Chapter 2.4.2).

Sections, lateral and medial to the PPN, containing the STN and the GiN respectively, were collected to verify the injection sites (Figure 5.1; despite accurate injections, some projection neurons will be unlabelled; see technical considerations, section 6.2.2). Animals with tracer injections largely restricted to the STN (Figure 5.1 A and B), and GiN (Figure 5.1 E) were used for this part of the study (n = 3). In two animals (J403 and J404), the retrobeads injected in the STN spread into the adjoining zona incerta (ZI; Figure 5.1 C). However, it has been reported that injections solely in the ZI result in the labelling of just a small number of neurons in the LDTg and PPN, most of which are cholinergic (Kita & Kita, 2010). Injections successfully placed in the STN also resulted in retrograde labelling of LDTg neurons (Figure 5.1 F).

One series of sections, from brains of rats injected with retrograde tracers, was also immunofluorescently labelled to reveal one of the following combinations: calbindin (Cy5) and ChAT (AMCA) or calretinin (Cy5) and ChAT (AMCA; see Table5.1). Control reactions were performed by omitting each of the primary antibodies in turn, which resulted in the complete absence of fluorescence for the omitted antibody (Methods Chapter 2.4.3). To quantify the number of retrogradely-labelled neurons in the PPN, and those that were immunopositive for calbindin, calretinin or ChAT, multichannel Z-stack images were acquired under the fluorescence microscope, using an Axiocam HRm digital camera in combination with the Axiovision 4.8.1 acquisition system (Zeiss). Concentric circles that defined segments S1 to S10 in the PPN were drawn on to the multichannel Z-stack images using Photoshop (Adobe) and these were then analysed using Image J software (Methods Chapter 2.4.4).

	Primary antibody	Species of origin	Dilution	Manufacturer	Fluorophore	Secondary antibody	Dilution	Manufacturer
1	Calbindin	mouse	1:5000	Swant	Cy5	donkey anti mouse	1:250	Jackson
	ChAT	goat	1:500	Chemicon	AMCA	donkey anti goat	1:100	Jackson
2	Calretinin	rabbit	1:5000	Swant	Cy5	donkey anti rabbit	1:250	Jackson
	ChAT	goat	1:500	Chemicon	AMCA	donkey anti goat	1: 100	Jackson

Table 5.1. Combinations of primary and secondary antibodies used for double-immunolabelling sections to reveal calbindin and ChAT (1) or calretinin and ChAT (2).

5.2.2. Activation of PPN projection neurons in control and lesioned rats

Unilateral 6-OHDA lesions were carried out in 30 Sprague-Dawley rats. Under isofluorane anaesthesia, animals were placed into a stereotaxic frame to perform an injection of 6-OHDA into the medial forebrain bundle fibres (see Methods Chapter 2.4.5 for exact coordinates). Twenty minutes prior to injection, animals were pre-treated with

desipramine to minimise 6-OHDA uptake by noradrenergic neurons (Schwarting & Huston, 1996b). The extent of the lesion was assessed two weeks after the surgery by challenging with apomorphine. A lesion was considered successful in animals that made 80 or more contraversive rotations in 20 min in response to apomorphine injection (Hudson et al., 1993; Methods Chapter 2.4.6; Table 5.2).

Animal ID	Rotations (first test)	Rotations (second test)	Result
C301	196		lesion
C302	48	137	lesion
C303	147		lesion
C304	<40	<40	none
C305	<40	44	partial
C306	<40	42	partial
C307	<40	155	lesion
C308	<40	<40	none
C309	46		partial
C310	107		lesion
C311	92		lesion
C312	176		lesion
C313	<40	<40	none
C314	<40	123	lesion
C315	<40	<40	none

Animal ID	Rotations (first test)	Rotations (second test)	Result
C316	<40	177	lesion
C317	<40	<40	none
C317 '	<40		none
C318	84		lesion
C319	86		lesion
C320	81		lesion
C321	115		lesion
C322	100		lesion
C323	172		lesion
C324	<40		none
C325	81		lesion
C326	<40	<40	none
J333	132		lesion
J334	120		lesion
J335	176		lesion

Table 5.2. Number of contraversive rotations observed over 20 min in response to subcutaneous injections of apomorphine for 30 rats. Those not demonstrating a full lesion when first tested (<80 rotations) were tested again before the extent of the lesion was stated. The prefix J for animal IDs indicate those animals for which the 6-OHDA lesion was carried out by Dr. Juan Mena-Segovia.

After confirming the extent of the lesion, the subthalamic nucleus (STN) and gigantocellular nucleus (GiN) of 16 lesioned rats and 6 control rats were injected with fluorescently labelled retrobeads, as before (see Methods Chapter 2.4.7). Two to three weeks after the tracer injections, the animals were deeply anaesthetised and perfuse-fixed (4% PFA). This was carried out between 6 and 8 pm, in order to minimise the variation in immediate early gene expression that can occur at different points of the sleep-wake cycle

(Mena-Segovia *et al.*, 2004b). Brainstem sections containing the PPN were collected in six series and stored in sodium azide (0.05% in PBS) until used. As before, sections lateral and medial to the PPN (containing the STN and the GiN, respectively) were collected to verify the injection sites. Sections containing the STN were immunolabelled to reveal FoxP2 in order to clearly visualise the STN (see Methods Chapter 2.4.7). Only the animals with the tracer injections largely restricted to the STN and the GiN were used in the study (Figure 5.1 D; 3 control and 3 lesioned animals). Two series of sections were also immunofluorescently labelled to reveal ChAT (AMCA) and the immediate early gene Egr1 (Cy5). Again, control reactions revealed a complete absence of fluorescence when each antibody was omitted individually (Methods Chapter 2.4.8).

Neuronal activity can induce the expression of specific genes, known as immediate early genes; one of the first identified and most studied is the transcription factor Egr1 (Sukhatme *et al.*, 1988; Tsai-Morris *et al.*, 1988). The expression of these genes is strongly linked to synaptic stimulation, but can also be induced by internal transduction pathways, meaning that their expression is not always an absolute marker of neuronal activation (see technical considerations, section 6.2.3). However, they are an important tool and have been widely used to identify and map active neurons (Hughes & Dragunow, 1995; Chaudhuri, 1997; Chaudhuri *et al.*, 1997; Herdegen & Leah, 1998; Chaudhuri *et al.*, 2000; Greer & Greenberg, 2008).

Because Egr1 is a nuclear transcription factor, neurons with labelling in their nucleus, but not in their cytoplasm, were regarded as immunopositive. The numbers and proportions of neurons immunopositive for Egr1 were quantified in control and lesioned animals for neurons projecting to the STN, GiN or both nuclei, using Stereo Investigator software (see Methods Chapter 2.4.8).

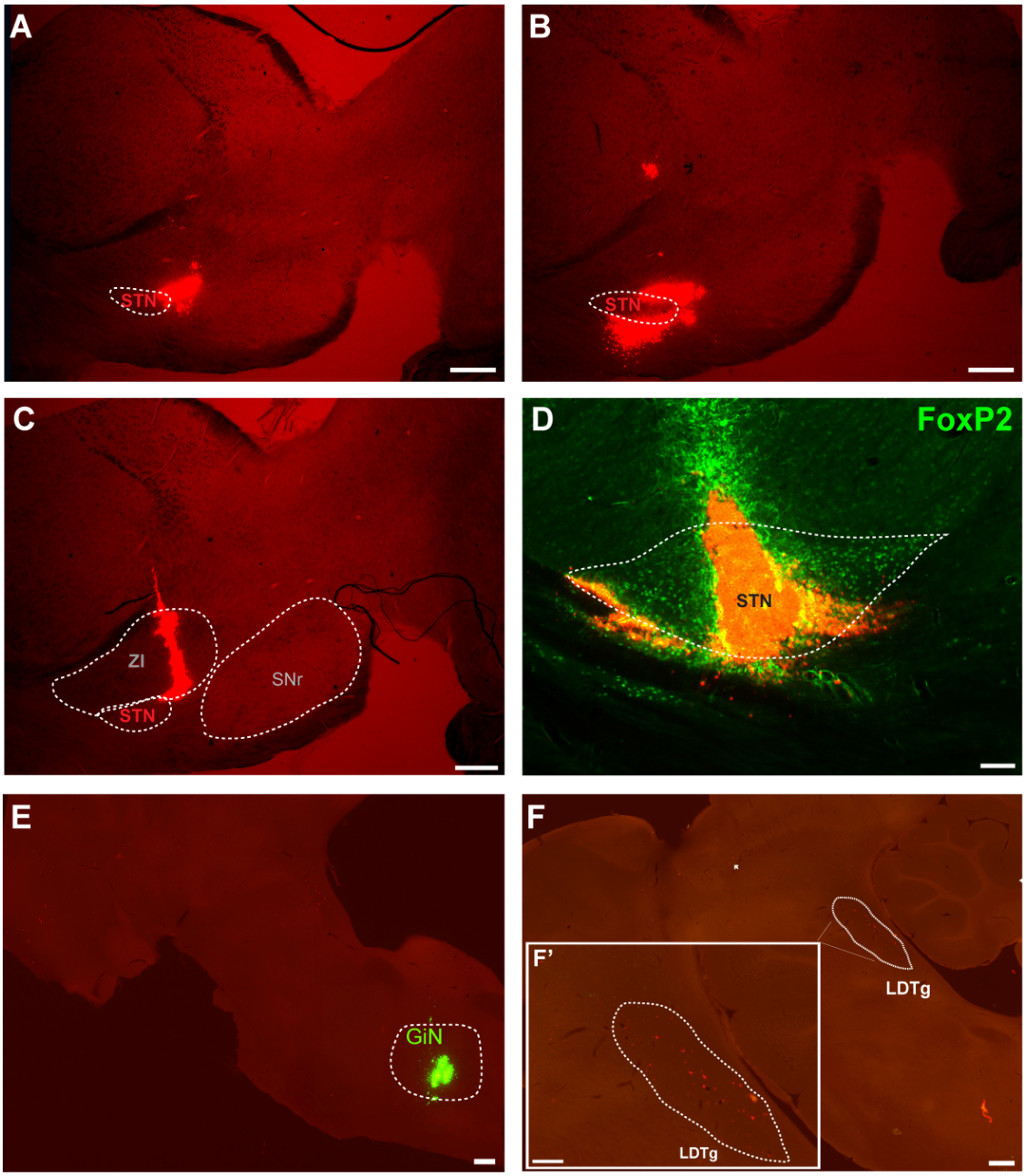


Figure 5.1. Fluorescently labelled retrobead injections in the STN and GiN

A and B.- Images of two medio-lateral levels of the STN (dotted line) where Cy3-retrobeads (red) were injected. C.- Cy3-retrobeads (red) that were injected into the caudal STN (seen in adjacent sections) are shown spreading into the zona incerta (ZI) but not the SNr. D.- High magnification image of a section containing the STN (dotted line) with Cy3-retrobead labelling in red, showing the injection site, and Alexa488 labelled FoxP2 in green showing the borders of the STN. E.- Injection of Alexa488-retrobeads (green) in the GiN (dotted line) of the same animal as panels A and B. F, F'.- Low and high magnification images of neurons in the LDTg (dotted line) retrogradely labelled from the STN (Cy3-retrobeads in red). Scale bars for A, B, C, E and F: 500 µm, D: 100 µm, F': 250 µm.

5.3. Results

5.3.1. The STN and GiN are targets of PPN projection neurons

To analyse the extent to which the PPN innervates the STN and GiN, fluorescently-labelled retrobeads were injected into both structures; Cy3 into the STN and Alexa488 into the GiN. Neurons of the PPN, retrogradely-labelled from the STN or GiN, displayed the typical granular fluorescence pattern of retrobead labelling, which is present in the cytoplasm and primary dendrites of the cell but not the nucleus (Figure 5.2 A, B and C). Neurons contained either red (Figure 5.2 A) or green (Figure 5.2 B) retrobeads and were clearly distinguishable from each other as well as from neurons containing both tracers (Figure 5.2 C).

Quantification of these labelled neurons in two series of sections revealed that 321 ± 30 PPN neurons projected to the STN, 200 ± 40 projected to the GiN and 27 ± 4 projected to both nuclei (mean ± SEM; $n = 6$). Significant differences were found between the numbers of neurons singly-projecting to either the STN or GiN; additionally, when each of these were compared to the numbers of double-projecting neurons they were found to be significantly more abundant (one way ANOVA; $F_{(2,15)} = 26.18$; $P < 0.001$).

Retrogradely labelled neurons projecting to either the STN, GiN or both nuclei were quantified for segments S1-S10 of the PPN and analysed for their distribution along the rostro-caudal axis (see Methods Chapter 2.4.4). Neurons projecting to the STN and GiN showed a non-uniform distribution (ANOVA on ranks, Kruskal-Wallis; STN, $H_{(9)} = 41.98$; GiN, $H_{(9)} = 33.25$; $P < 0.001$). Subsequent pairwise multiple comparisons indicated that STN-projecting neurons were more abundant in segments S5, S6, S7 and S8 individually than in S1, and more abundant in segment S7 than in segment S2 and segment

S10. Additionally, GiN-projecting neurons were more abundant in segments S5, S6, S7 and S8 individually than in segment S1 (Dunn's test; $P < 0.05$; Figure 5.2 D and E).

PPN neurons projecting to both nuclei were found to be non-uniformly distributed along the rostro-caudal axis of the PPN (ANOVA on ranks; Kruskal-Wallis; $H_{(9)} = 25.99$; $P < 0.002$); however, no differences were found between specific PPN segments (Dunn's test; $P > 0.05$; Figure 5.2 F).

5.3.2. Cholinergic PPN neurons project to the STN and GiN

Neurons of the PPN projecting to either the STN, GiN or both nuclei were further characterised to determine the numbers and distributions of those that were cholinergic (Figure 5.3, 5.4 A). The quantification in two series of sections revealed that a similar number of cholinergic neurons projected to the STN (38 ± 2) and the GiN (45 ± 12; student's t-test, $t_{(4)} = -0.584$, $P = 0.590$), and very few sent projections to both nuclei (7 ± 1; mean ± SEM; *n*=3; less than STN-projecting neurons, $t_{(4)} = 16.440$, $P < 0.001$; similar to GiN-projecting neurons, $t_{(4)} = 3.201$, $P = 0.033$). The cholinergic neurons accounted for 12 ± 1 % of the PPN neurons projecting to the STN; a higher proportion projected to the GiN (19 ± 1 %; student's t-test, $t_{(4)} = -5.026$, $P = 0.007$), whereas a similar proportion to each of these projected to both nuclei (26 ± 7 %; Rank sum test; STN, Mann-Whitney $U = 1$, $P = 0.2$; GiN, Mann-Whitney $U = 3$, $P = 0.7$).

The distributions of the cholinergic PPN neurons projecting to either the STN (Figure 5.4 B), GiN (Figure 5.4 C) or to both nuclei (Figure 5.4 D) were non-uniform (STN, ANOVA on ranks, Kruskal-Wallis, $H_{(9)} = 22.745$, $P = 0.007$; GiN and both nuclei, one way ANOVA, $F_{(8,18)} = 3.29$, $P = 0.017$, and $F_{(8,18)} = 6.11$, $P < 0.001$, respectively). No differences in neuronal number were found between specific segments of the PPN (Dunn's method; $P > 0.05$).

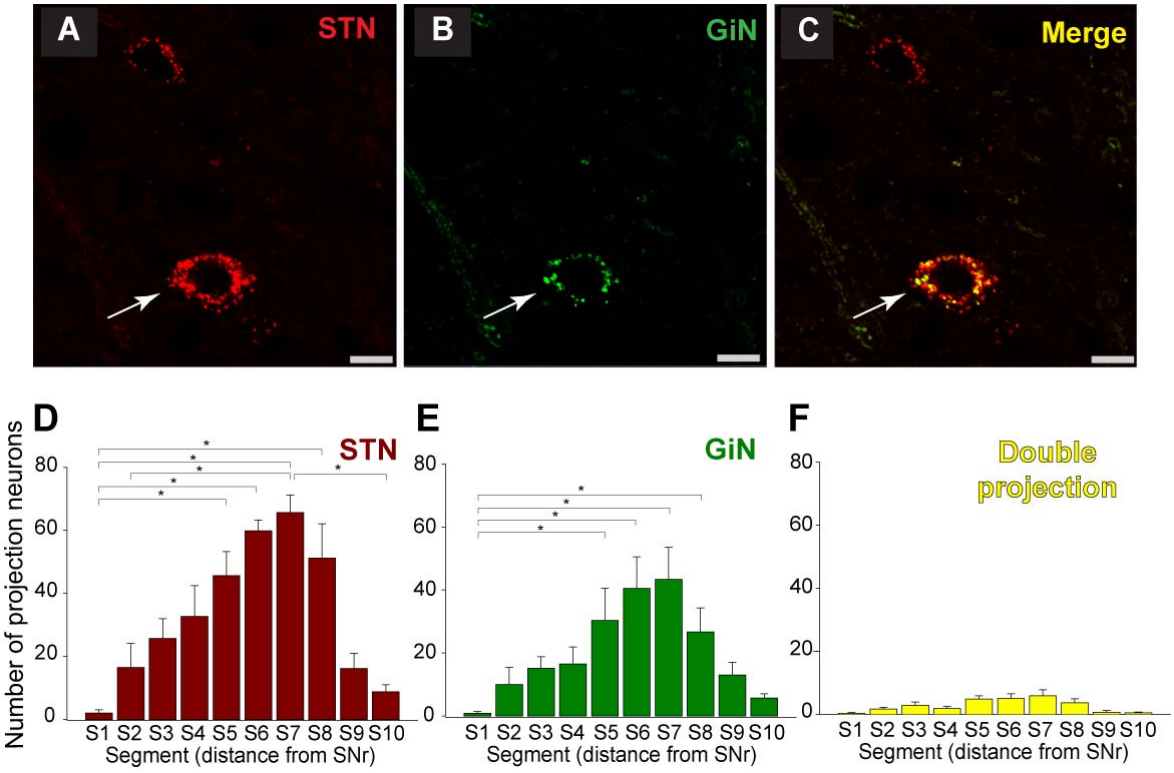


Figure 5.2. Distribution of PPN neurons projecting to the STN, GiN or both nuclei

Fluorescent images of a PPN neuron retrogradely labelled from both the STN (A) and GiN (B; merged image, C). Histograms showing the number of neurons per PPN segment that project to the STN (D), GiN (E), or both nuclei (F; n = 6; columns represent means; error bars indicate SEM; * denotes a significant difference between segments). Scale bars in panel A: 10 µm.

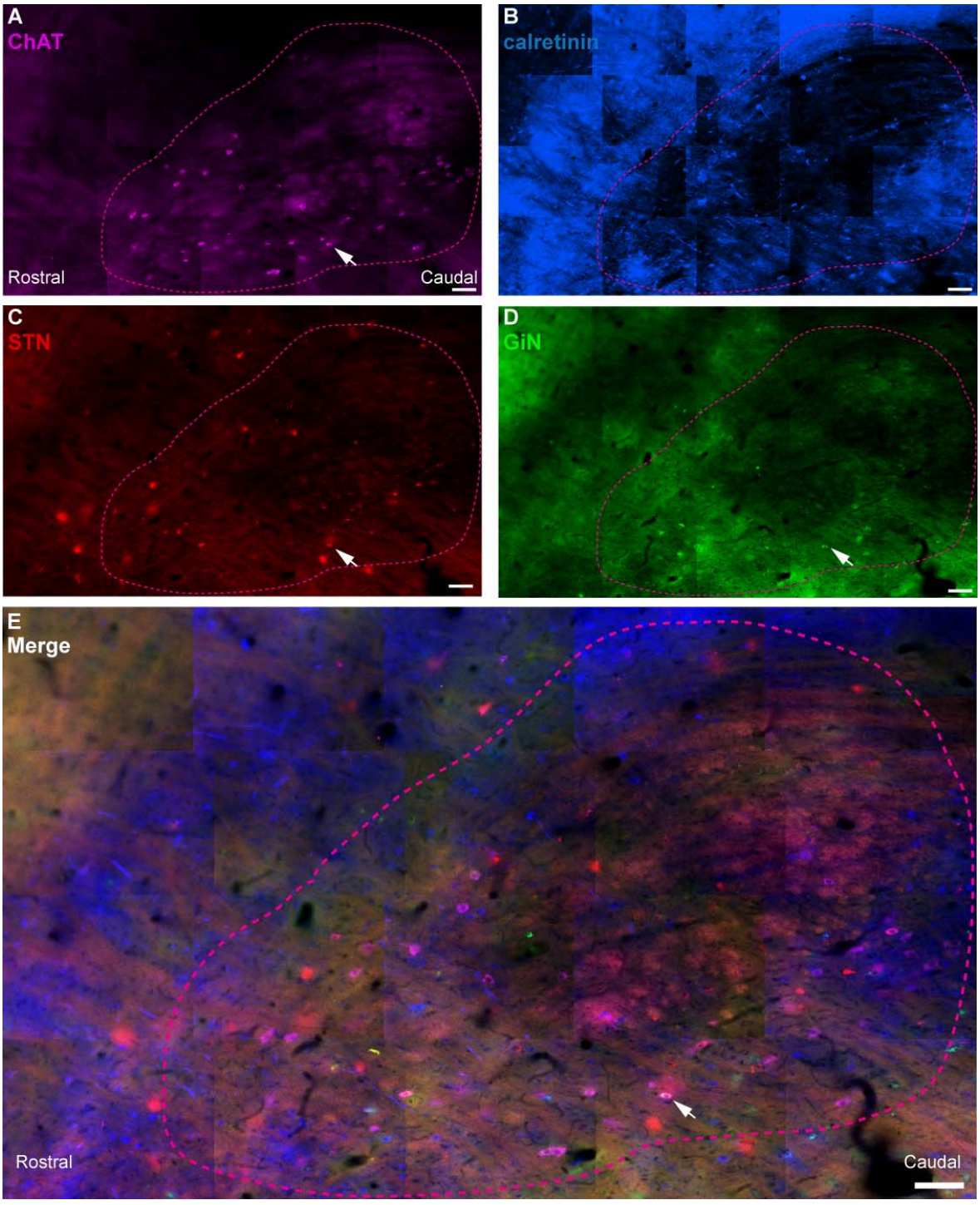


Figure 5.3. ChAT and calretinin labelling in STN- and GiN-projecting neurons of the PPN

Montage of fluorescent images showing ChAT (A; magenta) and calretinin (B; blue) immunolabelling in the PPN (dotted lines, as determined by cholinergic neurons), together with STN- and GiN-projecting neurons (C and D, red and green retrobeads, respectively). E.- Merged image of panels A-D. White arrows show a cholinergic neuron projecting to both the STN and GiN. Scale bars: 100 µm.

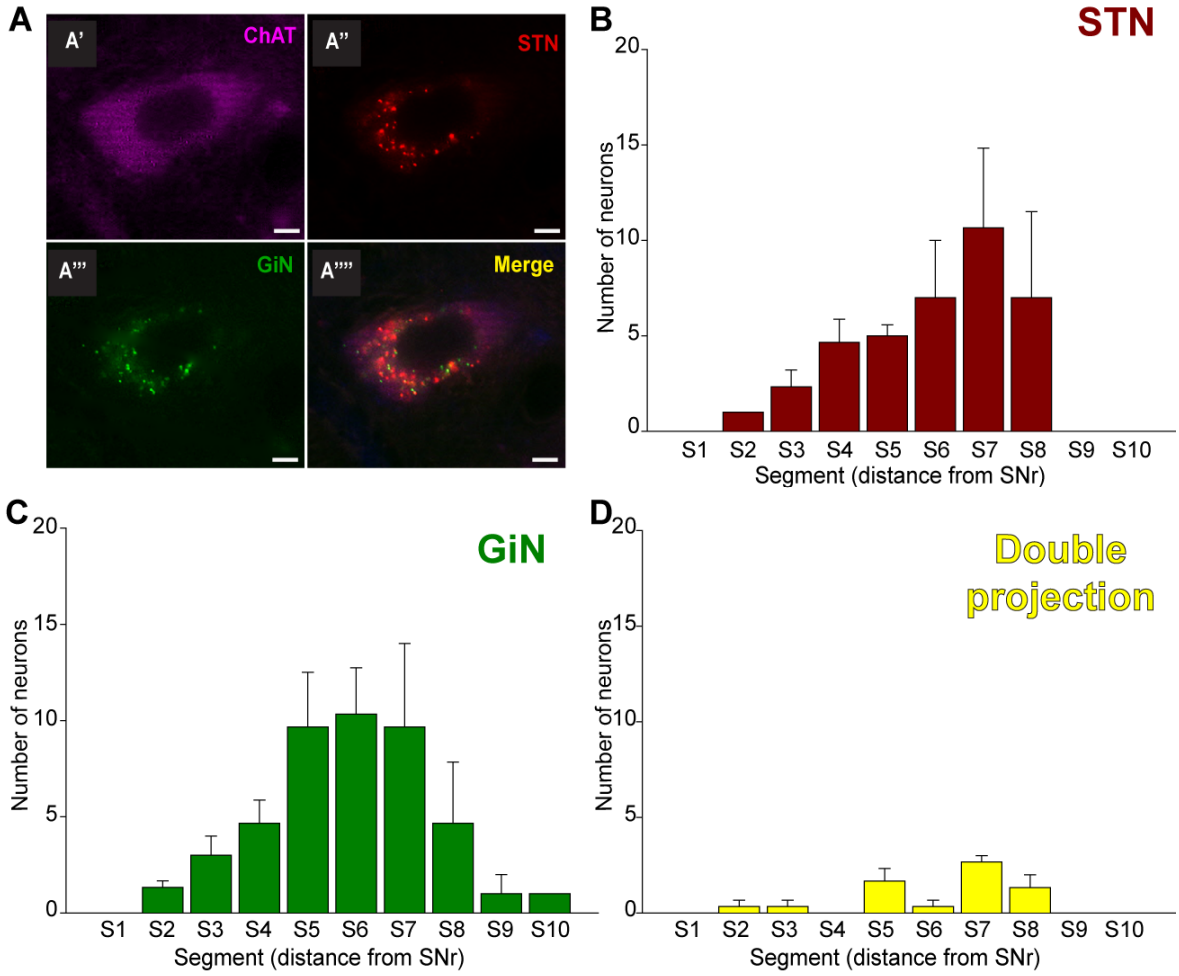


Figure 5.4. Distribution of cholinergic PPN neurons projecting to the STN, GiN or both nuclei

A.- Fluorescent image of a cholinergic PPN neuron (ChAT-positive, A') retrogradely labelled from both the STN (A'') and GiN (A'''; merged image in A''''). Histograms above show the number of cholinergic neurons per PPN segment that project to the STN (B), GiN (C), or both nuclei (D; *n* = 3; columns represent means; error bars indicate SEM). Scale bar: 10 µm.

5.3.3. Projections of calbindin- and calretinin-positive neurons of the PPN

The STN- and GiN-projecting neurons of the PPN were also analysed to assess whether they expressed calbindin or calretinin. The quantification of one series of sections revealed that STN-projecting neurons containing calbindin or calretinin numbered 8 ± 1 and 13 ± 3 respectively (mean ± SEM; n = 3). No GiN-projecting neurons contained calbindin, but 9 ± 5 contained calretinin; interestingly, no neurons projecting to both nuclei were observed to contain calbindin or calretinin. A similar number of calretinin-positive neurons projected to either the STN or GiN (student's t-test; $t_{(4)} = 0.81$; $P = 0.465$).

When expressed as a proportion of the neurons projecting to the STN, calbindin neurons accounted for 5 ± 0.5 % of the total and calretinin neurons accounted for 7 ± 1 %. In comparison, cholinergic neurons accounted for 12 ± 1 % of the STN-projecting neurons, similar to calretinin-positive neurons ($t_{(4)} = 2.21$, $P = 0.092$), but significantly higher than calbindin-positive neurons ($t_{(4)} = 3.26$, $P = 0.031$). Although no calbindin neurons were found to project to the GiN, calretinin neurons made up 7 ± 2 % of PPN neurons projecting to GiN; cholinergic neurons accounted for a greater proportion of this projection (19 ± 1 %, $t_{(4)} = 3.59$, $P = 0.023$). Calbindin- and calretinin-positive neurons did not project to both nuclei, but cholinergic neurons made up 26 ± 7 % of the projection.

The distributions of STN-projecting neurons containing calbindin and calretinin were uniform and non-uniform respectively (ANOVA on ranks, Kruskal-Wallis, $H_{(9)} = 13.39$, $P = 0.146$, Figure 5.5 A; one way ANOVA, $F_{(8,18)} = 3.174$, $P = 0.02$, Figure 5.5 B,). Despite the non-uniform distribution of the calretinin-positive neurons, no differences were seen between specific segments (Bonferroni; $P > 0.05$). The GiN-projecting neurons containing calretinin were uniformly distributed along the rostro-caudal axis of the PPN (ANOVA on ranks; Kruskal-Wallis; $H_{(9)} = 11.758$; $P = 0.227$; Figure 5.5 D).

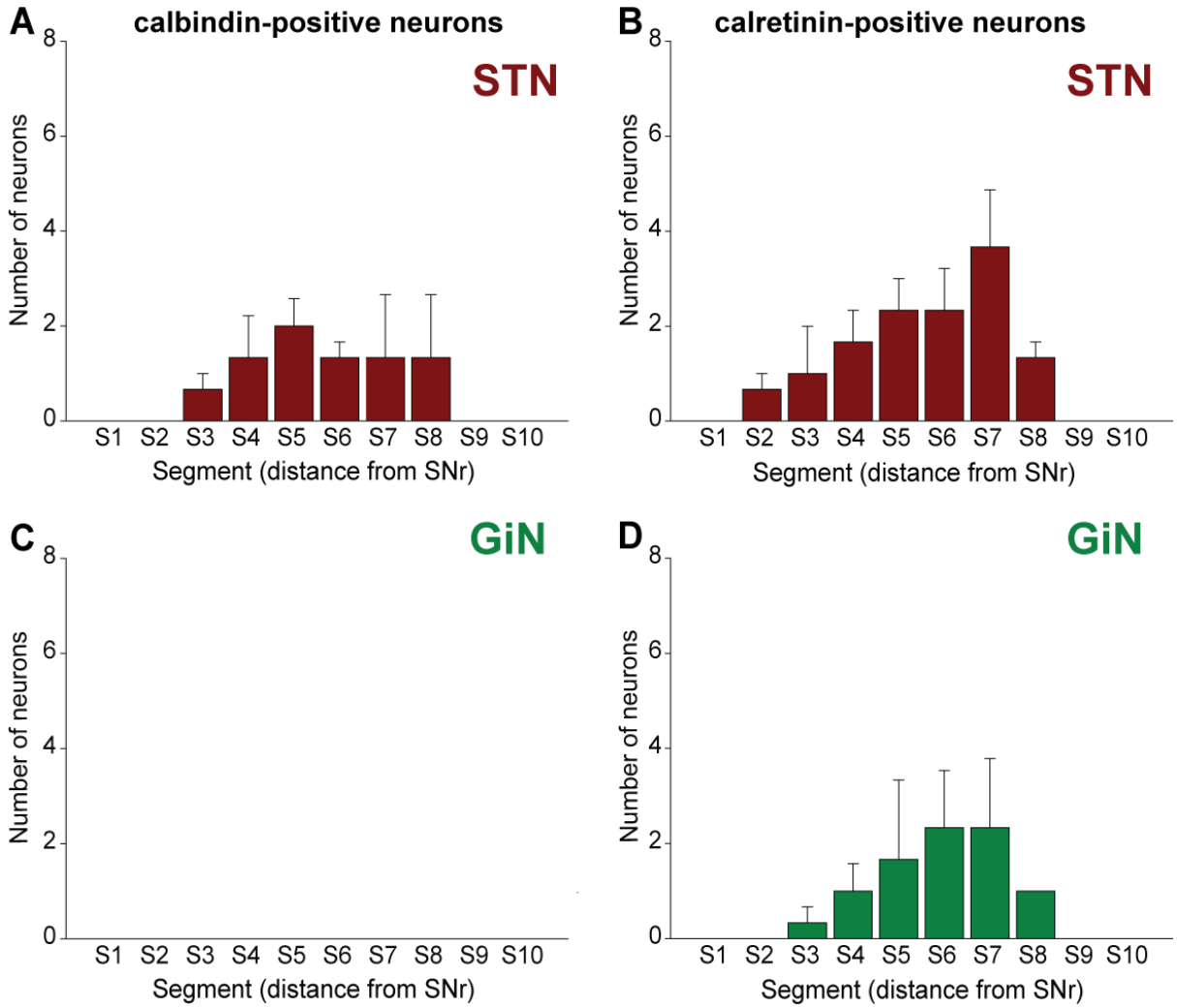


Figure 5.5. Distribution of STN- or GiN-projecting PPN neurons that contain calbindin or calretinin

Histograms above show the number of STN- and GiN-projecting PPN neurons that contain calbindin (A and C, respectively) or calretinin (B and D, respectively) in the rostro-caudal segments of the PPN (columns represent means; error bars indicate SEM; $n = 3$).

5.3.4. The expression of the immediate early gene Egr1 in PPN projection neurons of control and 6-OHDA lesioned animals

The presence of the immediately early gene, Egr1, was assessed in STN- and GiN-projecting neurons of the PPN, in both control and 6-OHDA lesioned animals, to analyse whether neuronal activity was affected by the lesion. Initially, the numbers of PPN neurons projecting to the STN, GiN or both nuclei, were quantified in control and 6-OHDA lesioned animals (see Table 5.3). No differences in the number of neurons were observed between control and lesioned animals for each of the targets examined (STN, student's t-test; $t_{(4)}$= 0.82, P= 0.456; GiN, $t_{(4)}$= 3.37, P = 0.028; STN/GiN, $t_{(4)}$= 1.05; P = 0.353; *n* = 3).

The presence of Egr1-immunoreactivity in these neurons was then assessed and quantified. The proportions of STN- showed statistically significant differences between control and lesioned animals (student's t-test; STN, $t_{(4)} = 3.13$, P = 0.035, Figure 5.6 A), but none were seen for GiN- and double-projecting neurons (student's t-test; GiN, $t_{(4)} = 0.96$, P = 0.39, Figure 5.6 C; STN/GiN, $t_{(4)} = 1.02$, P = 0.367, Figure 5.6 E; *n* = 3).

The distributions of Egr1-positive projection neurons were then analysed for both control and lesioned animals. Egr1-positive STN- and GiN-projecting neurons were non-uniformly distributed in both control and lesioned animals (control STN, ANOVA on ranks, Kruskal-Wallis, $H_{(9)} = 19.06$, P = 0.025; 6-OHDA STN, one way ANOVA, $F_{(9,20)} = 3.81$, P = 0.006; Figure 5.6 B; control GiN, Kruskal-Wallis, $H_{(9)} = 20.35$, P = 0.016; 6-OHDA GiN, $H_{(9)} = 21.24$, P = 0.012; Figure 5.6 D), however, no differences were found between specific segments of the PPN (Dunn's test, P > 0.05). In contrast, double-projecting neurons positive for Egr1 were uniformly distributed in both control and lesioned animals (ANOVA on ranks, Kruskal-Wallis; control, $H_{(9)} = 8.419$, P = 0.493; 6-OHDA, $H_{(9)} = 8.117$, P = 0.522; Figure 5.6 F).

	Rat ID	STN-projecting neurons			
		Total number	Erg1-positive	% Erg1-positive	SEM (±)
Control	C328	357	11	3.1	
	C327	375	10	2.7	
	C331	217	13	6.0	
	Mean	**316.3**	**11.3**	**3.9**	**1.0**
6-OHDA	C312	414	29	7.0	
	C316	298	40	13.4	
	C325	388	47	12.1	
	Mean	**366.7**	**38.7**	**10.8**	**2.0**
	Rat ID	**GiN-projecting neurons**			
		Total number	**Erg1-positive**	**% Erg1-positive**	**SEM (±)**
Control	C328	173	2	1.2	
	C327	185	4	2.2	
	C331	112	8	7.1	
	Mean	**156.7**	**4.7**	**3.5**	**1.9**
6-OHDA	C312	67	2	3.0	
	C316	57	3	5.3	
	C325	93	10	10.8	
	Mean	**72.3**	**5.0**	**6.3**	**2.3**
	Rat ID	**STN/GiN double-projecting neurons**			
		Total number	**Erg1-positive**	**% Erg1-positive**	**SEM (±)**
Control	C328	30	0	0.0	
	C327	23	1	4.3	
	C331	22	2	9.1	
	Mean	**25.0**	**1.0**	**4.5**	**2.6**
6-OHDA	C312	19	0	0.0	
	C316	9	1	11.1	
	C325	28	9	32.1	
	Mean	**18.7**	**3.3**	**14.4**	**9.4**

Table 5.3. Total number of PPN neurons projecting to the STN, GiN or both nuclei in control and 6-OHDA lesioned animals, together with the numbers and proportions of these that were Egr1-positive (individual animals and means ± SEM; $n = 3$).

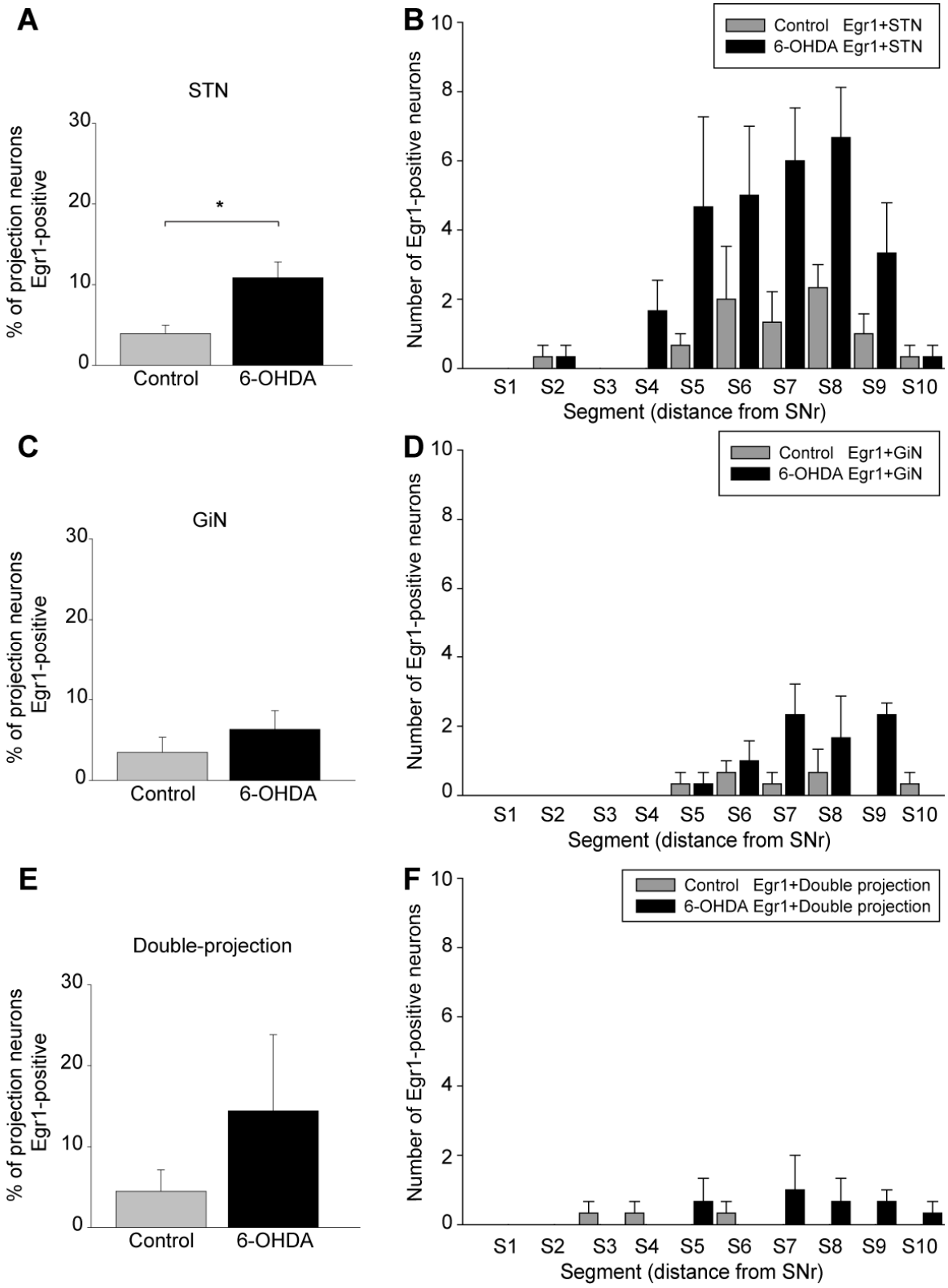


Figure 5.6. Proportions and distributions of STN- (A and B), GiN- (C and D) and double-projecting PPN neurons (E and F) that were positive for Egr1 in control and 6-OHDA lesioned animals (columns represent means, bars represent SEM; * denotes a significant difference; $n = 3$).

5.4. Discussion

The results of this chapter show that there are greater numbers of neurons projecting to the STN than to the GiN, and neurons projecting to the STN or GiN alone than to both nuclei together. Furthermore, these neurons are not uniformly distributed along the rostro-caudal axis of the PPN and express calbindin, calretinin and cholinergic markers to differing degrees. Additionally, it was shown that the expression of Egr1, a marker for neuronal activation, significantly change between control and 6-OHDA lesioned animals in the STN- projecting neurons but not in GiN- and double-projecting neurons of the PPN.

It should be noted that Egr1 expression might not be representative of neuronal activation, indeed, those negative for Egr1 might in fact be positive (false negatives may exist). Future experiments with additional immediate early genes could be used to address this point. It is also necessary to consider that not all STN- or GiN-projecting neurons of the PPN will have been labelled by the tracer injections (Kobbert *et al.*, 2000; Lanciego & Wouterlood, 2011). Factors influencing the numbers of neurons that were retrogradely-labelled include: 1) the accuracy of the injection, 2) the amount of tracer injected and 3) the time allowed between tracer injections and perfusion-fixation (Apps & Ruigrok, 2007).

PPN neurons projecting to the STN were non-uniformly distributed along the rostro-caudal axis of the PPN and 12 ± 1 % of these were cholinergic (ChAT-positive), leaving nearly 90% of this projection non-cholinergic. This is in agreement with a previous report, which also describes the types of fibres innervating the STN (Kita & Kita, 2010). It was shown that the two types of fibres, previously described by Bevan and Bolam (1995), thin fibres with small en-passant boutons and thicker fibres terminating in clumps of larger boutons, are likely to be cholinergic and non-cholinergic respectively (Kita & Kita, 2010).

It is possible that the cholinergic neurons elicit an excitatory effect upon STN neurons, as it has been shown that the application of acetylcholine can induce excitation in STN neurons (Feger *et al.*, 1979). As for the non-cholinergic component of this projection, it is likely that its effect will be more heterogeneous as it is composed of both inhibitory GABAergic and excitatory glutamatergic neurons (Bevan & Bolam, 1995). Results in this chapter show that a small proportion of non-cholinergic neurons are calbindin- or calretinin-positive, but it is difficult to surmise what effect these might have upon neurons of the STN given their small number.

When PPN neurons projecting to the STN were assessed for their expression of the immediate early gene Egr1, a marker of neuronal activation, significant differences were seen between control and 6-OHDA lesioned animals. This is in agreement with previous studies showing that the metabolic activity of the PPN has been seen to increase in the 6-OHDA lesioned rat model of Parkinson's disease, together with the activity of the STN (Carlson *et al.*, 1999; Hirsch *et al.*, 2000; Orieux *et al.*, 2000; Breit *et al.*, 2008). There is also an increased release of glutamate in the PPN in the 6-OHDA lesioned rat, attributable to an overactive STN, which could increase the activity of PPN neurons (Blanco-Lezcano et al., 2005). However, other studies suggest that the PPN is hypoactive in MPTP-treated primates (Mitchell *et al.,* 1989; Nandi *et al.*, 2002b; Nandi *et al.*, 2002c; Jenkinson *et al.*, 2004; Jenkinson *et al.*, 2005; Kringelbach *et al.*, 2007; Jenkinson *et al.*, 2009) or hyperactive in 6-OHDA lesioned animals (Breit *et al.*, 2001; Breit *et al.*, 2006).

In recent years the PPN has been used as a target for low frequency deep brain stimulation (DBS) to treat symptoms of Parkinson's disease, such as akinesia, by attenuating the inhibition thought to be imposed upon the PPN (Nandi *et al.*, 2002c; Jenkinson *et al.*, 2004; Jenkinson *et al.*, 2005). In contrast, high frequency stimulation decreases movement in non-parkinsonian animals (Jenkinson *et al.*, 2004; Jenkinson *et al.*,

2006). When low frequency stimulation of the PPN is combined with L-DOPA treatment, it serves better than L-DOPA alone in animal models of Parkinson's disease (Jenkinson et al., 2005) and in Parkinson's disease patients (Hamani *et al.*, 2007; Lozano & Snyder, 2008; Pierantozzi *et al.*, 2008).

When stimulating the PPN, it is pertinent not to forget that many projection neurons of the PPN also target the lower brainstem, pons, medulla and spinal cord (Grofova & Keane, 1991). Results in this chapter show that PPN neurons projecting to the GiN (situated in the lower brainstem) were non-uniformly distributed along the rostro-caudal axis of the PPN; 19 ± 1 % were cholinergic (ChAT-positive) and 7 ± 2 % were calretinin-positive. The percentage of cholinergic neurons was slightly higher than those previously reported for the cat (5.2%; Mitani *et al*., 1988), although this could be due to species differences or variability in injections between the two studies.

Similar to the STN-projecting neurons, and increase in the proportions of Egr-1-positive neurons was observed between GiN-projecting neurons or double-projecting neurons in 6-OHDA lesioned animals compared to control animals. However, the power of the performed Student's t-test was below the desire power and no statistically significant differences were found between them. This suggests that the hyperactivity seen in the PPN in other studies may not exist in neurons projecting to the GiN or both nuclei, but a larger study is necessary to confirm these results. However, certain caveats need to be considered: 1) Egr1 expression does not always reflect neuronal activation (Chaudhuri *et al.*, 2000), 2) expression of other immediate early genes might be more suitable to assess neuronal activation in the PPN and 3) the sample of neurons in this study was relatively small and could be increased.

Overall, this chapter has shown that the neurons of the PPN projecting to the STN and GiN are mainly non-cholinergic (74-88 %) and rarely positive for calbindin or calretinin (0-7 %). Evidence has been found suggesting that these neurons may increase their activity in the 6-OHDA lesioned rat model of Parkinson's disease, although a larger study is necessary to confirm this observation. These findings, and those of previous chapters, extend our knowledge of the complex nature of the PPN, its neuronal architecture and its connectivity with other regions of the nervous system, but in doing so they open more questions about its roles in brain function.

6. General discussion

6.1. Overview of the chapters

6.1.1. Introduction

This thesis has examined the neuronal subtypes of the PPN, their neurochemical phenotypes, their distributions and their connections with other brain regions. In Chapter 3, calbindin- and calretinin-positive neurons of the PPN were stereologically quantified and their distribution along its rostro-caudal axis analysed. The study of these neurons was then extended in Chapter 4 to assess which neurotransmitter these neurons might use: acetylcholine, GABA or glutamate. Chapter 5 examined neurons of the PPN that project to the subthalamic nucleus and/or the gigantocellular nucleus, as representative targets for its ascending and descending projections, respectively. The distributions and neurochemical phenotypes of these neurons were examined, as was their expression of the immediate early gene Egr1, in control and 6-OHDA lesioned animals. Each of these chapters will be summarised in the sections that follow.

6.1.2. Chapter 3: Calbindin- and calretinin-positive neurons in the PPN

The first study of this thesis provided anatomical evidence that calbindin- and calretinin-positive neurons are as abundant as cholinergic neurons in the PPN, and that these neurons are non-uniformly distributed along the rostro-caudal axis of the PPN. Cholinergic and GABAergic neurons of the PPN have previously been quantified using a stereological approach and were found to account for approximately 3,000 and 6,600 neurons respectively (Mena-Segovia *et al.*, 2009). Calbindin and calretinin are calcium-binding proteins that have helped to identify neuronal subtypes in other regions of the brain, most notably the hippocampus, cortex, basal ganglia and basal forebrain (Fortin & Parent, 1996; Parent *et al.*, 1996; Airaksinen *et al.*, 1997; Gritti *et al.*, 2003; Staiger *et al.*, 2004; Klausberger & Somogyi, 2008). For this reason, and the fact that these proteins can alter the electrophysiological properties of neurons in which they are expressed (Schwaller

et al., 2002), their presence in neurons of the PPN was analysed. Stereological estimates of these neurons showed that approximately 2,300 calbindin-positive neurons and 2,500 calretinin-positive neurons are present in the rat PPN of one hemisphere. The distributions of these neurons along the rostro-caudal axis of the PPN showed greater numbers in the central segments of the PPN. However, the volumes of these segments were generally larger, and when density distributions were analysed, no specific differences between any of the rostro-caudal segments were observed.

6.1.3. Chapter 4: Neurotransmitters expressed by calbindin- and calretinin-positive neurons of the PPN

In Chapter 3, it was found that calbindin- and calretinin-positive neurons are present in similar numbers to cholinergic neurons in the PPN; roughly half as abundant as GABAergic neurons (Mena-Segovia *et al.*, 2009). The next step was to determine what proportions of these calbindin- and calretinin-positive neurons use acetylcholine, GABA or glutamate as their neurotransmitter (as these are the major neurotransmitters known to be used in the PPN).

Two approaches were used to examine the proportions of these neurons that were cholinergic; double-immunoperoxidase labelling for ChAT with either calbindin or calretinin and triple-immunofluorescent labelling to reveal all three markers. Calbindin-positive neurons displaying immunoreactivity for ChAT accounted for only 0.2% of all calbindin neurons in the double-immunoperoxidase labelling study, whereas none were ChAT-positive when triple-immunofluorescent labelling was examined (within in the margin of error). A larger proportion of calretinin-positive neurons were ChAT-immunopositive; 13% for double-immunoperoxidase labelling and 5% for triple-immunofluorescent labelling.

Interestingly, 24% of calbindin-positive neurons were calretinin-positive and 25% of calretinin-positive neurons were calbindin-positive, showing that calbindin- and calretinin-positive neurons of the PPN can be split into three groups: those containing only calbindin or calretinin and those containing both. The functional implications of this are as yet unknown, but the consequences of single PPN neurons containing both calcium-binding proteins could be significant for their physiological activity. For example, in the hippocampus, GABAergic interneurons containing different combinations of calcium-binding proteins have been described as having different physiological properties (Klausberger *et al.*, 2003).

Immunolabelling also revealed that a large proportion of calbindin- and calretinin-positive neurons were not cholinergic; 99.8-100% of calbindin-positive neurons and 87-95% of calretinin-positive neurons. It is likely therefore that these neurons use GABA or glutamate as their neurotransmitter. To test this, *in situ* hybridisation of GAD65/67 mRNA and VGluT2 mRNA was performed, to label GABAergic and glutamatergic neurons respectively, in combination with immunoperoxidase labelling for calbindin or calretinin. This showed that about a third of both calbindin- and calretinin-positive neurons were GABAergic (39% and 28% respectively) and about two thirds glutamatergic (67% and 74% respectively). Similar to previous reports (Mena-Segovia *et al.*, 2009; Wang & Morales, 2009), it was shown that GABAergic neurons were more concentrated in the rostral PPN and glutamatergic neurons were more concentrated in the caudal PPN; the calbindin and calretinin content of these did not significantly alter their distribution. This rostral and caudal bias of GABAergic and glutamatergic neurons might explain, or be explained by, the differential afferents and efferents of these regions.

6.1.4. Chapter 5: Connectivity and activation of PPN neurons

Projections of PPN neurons to the STN and GiN were examined in Chapter 5. Their neurochemical nature was also assessed by immunofluorescent labelling for ChAT, calbindin or calretinin. For each of the three animals injected with retrograde tracers, in the STN and GiN, roughly 330 PPN neurons projected only to the STN, 250 only to the GiN and 30 to both nuclei (significantly less than single projecting neurons). These numbers of singly-projecting neurons are similar to those seen in other studies (Grofova & Keane, 1991; Kita & Kita, 2010), however, others report a smaller projection to the STN of the cat and primate (Carpenter *et al.*, 1981). Although all projection neurons were non-uniformly distributed along the rostro-caudal axis of the PPN, only the STN-projecting neurons showed specific differences between PPN segments; more neurons were found in the middle of the PPN than in rostral regions. This distribution is similar to the cholinergic and non-cholinergic neurons of the PPN that project to the STN (Kita & Kita, 2010).

About one fifth of projection neurons were found to be cholinergic, accounting for 12% of the STN-projecting neurons, 19% of the GiN-projecting neurons (slightly higher than previously reported; Mitani *et al.*, 1998) and 26% of those projecting to both nuclei. As for the projection neurons as a whole, cholinergic neurons projecting to the STN, GiN or both nuclei were non-uniformly distributed along the rostro-caudal axis of the PPN. These results suggest that, unlike previously suggested (Woolf & Butcher, 1986), cholinergic neurons account for the minority of projection neurons to both the STN and GiN. It is likely that many of these projection neurons are of a GABAergic or glutamatergic phenotype; indeed, GABAergic and glutamatergic projections from the PPN to the STN have been documented previously (Bevan & Bolam, 1995).

A much smaller proportion of projection neurons were found to be calbindin- or calretinin-positive. Five percent and 7% of the STN-projecting neurons were calbindin- and calretinin-positive respectively. Seven percent of GiN-projecting neurons contained calretinin but none contained calbindin; double-projecting neurons contained neither calbindin nor calretinin. Calbindin-positive neurons projecting to the STN and calretinin-positive neurons projecting the GiN were uniformly distributed along the rostro-caudal axis of the PPN, but calretinin-positive neurons projecting to the STN were non-uniformly distributed (with no specific differences between segments). The vast majority of neurons projecting to either the STN, GiN or both nuclei are not calbindin- or calretinin-positive, despite the fact that there are large numbers of calbindin- or calretinin-positive neurons in the PPN (see Chapter 3). Therefore, it is likely that these neurons, a third of which are GABAergic and two thirds of which are glutamatergic, are projecting to other targets of the PPN or contributing to local connections within the PPN.

These projection neurons were then analysed for their expression of the immediate early gene Egr1, in control and 6-OHDA lesioned animals, with a view to understanding whether they were more likely to be activated in health or disease. In each of these groups of projection neurons, only in STN-projection neurons were found significant differences between control and lesioned animals. However, several factors should be taken into account when considering the results of this study; the relatively small number of animals used, the suitability of Egr1 as a marker of neuronal activation and the targeting of tracer injections in lesioned animals (all of these factors will be discussed in the section that follows on technical considerations).

6.1.5. Summary

It is crucial to understand how the PPN is able to accomplish its physiological roles in health, and how those roles are affected in pathological conditions such as Parkinson's disease. In order to investigate this, the overall aim of this thesis was to provide new insights into the anatomy, connectivity and activation of PPN neurons for both control and 6-OHDA lesioned animals.

This thesis has shown that calbindin- and calretinin-positive neurons are present in substantial numbers in the PPN, and that the vast majority are either GABAergic or glutamatergic. This builds upon the studies of Dun *et al.* (1995), Parent *et al.* (1996) and Fortin and Parent (1999) who showed the presence of calbindin- and calretinin-positive neurons in the PPN of rats and primates. Furthermore, the thesis has shown that these neurons are concentrated in either the rostral or caudal PPN dependent upon their expression of GABAergic or glutamatergic markers, respectively. These results correlate well with the studies of Wang and Morales (2009) and Mena-Segovia *et al.* (2009) that describe higher numbers of GABAergic neurons in the rostral PPN and higher numbers of glutamatergic neurons in the caudal PPN.

Calbindin- and calretinin-positive neurons, in addition to cholinergic neurons, were seen to provide a relatively restricted innervation of the subthalamic and gigantocellular nuclei (representative ascending and descending targets of the PPN, respectively), implying that other cell populations of the PPN, possibly GABAergic or glutamatergic neurons, may be responsible for the majority of these projections. This extends the work of Bevan and Bolam (1995) and Kita and Kita (2010) who described cholinergic, GABAergic and glutamatergic inputs to the STN from the rat PPN in the rat and the work of Grofova

and Keane (1991) and Mitani *et al.* (1988) who described the cholinergic PPN projection to the GiN in the rat and cat, respectively.

The activation of PPN neurons projecting to the STN and/or GiN was assessed by their expression of the immediate early gene Egr1; statistically significant differences were found only in STN-projecting neurons between control and 6-OHDA lesioned animals. The expression of Egr1 has previously been used as a marker of neuronal activation, but it might be the case that other immediate early genes better reflect the activation of neurons in the rat PPN (Chaudhuri *et al.*, 1995; Hughes & Dragunow, 1995; Chaudhuri *et al.*, 1997; Herdegen & Leah, 1998; Chaudhuri *et al.*, 2000). Neuronal activation may increase within the PPN of the 6-OHDA lesioned rat as other studies have suggested (Carlson *et al.*, 1999; Hirsch *et al.*, 2000; Orieux *et al.*, 2000; Breit *et al.*, 2008). However, this was only seen in PPN neurons projecting to the STN in the current study and further investigation of immediate early gene expression or electrophysiological recordings will be necessary to determine whether other populations of PPN neurons increase or decrease their activity in the 6-OHDA model. Only then could these findings be used to help explain why low frequency deep brain stimulation of the PPN is therapeutic in the treatment of Parkinson's disease (Jenkinson *et al.*, 2005; Hamani *et al.*, 2007; Lozano & Snyder, 2008; Jenkinson *et al.*, 2009).

6.2. Technical considerations

6.2.1. *In situ* hybridisation

In situ hybridisation labelling of GAD65/67 or VGluT2 mRNA was used in Chapter 4 to reveal GABAergic and glutamatergic neurons of the PPN, respectively. Labelling the nucleus of GABAergic and glutamatergic neurons with these markers allowed individual neurons to be classified. Immunoperoxidase labelling for either of these

makers does not guarantee the labelling of the soma; GAD65/67 immunolabelling results in high levels of non-specific labelling in the brainstem, whereas VGluT2 is rapidly transported to synaptic terminals, away from the soma (Mena-Segovia *et al.*, 2009; Wang & Morales, 2009). In the initial stages of the current study, different antibodies against GAD65, GAD67 and GABA were evaluated for their immunolabelling of GABAergic neurons in the PPN, but none were visible above levels of background labelling. Additionally, the presence of GABAergic neurons in the PPN was evaluated in two types of transgenic mouse (GAD65/GFP- or GAD67/GFP-expressing). However, GFP-positive neurons in these animals were much less abundant than GAD65/67 mRNA-positive neurons observed by *in situ* hybridisation in the rat PPN. As a result of these initial experiments, it was decided that *in situ* hybridisation would be the best method by which to evaluate GABAergic neurons of the PPN.

Radioactive, rather than fluorescent, *in situ* hybridisation labelling was used for this study due to its higher sensitivity; however, there are limitations to this technique. For radioactive *in situ* hybridisation, tissue is dehydrated onto slides and immersed in a photographic emulsion, which creates a thin layer of gelatin on the top of the tissue containing light-sensitive silver halides. The developing solution then reduces, into metallic silver, only the silver halides that were exposed to a sufficient amount of radioactivity, as a result of lying directly above neurons containing radioactive riboprobes. These silver granules, visible on the surface of the tissue, allow neurons containing the riboprobes to be analysed.

This process is greatly affected by the thickness of the tissue. Riboprobe-containing neurons located at the bottom of the section (closest to the slide) are unlikely to have a sufficient enough effect as to result in the formation of silver granules on the surface of the tissue. This problem can be overcome by using thin sections (approximately 5 μm in

thickness, after shrinkage due to dehydration), but cutting sections this thin and maintaining their integrity is technically challenging. Sections used in Chapter 4 were cut at 18 μm and shrank to approximately 6-8 μm after dehydration, enabling most of the neurons containing radioactive riboprobes to be labelled.

6.2.2. Retrograde tracer injections

For the retrograde tracer experiments in Chapter 5, red and green retrobeads (fluorescently-labelled latex microspheres) were injected in the STN and GiN to label STN- and GiN-projecting neurons of the PPN. These retrobeads have distinct advantages over other retrograde tracers; they are transported in a strictly retrograde fashion, diffuse only minimally from the site of injection and can persist for long periods of time in the tissue, due to their lack of cytotoxicity (Katz *et al.*, 1984; Katz & Iarovici, 1990; Lanciego & Wouterlood, 2011). Furthermore, these tracers do not require additional histological processing, thus reducing non-specific labelling.

However, there are limitations to this technique; not all STN- or GiN-projecting neurons of the PPN are labelled by the tracer injections, which could result in false negatives (Kobbert *et al.*, 2000; Lanciego & Wouterlood, 2011). To increase the chances of STN- and GiN-projecting neurons being labelled an appropriate volume of retrobeads needs to be injected, injections need to be accurate and enough time needs to be given to allow the transport of the retrobeads to the neurons of the PPN.

Red and green retrobeads are observed in the cytoplasm and primary dendrites of retrogradely labelled neurons; specifically in the form of either red, green or yellow cytoplasmic grains (Katz & Iarovici, 1990). The mechanism underlying the retrograde transport of these beads is not fully known and neither is the explanation for why yellow grains appear. However, Katz & Iarovici (1990) state that yellow grains could result from

overlapping red and green grains or instances where organelles containing red and green grains have fused.

6.2.3. Immediate early gene expression

In Chapter 5, the expression of the immediate early gene Egr1 was used as a marker of neuronal activation. When used for this purpose, there are some important methodological points to consider; ketamine (used as an anaesthetic) can transiently interfere with the induction of immediate early genes, those of the *fos* family can be affected by apomorphine (Sommer *et al.*, 1993) and the expression of others can be differentially induced by neurotoxin-related axonal degeneration (Duchemin *et al.*, 1992; Jenkins *et al.*, 1993). However, all of these considerations were taken into account when performing the procedures in Chapter 5. Firstly, the animals were perfuse-fixed immediately after being anaesthetised with ketamine, thus not allowing sufficient time for it to affect the induction of immediate early genes. Secondly, based upon previous studies (Dragunow & Faull, 1989), the time between apomorphine injections (used to test the extent of the lesion) and perfusion of the animals was long enough for immediate early gene expression to return to baseline levels. Thirdly, in order to observe the immediate early gene expression that was due to the lesion, and not due to the acute effects of the neurotoxin, animals were perfuse-fixed four weeks after lesion surgery (Dragunow & Faull, 1989).

6.3. Future directions

6.3.1. Further stereological analyses of PPN neurons

In Chapter 3 of this thesis, the numbers of calbindin- and calretinin-positive neurons in the PPN were quantified. This was done using a stereological method, similar to that previously used to estimate the number of GABAergic and cholinergic neurons in

the PPN and the number of neurons in nuclei of the basal ganglia (Oorschot, 1996; Mena-Segovia *et al.*, 2009). The definitive number of glutamatergic neurons in the PPN is yet to be established, as is the total number of neurons present in the PPN; these numbers could be quantified, using similar methods, to further characterise the neuronal make-up of the PPN. Furthermore, GABAergic neurons of the PPN could be differentiated based upon their expression of GAD65 or GAD67 mRNA. In Chapter 4, GABAergic neurons of the PPN were labelled by *in situ* hybridisation using a combination of GAD65 and GAD67 mRNA riboprobes, but future studies could assess the number, distribution and electrophysiological properties of each individually to determine whether any differences between the two exist.

6.3.2. Electrophysiological characterisation of PPN neuron subtypes

Subdividing neurons of the PPN by their neurochemistry (as shown in Chapters 4 and 5) is the first step in defining what the function of these neurons, and the PPN as a whole, might be. Diverse subtypes of neurons have been identified among cholinergic and non-cholinergic neurons of the PPN, based upon their electrophysiological activity during cortical slow oscillations and global brain state transitions (Mena-Segovia *et al.*, 2008a; Ros *et al.*, 2010). Therefore, the next logical step would be to conduct *in vivo* electrophysiological experiments to record the activity of PPN neurons identified in this thesis.

This could be done by juxtacellularly labelling neurons at the end of an electrophysiological experiment and labelling perfuse-fixed tissue to determine their neurochemical phenotypes post-hoc (Mena-Segovia *et al.*, 2004a; Mena-Segovia *et al.*, 2006; Mena-Segovia *et al.*, 2008a; Mena-Segovia *et al.*, 2008b; Ros *et al.*, 2010; Mena-Segovia & Bolam, 2011). Immunoperoxidase labelling could be used to identify calbindin- and calretinin-positive neurons and their neurotransmitters could be identified through the

use of *in situ* hybridisation (see technical considerations for the suitability of each technique) (Lanciego & Wouterlood, 2011). These methods could provide information about the firing patterns of the neurons during different brain states and cortical oscillations. Juxtacellular labelling, in combination with neuronal reconstruction and electron microscopy, could also help to establish their full axonal arbourisations and synaptic targets, respectively.

6.3.3. Establishing the neurotransmitters of PPN projection neurons

In Chapter 5, the neurons projecting to the STN and GiN were analysed for their expression of ChAT, which showed that a large proportion of them were ChAT-negative (non-cholinergic). This suggested that they might be positive for either of the two other major neurotransmitters found in neurons of the PPN, GABA or glutamate. As discussed previously (see technical considerations), the only feasible way to label these neurons is by *in situ* hybridisation. In order to use tracer-injected tissue for *in situ* hybridisation, animals should be perfuse-fixed using RNAase-free solutions and the tissue stored under RNAase-free conditions. This was not done for experiments in Chapter 5, but could be done in the future to confirm the neurochemical phenotypes of STN- and GiN-projecting neurons of the PPN. It should be noted that the STN and GiN are not the only targets of PPN projection neurons; PPN efferents also target the basal ganglia, thalamus, cortex, brainstem, cerebellum and spinal cord. Anterograde and retrograde tracers could be used to investigate the number of PPN neurons projecting to these targets. Additionally, these could be used to identify the contributions of other brain regions to PPN activity through their inputs to rostral or caudal regions.

6.3.4. Immediate early gene-expression in the PPN

The expression of immediate early genes can be induced in response to synaptic stimulation (Hughes & Dragunow, 1995; Herdegen & Leah, 1998), however, the expression of these genes can also be affected by several other factors (Chaudhuri *et al.*, 2000). In Chapter 5 it was observed that, only in STN-projection neurons, a larger proportion was positive for Egr1 6-OHDA lesioned animals compared to control animals. However, statistically similar numbers of GiN- and double-projecting PPN neurons were positive for Egr1 in control and 6-OHDA lesioned animals. It is likely that differences between control and lesioned animals exist, but greater numbers of animals would need to be tested in order to demonstrate significant statistical differences. Therefore, an obvious extension to this project would be to examine more animals to assess whether this was the case.

Another approach would be to assess the expression of additional immediate early genes, which could help to assess neuronal activation in STN- and GiN-projection neurons in the PPN of control and 6-OHDA lesioned rats. Additionally, the expression of immediate early genes could be examined in the MPTP-treated primate model of Parkinson's disease, and control animals, to assess the effect of MPTP treatment on neuronal activation and to compare this model against the 6-OHDA lesioned rat.

7. REFERENCES

Acsady, L., Halasy, K. & Freund, T.F. (1993) Calretinin is present in non-pyramidal cells of the rat hippocampus--III. Their inputs from the median raphe and medial septal nuclei. *Neuroscience*, **52**, 829-841.

Aihara, Y., Mashima, H., Onda, H., Hisano, S., Kasuya, H., Hori, T., Yamada, S., Tomura, H., Yamada, Y., Inoue, I., Kojima, I. & Takeda, J. (2000) Molecular cloning of a novel brain-type Na(+)-dependent inorganic phosphate cotransporter. *J Neurochem*, **74**, 2622-2625.

Ainge, J.A., Jenkins, T.A. & Winn, P. (2004) Induction of c-fos in specific thalamic nuclei following stimulation of the pedunculopontine tegmental nucleus. *Eur J Neurosci*, **20**, 1827-1837.

Airaksinen, M.S., Thoenen, H. & Meyer, M. (1997) Vulnerability of midbrain dopaminergic neurons in calbindin-D_{28k}-deficient mice: Lack of evidence for a neuroprotective role of endogenous calbindin in MPTP-treated and weaver mice. *Eur J Neurosci*, **9**, 120-127.

Albin, R.L., Young, A.B. & Penney, J.B. (1989) The functional anatomy of basal ganglia disorders. *Trends in Neurosciences*, **12**, 366-375.

Alderson, H.L., Latimer, M.P. & Winn, P. (2006) Intravenous self-administration of nicotine is altered by lesions of the posterior, but not anterior, pedunculopontine tegmental nucleus. *Eur J Neurosci*, **23**, 2169-2175.

Alderson, H.L., Latimer, M.P. & Winn, P. (2008) A functional dissociation of the anterior and posterior pedunculopontine tegmental nucleus: excitotoxic lesions have differential effects on locomotion and the response to nicotine. *Brain Struct Funct*, **213**, 247-253.

Alexander, G.E. & Crutcher, M.D. (1990) Functional architecture of basal ganglia circuits: neural substrates of parallel processing. *Trends in Neurosciences*, **13**, 266-271.

Alfahel-Kakunda, A. & Silverman, W.F. (1997) Calcium-binding proteins in the substantia nigra and ventral tegmental area during development: correlation with dopaminergic compartmentalization. *Developmental Brain Research*, **103**, 9-20.

Apps, R. & Ruigrok, T.J. (2007) A fluorescence-based double retrograde tracer strategy for charting central neuronal connections. *Nat Protoc*, **2**, 1862-1868.

Arai, R., Winsky, L., Arai, M. & Jacobowitz, D.M. (1991) Immunohistochemical localization of calretinin in the rat hindbrain. *J Comp Neurol*, **310**, 21-44.

Aravamuthan, B.R., Bergstrom, D.A., French, R.A., Taylor, J.J., Parr-Brownlie, L.C. & Walters, J.R. (2008) Altered neuronal activity relationships between the pedunculopontine nucleus and motor cortex in a rodent model of Parkinson's disease. *Exp Neurol*, **213**, 268-280.

Armstrong, D.M., Saper, C.B., Levey, A.I., Wainer, B.H. & Terry, R.D. (1983) Distribution of cholinergic neurons in rat brain: demonstrated by the immunocytochemical localization of choline acetyltransferase. *J Comp Neurol*, **216**, 53-68.

Baghdoyan, H.A., Rodrigo-Angulo, M.L., McCarley, R.W. & Hobson, J.A. (1987) A neuroanatomical gradient in the pontine tegmentum for the cholinoceptive induction of desynchronized sleep signs. *Brain Res*, **414**, 245-261.

Baimbridge, K.G., Celio, M.R. & Rogers, J.H. (1992) Calcium-binding proteins in the nervous system. *Trends in Neurosciences*, **15**, 303-308.

Barroso-Chinea, P., Castle, M., Aymerich, M.S. & Lanciego, J.L. (2008) Expression of vesicular glutamate transporters 1 and 2 in the cells of origin of the rat thalamostriatal pathway. *J Chem Neuroanat*, **35**, 101-107.

Barroso-Chinea, P., Rico, A.J., Conte-Perales, L., Gomez-Bautista, V., Luquin, N., Sierra, S., Roda, E. & Lanciego, J.L. (2011) Glutamatergic and cholinergic pedunculopontine neurons innervate the thalamic parafascicular nucleus in rats: changes following experimental parkinsonism. *Brain Struct Funct*, **216**, 319-330.

Benabid, A.L. (2003) Deep brain stimulation for Parkinson's disease. *Curr Opin Neurobiol*, **13**, 696-706.

Beninato, M. & Spencer, R.F. (1986) A cholinergic projection to the rat superior colliculus demonstrated by retrograde transport of horseradish peroxidase and choline acetyltransferase immunohistochemistry. *J Comp Neurol*, **253**, 525-538.

Bennett, B.D. & Bolam, J.P. (1993) Characterisation of calretinin-immunoreactive neurones in the rat striatum. *Brain Res*, **609**, 137-148.

Bergman, H. & Deuschl, G. (2002) Pathophysiology of Parkinson's disease: from clinical neurology to basic neuroscience and back. *Mov Disord*, **17 Suppl 3**, S28-40.

Betarbet, R., Sherer, T.B. & Greenamyre, J.T. (2002) Animal models of Parkinson's disease. *Bioessays*, **24**, 308-318.

Betarbet, R., Sherer, T.B. & Greenamyre, J.T. (2005) Ubiquitin-proteasome system and Parkinson's diseases. *Exp Neurol*, **191 Suppl 1**, S17-27.

Bethlem, J. & Den Hartog Jager, W.A. (1960) The incidence and characteristics of Lewy bodies in idiopathic paralysis agitans (Parkinson's disease). *J Neurol Neurosurg Psychiatry*, **23**, 74-80.

Bevan, M.D. & Bolam, J.P. (1995) Cholinergic, GABAergic, and glutamate-enriched inputs from the mesopontine tegmentum to the subthalamic nucleus in the rat. *J Neurosci*, **15**, 7105-7120.

Bevan, M.D., Booth, P.A., Eaton, S.A. & Bolam, J.P. (1998) Selective innervation of neostriatal interneurons by a subclass of neuron in the globus pallidus of the rat. *J Neurosci*, **18**, 9438-9452.

Blanco-Lezcano, L., Rocha-Arrieta, L.L., Alvarez-Gonzalez, L., Martinez-Marti, L., Pavon-Fuentes, N., Gonzalez-Fraguela, M.E., Bauza-Calderin, Y. & Coro-Grave de Peralta, Y. (2005) The effects of lesions in the compact part of the substantia nigra on glutamate and GABA release in the pedunculopontine nucleus. *Rev Neurol*, **40**, 23-29.

Bolam, J.P., Brown, M.T.C., Moss, J. & Magill, P.J. (2009) *Basal Ganglia: Internal Organization.* In Squire, L.R (eds), *Encyclopedia of Neuroscience, vol 2.* Academic Press, Oxford, pp. 97-104.

Bolam, J.P., Francis, C.M. & Henderson, Z. (1991) Cholinergic input to dopaminergic neurons in the substantia nigra: a double immunocytochemical study. *Neuroscience*, **41**, 483-494.

Bolam, J.P., Hanley, J.J., Booth, P.A. & Bevan, M.D. (2000) Synaptic organisation of the basal ganglia. *J Anat*, **196**, 527-542.

Bolam, J.P., Wainer, B.H. & Smith, A.D. (1984) Characterization of cholinergic neurons in the rat neostriatum. A combination of choline acetyltransferase immunocytochemistry, Golgi-impregnation and electron microscopy. *Neuroscience*, **12**, 711-718.

Bonci, A. & Malenka, R.C. (1999) Properties and plasticity of excitatory synapses on dopaminergic and GABAergic cells in the ventral tegmental area. *J Neurosci*, **19**, 3723-3730.

Braak, E., Sandmann-Keil, D., Rub, U., Gai, W.R., de Vos, R.A.I., Steur, E.N.H.J., Arai, K. & Braak, H. (2001) alpha-synuclein immunopositive Parkinson's disease-related inclusion bodies in lower brain stem nuclei. *Acta Neuropathologica*, **101**, 195-201.

Braak, H., Del Tredici, K., Rub, U., de Vos, R.A., Jansen Steur, E.N. & Braak, E. (2003a) Staging of brain pathology related to sporadic Parkinson's disease. *Neurobiol Aging*, **24**, 197-211.

Braak, H., Ghebremedhin, E., Rub, U., Bratzke, H. & Del Tredici, K. (2004) Stages in the development of Parkinson's disease-related pathology. *Cell Tissue Res*, **318**, 121-134.

Braak, H., Rub, U., Gai, W.P. & Del Tredici, K. (2003b) Idiopathic Parkinson's disease: possible routes by which vulnerable neuronal types may be subject to neuroinvasion by an unknown pathogen. *J Neural Transm*, **110**, 517-536.

Brantley, R.K. & Bass, A.H. (1988) Cholinergic neurons in the brain of a teleost fish (Porichthys notatus) located with a monoclonal antibody to choline acetyltransferase. *J Comp Neurol*, **275**, 87-105.

Breit, S., Bouali-Benazzouz, R., Benabid, A.L. & Benazzouz, A. (2001) Unilateral lesion of the nigrostriatal pathway induces an increase of neuronal activity of the pedunculopontine nucleus, which is reversed by the lesion of the subthalamic nucleus in the rat. *Eur J Neurosci*, **14**, 1833-1842.

Breit, S., Lessmann, L., Benazzouz, A. & Schulz, J.B. (2005) Unilateral lesion of the pedunculopontine nucleus induces hyperactivity in the subthalamic nucleus and substantia nigra in the rat. *Eur J Neurosci*, **22**, 2283-2294.

Breit, S., Lessmann, L., Unterbrink, D., Popa, R.C., Gasser, T. & Schulz, J.B. (2006) Lesion of the pedunculopontine nucleus reverses hyperactivity of the subthalamic nucleus and substantia nigra pars reticulata in a 6-hydroxydopamine rat model. *Eur J Neurosci*, **24**, 2275-2282.

Breit, S., Martin, A., Lessmann, L., Cerkez, D., Gasser, T. & Schulz, J.B. (2008) Bilateral changes in neuronal activity of the basal ganglia in the unilateral 6-hydroxydopamine rat model. *J Neurosci Res*, **86**, 1388-1396.

Camp, A.J. & Wijesinghe, R. (2009) Calretinin: modulator of neuronal excitability. *Int J Biochem Cell Biol*, **41**, 2118-2121.

Canteras, N.S., Shammah-Lagnado, S.J., Silva, B.A. & Ricardo, J.A. (1990) Afferent connections of the subthalamic nucleus: a combined retrograde and anterograde horseradish peroxidase study in the rat. *Brain Res*, **513**, 43-59.

Carlson, J.D., Pearlstein, R.D., Buchholz, J., Iacono, R.P. & Maeda, G. (1999) Regional metabolic changes in the pedunculopontine nucleus of unilateral 6-hydroxydopamine Parkinson's model rats. *Brain Res*, **828**, 12-19.

Carpenter, M.B., Carleton, S.C., Keller, J.T. & Conte, P. (1981) Connections of the subthalamic nucleus in the monkey. *Brain Res*, **224**, 1-29.

Celada, P., Paladini, C.A. & Tepper, J.M. (1999) GABAergic control of rat substantia nigra dopaminergic neurons: Role of globus pallidus and substantia nigra pars reticulata. *Neuroscience*, **89**, 813-825.

Celio, M.R. (1990) Calbindin D-28k and parvalbumin in the rat nervous system. *Neuroscience*, **35**, 375-475.

Charara, A. & Parent, A. (1994) Brainstem dopaminergic, cholinergic and serotoninergic afferents to the pallidum in the squirrel monkey. *Brain Res*, **640**, 155-170.

Charara, A., Smith, Y. & Parent, A. (1996) Glutamatergic inputs from the pedunculopontine nucleus to midbrain dopaminergic neurons in primates: phaseolus vulgaris-leucoagglutinin anterograde labeling combined with postembedding glutamate and GABA immunohistochemistry. *J Comp Neurol*, **364**, 254-266.

Chard, P.S., Bleakman, D., Christakos, S., Fullmer, C.S. & Miller, R.J. (1993) Calcium buffering properties of calbindin D28k and parvalbumin in rat sensory neurones. *J Physiol*, **472**, 341-357.

Chaudhuri, A. (1997) Neural activity mapping with inducible transcription factors. *Neuroreport*, **8 (13)**, iii-vii.

Chaudhuri, A., Matsubara, J.A. & Cynader, M.S. (1995) Neuronal activity in primate visual cortex assessed by immunostaining for the transcription factor Zif268. *Vis Neurosci*, **12**, 35-50.

Chaudhuri, A., Nissanov, J., Larocque, S. & Rioux, L. (1997) Dual activity maps in primate visual cortex produced by different temporal patterns of zif268 mRNA and protein expression. *Proc Natl Acad Sci U S A*, **94**, 2671-2675.

Chaudhuri, A., Zangenehpour, S., Rahbar-Dehgan, F. & Ye, F. (2000) Molecular maps of neural activity and quiescence. *Acta Neurobiol Exp*, **60**, 403-410.

Clarke, P.B., Hommer, D.W., Pert, A. & Skirboll, L.R. (1987) Innervation of substantia nigra neurons by cholinergic afferents from pedunculopontine nucleus in the rat: neuroanatomical and electrophysiological evidence. *Neuroscience*, **23**, 1011-1019.

Cornwall, J., Cooper, J.D. & Phillipson, O.T. (1990) Afferent and efferent connections of the laterodorsal tegmental nucleus in the rat. *Brain Res Bull*, **25**, 271-284.

Cote, P.Y. & Parent, A. (1992) Calbindin D-28k and choline acetyltransferase are expressed by different neuronal populations in pedunculopontine nucleus but not in nucleus basalis in squirrel monkeys. *Brain Res*, **593**, 245-252.

Cragg, S.J., Baufreton, J., Xue, Y., Bolam, J.P. & Bevan, M.D. (2004) Synaptic release of dopamine in the subthalamic nucleus. *Eur J Neurosci*, **20**, 1788-1802.

Damier, P., Hirsch, E.C., Agid, Y. & Graybiel, A.M. (1999a) The substantia nigra of the human brain. I. Nigrosomes and the nigral matrix, a compartmental organization based on calbindin D(28K) immunohistochemistry. *Brain*, **122**, 1421-1436.

Damier, P., Hirsch, E.C., Agid, Y. & Graybiel, A.M. (1999b) The substantia nigra of the human brain. II. Patterns of loss of dopamine-containing neurons in Parkinson's disease. *Brain*, **122**, 1437-1448.

Datta, S. & Siwek, D.F. (1997) Excitation of the brain stem pedunculopontine tegmentum cholinergic cells induces wakefulness and REM sleep. *J Neurophysiol*, **77**, 2975-2988.

DeLong, M.R. (1990) Primate models of movement disorders of basal ganglia origin. *Trends in Neurosciences*, **13**, 281-285.

Den, H.J.W. & Bethlem, J. (1960) The distribution of Lewy bodies in the central and autonomic nervous systems in idiopathic paralysis agitans. *J Neurol Neurosurg Psychiatry*, **23**, 283-290.

Dragunow, M. & Faull, R. (1989) The use of c-fos as a metabolic marker in neuronal pathway tracing. *J Neurosci Methods*, **29**, 261-265.

Duchemin, A.M., Gudehithlu, K.P., Neff, N.H. & Hadjiconstantinou, M. (1992) c-fos mRNA in mouse brain after MPTP treatment. *Neurochem Int*, **20**, 281-287.

Duda, J.E., Lee, V.M. & Trojanowski, J.Q. (2000) Neuropathology of synuclein aggregates. *J Neurosci Res*, **61**, 121-127.

Dun, N.J., Dun, S.L. & Forstermann, U. (1994) Nitric oxide synthase immunoreactivity in rat pontine medullary neurons. *Neuroscience*, **59**, 429-445.

Dun, N.J., Dun, S.L., Hwang, L.L. & Forstermann, U. (1995) Infrequent co-existence of nitric oxide synthase and parvalbumin, calbindin and calretinin immunoreactivity in rat pontine neurons. *Neurosci Lett*, **191**, 165-168.

Eckenstein, F. & Thoenen, H. (1982) Production of specific antisera and monoclonal antibodies to choline acetyltransferase: characterization and use for identification of cholinergic neurons. *EMBO J*, **1**, 363-368.

Edley, S.M. & Graybiel, A.M. (1983) The afferent and efferent connections of the feline nucleus tegmenti pedunculopontinus, pars compacta. *J Comp Neurol*, **217**, 187-215.

el Mansari, M., Sakai, K. & Jouvet, M. (1989) Unitary characteristics of presumptive cholinergic tegmental neurons during the sleep-waking cycle in freely moving cats. *Exp Brain Res*, **76**, 519-529.

el Mansari, M., Sakai, K. & Jouvet, M. (1990) Responses of presumed cholinergic mesopontine tegmental neurons to carbachol microinjections in freely moving cats. *Exp Brain Res*, **83**, 115-123.

El Mestikawy, S., Wallen-Mackenzie, A., Fortin, G.M., Descarries, L. & Trudeau, L.E. (2011) From glutamate co-release to vesicular synergy: vesicular glutamate transporters. *Nat Rev Neurosci*, **12**, 204-216.

Erlander, M.G., Tillakaratne, N.J.K., Feldblum, S., Patel, N. & Tobin, A.J. (1991) Two genes encode distinct glutamate decarboxylases. *Neuron*, **7**, 91-100.

Erro, E., Lanciego, J.L. & Gimenez-Amaya, J.M. (1999) Relationships between thalamostriatal neurons and pedunculopontine projections to the thalamus: a neuroanatomical tract-tracing study in the rat. *Exp Brain Res*, **127**, 162-170.

Fearnley, J.M. & Lees, A.J. (1991) Ageing and Parkinson's disease: substantia nigra regional selectivity. *Brain*, **114**, 2283-2301.

Feger, J., Hammond, C. & Rouzaire-Dubois, B. (1979) Pharmacological properties of acetylcholine-induced excitation of subthalamic nucleus neurones. *Br J Pharmacol*, **65**, 511-515.

Florio, T., Scarnati, E., Confalone, G., Minchella, D., Galati, S., Stanzione, P., Stefani, A. & Mazzone, P. (2007) High-frequency stimulation of the subthalamic nucleus modulates the activity of pedunculopontine neurons through direct activation of excitatory fibres as well as through indirect activation of inhibitory pallidal fibres in the rat. *Eur J Neurosci*, **25**, 1174-1186.

Ford, B., Holmes, C.J., Mainville, L. & Jones, B.E. (1995) GABAergic neurons in the rat pontomesencephalic tegmentum: codistribution with cholinergic and other tegmental neurons projecting to the posterior lateral hypothalamus. *J Comp Neurol*, **363**, 177-196.

Fortin, M. & Parent, A. (1996) Calretinin as a marker of specific neuronal subsets in primate substantia nigra and subthalamic nucleus. *Brain Res*, **708**, 201-204.

Fortin, M. & Parent, A. (1999) Calretinin-immunoreactive neurons in primate pedunculopontine and laterodorsal tegmental nuclei. *Neuroscience*, **88**, 535-547.

Fremeau, R.T., Jr., Burman, J., Qureshi, T., Tran, C.H., Proctor, J., Johnson, J., Zhang, H., Sulzer, D., Copenhagen, D.R., Storm-Mathisen, J., Reimer, R.J., Chaudhry, F.A. & Edwards, R.H. (2002) The identification of vesicular glutamate transporter 3 suggests novel modes of signaling by glutamate. *Proc Natl Acad Sci U S A*, **99**, 14488-14493.

Fremeau, R.T., Jr., Voglmaier, S., Seal, R.P. & Edwards, R.H. (2004) VGLUTs define subsets of excitatory neurons and suggest novel roles for glutamate. *Trends in Neurosciences*, **27**, 98-103.

Fremeau, R.T., Troyer, M.D., Pahner, I., Nygaard, G.O., Tran, C.H., Reimer, R.J., Bellocchio, E.E., Fortin, D., Storm-Mathisen, J. & Edwards, R.H. (2001) The expression of vesicular glutamate transporters defines two classes of excitatory synapse. *Neuron*, **31**, 247-260.

Futami, T., Takakusaki, K. & Kitai, S.T. (1995) Glutamatergic and cholinergic inputs from the pedunculopontine tegmental nucleus to dopamine neurons in the substantia nigra pars compacta. *Neurosci Res*, **21**, 331-342.

Garcia-Rill, E. (1986) The basal ganglia and the locomotor regions. *Brain Research*, **396**, 47-63.

Garcia-Rill, E. (1991) The pedunculopontine nucleus. *Prog Neurobiol*, **36**, 363-389.

Garcia-Rill, E., Houser, C.R., Skinner, R.D., Smith, W. & Woodward, D.J. (1987) Locomotion-inducing sites in the vicinity of the pedunculopontine nucleus. *Brain Res Bull*, **18**, 731-738.

Garcia-Rill, E., Kinjo, N., Atsuta, Y., Ishikawa, Y., Webber, M. & Skinner, R.D. (1990) Posterior midbrain-induced locomotion. *Brain Research Bulletin*, **24**, 499-508.

Garcia-Rill, E., Simon, C., Smith, K., Kezunovic, N. & Hyde, J. (2011) The pedunculopontine tegmental nucleus: from basic neuroscience to neurosurgical applications. *Journal of Neural Transmission*, **118**, 1397-1407.

Garcia-Rill, E. & Skinner, R.D. (1987a) The mesencephalic locomotor region. I. Activation of a medullary projection site. *Brain Res*, **411**, 1-12.

Garcia-Rill, E. & Skinner, R.D. (1987b) The mesencephalic locomotor region. II. Projections to reticulospinal neurons. *Brain Res*, **411**, 13-20.

Garcia-Rill, E. & Skinner, R.D. (1988) Modulation of rhythmic function in the posterior midbrain. *Neuroscience*, **27**, 639-654.

Garcia-Rill, E., Skinner, R.D., Miyazato, H. & Homma, Y. (2001) Pedunculopontine stimulation induces prolonged activation of pontine reticular neurons. *Neuroscience*, **104**, 455-465.

Geisler, S. & Zahm, D.S. (2005) Afferents of the ventral tegmental area in the rat-anatomical substratum for integrative functions. *J Comp Neurol*, **490**, 270-294.

German, D.C., Manaye, K.F., Sonsalla, P.K. & Brooks, B.A. (1992) Midbrain dopaminergic cell loss in Parkinson's disease and MPTP-induced parkinsonism: sparing of calbindin-D28k-containing cells. *Ann N Y Acad Sci*, **648**, 42-62.

Gonya-Magee, T. & Anderson, M.E. (1983) An electrophysiological characterization of projections from the pedunculopontine area to entopeduncular nucleus and globus pallidus in the cat. *Exp Brain Res*, **49**, 269-279.

Good, C.H. & Lupica, C.R. (2009) Properties of distinct ventral tegmental area synapses activated via pedunculopontine or ventral tegmental area stimulation in vitro. *J Physiol*, **587**, 1233-1247.

Gould, E., Woolf, N.J. & Butcher, L.L. (1989) Cholinergic projections to the substantia nigra from the pedunculopontine and laterodorsal tegmental nuclei. *Neuroscience*, **28**, 611-623.

Granata, A.R. & Kitai, S.T. (1989) Intracellular analysis of excitatory subthalamic inputs to the pedunculopontine neurons. *Brain Research*, **488**, 57-72.

Granata, A.R. & Kitai, S.T. (1991) Inhibitory substantia nigra inputs to the pedunculopontine neurons. *Exp Brain Res*, **86**, 459-466.

Gras, C., Herzog, E., Bellenchi, G.C., Bernard, V., Ravassard, P., Pohl, M., Gasnier, B., Giros, B. & El Mestikawy, S. (2002) A third vesicular glutamate transporter expressed by cholinergic and serotoninergic neurons. *J Neurosci*, **22**, 5442-5451.

Graybiel, A.M. (1998) The basal ganglia and chunking of action repertoires. *Neurobiology of Learning & Memory*, **70**, 119-136.

Graybiel, A.M., Aosaki, T., Flaherty, A.W. & Kimura, M. (1994) The basal ganglia and adaptive motor control. *Science*, **265**, 1826-1831.

Greene, R.W., Gerber, U. & McCarley, R.W. (1989) Cholinergic activation of medial pontine reticular formation neurons in vitro. *Brain Res*, **476**, 154-159.

Greer, P.L. & Greenberg, M.E. (2008) From synapse to nucleus: calcium-dependent gene transcription in the control of synapse development and function. *Neuron*, **59**, 846-860.

Grillner, S., Wallen, P., Saitoh, K., Kozlov, A. & Robertson, B. (2008) Neural bases of goal-directed locomotion in vertebrates--an overview. *Brain Res Rev*, **57**, 2-12.

Gritti, I., Manns, I.D., Mainville, L. & Jones, B.E. (2003) Parvalbumin, calbindin, or calretinin in cortically projecting and GABAergic, cholinergic, or glutamatergic basal forebrain neurons of the rat. *J Comp Neurol*, **458**, 11-31.

Grofova, I. & Keane, S. (1991) Descending brainstem projections of the pedunculopontine tegmental nucleus in the rat. *Anat Embryol (Berl)*, **184**, 275-290.

Grofova, I. & Zhou, M. (1998) Nigral innervation of cholinergic and glutamatergic cells in the rat mesopontine tegmentum: light and electron microscopic anterograde tracing and immunohistochemical studies. *J Comp Neurol*, **395**, 359-379.

Gulyas, A.I., Toth, K., Danos, P. & Freund, T.F. (1991) Subpopulations of GABAergic neurons containing parvalbumin, calbindin D28k, and cholecystokinin in the rat hippocampus. *J Comp Neurol*, **312**, 371-378.

Haber, S.N., Lynd, E., Klein, C. & Groenewegen, H.J. (1990) Topographic organization of the ventral striatal efferent projections in the rhesus monkey: an anterograde tracing study. *J Comp Neurol*, **293**, 282-298.

Hall, W.C., Fitzpatrick, D., Klatt, L.L. & Raczkowski, D. (1989) Cholinergic innervation of the superior colliculus in the cat. *J Comp Neurol*, **287**, 495-514.

Hallanger, A.E., Levey, A.I., Lee, H.J., Rye, D.B. & Wainer, B.H. (1987) The origins of cholinergic and other subcortical afferents to the thalamus in the rat. *J Comp Neurol*, **262**, 105-124.

Hallanger, A.E. & Wainer, B.H. (1988a) Ascending projections from the pedunculopontine tegmental nucleus and the adjacent mesopontine tegmentum in the rat. *J Comp Neurol*, **274**, 483-515.

Hallanger, A.E. & Wainer, B.H. (1988b) Ultrastructure of ChAT-immunoreactive synaptic terminals in the thalamic reticular nucleus of the rat. *J Comp Neurol*, **278**, 486-497.

Hamani, C., Stone, S., Laxton, A. & Lozano, A.M. (2007) The pedunculopontine nucleus and movement disorders: anatomy and the role for deep brain stimulation. *Parkinsonism & related disorders*, **13 Suppl 3**, S276-280.

Hammond, C., Rouzaire-Dubois, B., Feger, J., Jackson, A. & Crossman, A.R. (1983) Anatomical and electrophysiological studies on the reciprocal projections between the subthalamic nucleus and nucleus tegmenti pedunculopontinus in the rat. *Neuroscience*, **9**, 41-52.

Hassani, O.K., Francois, C., Yelnik, J. & Feger, J. (1997) Evidence for a dopaminergic innervation of the subthalamic nucleus in the rat. *Brain Res*, **749**, 88-94.

Hazrati, L.N. & Parent, A. (1992) Projection from the deep cerebellar nuclei to the pedunculopontine nucleus in the squirrel monkey. *Brain Res*, **585**, 267-271.

Heizmann, C.W. (1984a) Parvalbumin, a relaxing factor in muscle and a neuronal marker in brain. *Prog Clin Biol Res*, **168**, 205-210.

Heizmann, C.W. (1984b) Parvalbumin, an intracellular calcium-binding protein; distribution, properties and possible roles in mammalian cells. *Experientia*, **40**, 910-921.

Herdegen, T. & Leah, J.D. (1998) Inducible and constitutive transcription factors in the mammalian nervous system: control of gene expression by Jun, Fos and Krox, and CREB/ATF proteins. *Brain Res Brain Res Rev*, **28**, 370-490.

Herrero, M.T., Hirsch, E.C., Javoy-Agid, F., Obeso, J.A. & Agid, Y. (1993) Differential vulnerability to 1-methyl-4-phenyl-1,2,3,6-tetrahydropyridine of dopaminergic and

cholinergic neurons in the monkey mesopontine tegmentum. *Brain Res*, **624**, 281-285.

Herzog, E., Bellenchi, G.C., Gras, C., Bernard, V., Ravassard, P., Bedet, C., Gasnier, B., Giros, B. & El Mestikawy, S. (2001) The existence of a second vesicular glutamate transporter specifies subpopulations of glutamatergic neurons. *J Neurosci*, **21**, RC181.

Hirsch, E.C., Graybiel, A.M., Duyckaerts, C. & Javoy-Agid, F. (1987) Neuronal loss in the pedunculopontine tegmental nucleus in Parkinson disease and in progressive supranuclear palsy. *Proc Natl Acad Sci U S A*, **84**, 5976-5980.

Hirsch, E.C., Perier, C., Orieux, G., Francois, C., Feger, J., Yelnik, J., Vila, M., Levy, R., Tolosa, E.S., Marin, C., Trinidad Herrero, M., Obeso, J.A. & Agid, Y. (2000) Metabolic effects of nigrostriatal denervation in basal ganglia. *Trends in neurosciences*, **23**, S78-85.

Hisano, S., Sawada, K., Kawano, M., Kanemoto, M., Xiong, G., Mogi, K., Sakata-Haga, H., Takeda, J., Fukui, Y. & Nogami, H. (2002) Expression of inorganic phosphate/vesicular glutamate transporters (BNPI/VGLUT1 and DNPI/VGLUT2) in the cerebellum and precerebellar nuclei of the rat. *Brain Res Mol Brain Res*, **107**, 23-31.

Hoshino, K., Hicks, T.P., Meguro, R., Hirano, S., Kase, M. & Norita, M. (1997) Cholinergic innervation of the lateralis medialis-suprageniculate nuclear complex

(LM-Sg) of the cat's thalamus: a double labeling immunohistochemical study. *Brain Res*, **747**, 151-155.

Hoshino, K., Katoh, Y.Y., Bai, W., Kaiya, T. & Norita, M. (2000) Distribution of terminals from pedunculopontine tegmental nucleus and synaptic organization in lateralis medialis-suprageniculate nucleus of cat's thalamus: anterograde tracing, immunohistochemical studies, and quantitative analysis. *Vis Neurosci*, **17**, 893-904.

Hoshino, K., Nagy, A., Eordegh, G., Benedek, G. & Norita, M. (2004) Two types of neuron are found within the PPT, a small percentage of which project to both the LM-SG and SC. *Exp Brain Res*, **155**, 421-426.

Hudson, J.L., van Horne, C.G., Stromberg, I., Brock, S., Clayton, J., Masserano, J., Hoffer, B.J. & Gerhardt, G.A. (1993) Correlation of apomorphine- and amphetamine-induced turning with nigrostriatal dopamine content in unilateral 6-hydroxydopamine lesioned rats. *Brain Res*, **626**, 167-174.

Hughes, P. & Dragunow, M. (1995) Induction of immediate-early genes and the control of neurotransmitter-regulated gene expression within the nervous system. *Pharmacol Rev*, **47**, 133-178.

Inglis, W.L., Olmstead, M.C. & Robbins, T.W. (2001) Selective deficits in attentional performance on the 5-choice serial reaction time task following pedunculopontine tegmental nucleus lesions. *Behav Brain Res*, **123**, 117-131.

Inglis, W.L. & Winn, P. (1995) The pedunculopontine tegmental nucleus: where the striatum meets the reticular formation. *Progress in Neurobiology*, **47**, 1-29.

Jackson, A. & Crossman, A.R. (1981) Subthalamic projection to nucleus tegmenti pedunculopontinus in the rat. *Neurosci Lett*, **22**, 17-22.

Jackson, A. & Crossman, A.R. (1983) Nucleus tegmenti pedunculopontinus: efferent connections with special reference to the basal ganglia, studied in the rat by anterograde and retrograde transport of horseradish peroxidase. *Neuroscience*, **10**, 725-765.

Jenkins, R., O'Shea, R., Thomas, K.L. & Hunt, S.P. (1993) c-jun expression in substantia nigra neurons following striatal 6-hydroxydopamine lesions in the rat. *Neuroscience*, **53**, 447-455.

Jenkinson, N., Nandi, D., Aziz, T.Z. & Stein, J.F. (2005) Pedunculopontine nucleus: a new target for deep brain stimulation for akinesia. *Neuroreport*, **16**, 1875-1876.

Jenkinson, N., Nandi, D., Miall, R.C., Stein, J.F. & Aziz, T.Z. (2004) Pedunculopontine nucleus stimulation improves akinesia in a Parkinsonian monkey. *Neuroreport*, **15**, 2621-2624.

Jenkinson, N., Nandi, D., Muthusamy, K., Ray, N.J., Gregory, R., Stein, J.F. & Aziz, T.Z. (2009) Anatomy, physiology, and pathophysiology of the pedunculopontine nucleus. *Mov Disord*, **24**, 319-328.

Jenkinson, N., Nandi, D., Oram, R., Stein, J.F. & Aziz, T.Z. (2006) Pedunculopontine nucleus electric stimulation alleviates akinesia independently of dopaminergic mechanisms. *Neuroreport*, **17**, 639-641.

Jensen, P.H. & Gai, W.P. (2001) Alpha-synuclein. Axonal transport, ligand interaction and neurodegeneration. *Adv Exp Med Biol*, **487**, 129-134.

Jhou, T.C., Geisler, S., Marinelli, M., Degarmo, B.A. & Zahm, D.S. (2009) The mesopontine rostromedial tegmental nucleus: A structure targeted by the lateral habenula that projects to the ventral tegmental area of Tsai and substantia nigra compacta. *J Comp Neurol*, **513**, 566-596.

Jones, B.E. (1991) Paradoxical Sleep and Its Chemical Structural Substrates in the Brain. *Neuroscience*, **40**, 637-656.

Jones, B.E. (2005) From waking to sleeping: neuronal and chemical substrates. *Trends Pharmacol Sci*, **26**, 578-586.

Jones, B.E. & Webster, H.H. (1988) Neurotoxic lesions of the dorsolateral pontomesencephalic tegmentum-cholinergic cell area in the cat. I. Effects upon the cholinergic innervation of the brain. *Brain Res*, **451**, 13-32.

Jones, B.E. & Yang, T.Z. (1985) The efferent projections from the reticular formation and the locus coeruleus studied by anterograde and retrograde axonal transport in the rat. *J Comp Neurol*, **242**, 56-92.

Kaneko, T. & Fujiyama, F. (2002) Complementary distribution of vesicular glutamate transporters in the central nervous system. *Neurosci Res*, **42**, 243-250.

Kaneko, T., Fujiyama, F. & Hioki, H. (2002) Immunohistochemical localization of candidates for vesicular glutamate transporters in the rat brain. *J Comp Neurol*, **444**, 39-62.

Katz, L.C., Burkhalter, A. & Dreyer, W.J. (1984) Fluorescent latex microspheres as a retrograde neuronal marker for in vivo and in vitro studies of visual cortex. *Nature*, **310**, 498-500.

Katz, L.C. & Iarovici, D.M. (1990) Green fluorescent latex microspheres: a new retrograde tracer. *Neuroscience*, **34**, 511-520.

Kaufling, J., Veinante, P., Pawlowski, S.A., Freund-Mercier, M.J. & Barrot, M. (2009) Afferents to the GABAergic tail of the ventral tegmental area in the rat. *J Comp Neurol*, **513**, 597-621.

Kemp, J.M. & Powell, T.P.S. (1971) The synaptic organization of the caudate nucleus. *Phil. Trans. R. Soc. Lond. B.*, **262**, 403-412.

Kinjo, N., Atsuta, Y., Webber, M., Kyle, R., Skinner, R.D. & Garcia-Rill, E. (1990) Medioventral medulla-induced locomotion. *Brain Res Bull*, **24**, 509-516.

Kiss, J., Magloczky, Z., Somogyi, J. & Freund, T.F. (1997) Distribution of calretinin-containing neurons relative to other neurochemically identified cell types in the medial septum of the rat. *Neuroscience*, **78**, 399-410.

Kita, H. & Kitai, S.T. (1987) Efferent projections of the subthalamic nucleus in the rat: light and electron microscopic analysis with the PHA-L method. *J Comp Neurol*, **260**, 435-452.

Kita, H. & Kitai, S.T. (1988) Glutamate decarboxylase immunoreactive neurons in rat neostriatum: their morphological types and populations. *Brain Res*, **447**, 346-352.

Kita, T. & Kita, H. (2010) Cholinergic and non-cholinergic mesopontine tegmental neurons projecting to the subthalamic nucleus in the rat. *Eur J Neurosci*, **33**, 433-443.

Klausberger, T., Magill, P.J., Marton, L.F., Roberts, J.D., Cobden, P.M., Buzsaki, G. & Somogyi, P. (2003) Brain-state- and cell-type-specific firing of hippocampal interneurons in vivo. *Nature*, **421**, 844-848.

Klausberger, T. & Somogyi, P. (2008) Neuronal diversity and temporal dynamics: the unity of hippocampal circuit operations. *Science*, **321**, 53-57.

Kobayashi, K., Hoshino, K., Homma, S., Takagi, S. & Norita, M. (2007) A possible monosynaptic pathway links the pedunculopontine tegmental nucleus to thalamostriatal neurons in the hooded rat. *Arch Histol Cytol*, **70**, 207-214.

Kobayashi, S. & Nakamura, Y. (2003) Synaptic organization of the rat parafascicular nucleus, with special reference to its afferents from the superior colliculus and the pedunculopontine tegmental nucleus. *Brain Res*, **980**, 80-91.

Kobbert, C., Apps, R., Bechmann, I., Lanciego, J.L., Mey, J. & Thanos, S. (2000) Current concepts in neuroanatomical tracing. *Prog Neurobiol*, **62**, 327-351.

Kolmac, C.I. & Mitrofanis, J. (1998) Patterns of brainstem projection to the thalamic reticular nucleus. *J Comp Neurol*, **396**, 531-543.

Kolmac, C.I., Power, B.D. & Mitrofanis, J. (1998) Patterns of connections between zona incerta and brainstem in rats. *J Comp Neurol*, **396**, 544-555.

Krauthamer, G.M., Grunwerg, B.S. & Krein, H. (1995) Putative cholinergic neurons of the pedunculopontine tegmental nucleus projecting to the superior colliculus consist of sensory responsive and unresponsive populations which are functionally distinct from other mesopontine neurons. *Neuroscience*, **69**, 507-517.

Kretsinger, R.H. & Nockolds, C.E. (1973) Carp muscle calcium-binding protein. II. Structure determination and general description. *J Biol Chem*, **248**, 3313-3326.

Kringelbach, M.L., Jenkinson, N., Owen, S.L. & Aziz, T.Z. (2007) Translational principles of deep brain stimulation. *Nat Rev Neurosci*, **8**, 623-635.

Krout, K.E., Belzer, R.E. & Loewy, A.D. (2002) Brainstem projections to midline and intralaminar thalamic nuclei of the rat. *J Comp Neurol*, **448**, 53-101.

Lanciego, J.L. & Wouterlood, F.G. (2011) A half century of experimental neuroanatomical tracing. *J Chem Neuroanat*, **42**, 157-183.

Lavoie, B. & Parent, A. (1994a) Pedunculopontine nucleus in the squirrel monkey: cholinergic and glutamatergic projections to the substantia nigra. *J Comp Neurol*, **344**, 232-241.

Lavoie, B. & Parent, A. (1994b) Pedunculopontine nucleus in the squirrel monkey: cholinergic and glutamatergic projections to the substantia nigra. *J Comp Neurol*, **344**, 232-241.

Lavoie, B. & Parent, A. (1994c) Pedunculopontine nucleus in the squirrel monkey: projections to the basal ganglia as revealed by anterograde tract-tracing methods. *J Comp Neurol*, **344**, 210-231.

Leonard, C.S., Kerman, I., Blaha, G., Taveras, E. & Taylor, B. (1995) Interdigitation of nitric oxide synthase-, tyrosine hydroxylase-, and serotonin-containing neurons in

and around the laterodorsal and pedunculopontine tegmental nuclei of the guinea pig. *J Comp Neurol*, **362**, 411-432.

Leonard, C.S. & Llinas, R. (1994) Serotonergic and cholinergic inhibition of mesopontine cholinergic neurons controlling REM sleep: an in vitro electrophysiological study. *Neuroscience*, **59**, 309-330.

Leonard, T.O. & Lydic, R. (1997) Pontine nitric oxide modulates acetylcholine release, rapid eye movement sleep generation, and respiratory rate. *J Neurosci*, **17**, 774-785.

Liu, H.M., Gao, J., Miao, H., Xiao, C.H., Sun, Y., Du, X., Yuan, H.H., Yu, H.L. & Gao, D.S. (2009) Influence of aging on the calbindin-D-28k immunoreactive positive dopaminergic neurons in the substantia nigra pars compacta of rats. *Neurosci Lett*, **468**, 3-6.

Losier, B.J. & Semba, K. (1993) Dual projections of single cholinergic and aminergic brainstem neurons to the thalamus and basal forebrain in the rat. *Brain Res*, **604**, 41-52.

Lozano, A.M. (2001) Deep brain stimulation for Parkinson's disease. *Parkinsonism Relat Disord*, **7**, 199-203.

Lozano, A.M. & Snyder, B.J. (2008) Deep brain stimulation for parkinsonian gait disorders. *J Neurol*, **255 Suppl 4**, 30-31.

Lydic, R. & Baghdoyan, H.A. (1993) Pedunculopontine stimulation alters respiration and increases ACh release in the pontine reticular formation. *Am J Physiol*, **264**, R544-554.

Marin, O., Smeets, W.J. & Gonzalez, A. (1998) Evolution of the basal ganglia in tetrapods: a new perspective based on recent studies in amphibians. *Trends Neurosci*, **21**, 487-494.

Masdeu, J.C., Alampur, U., Cavaliere, R. & Tavoulareas, G. (1994) Astasia and gait failure with damage of the pontomesencephalic locomotor region. *Ann Neurol*, **35**, 619-621.

Matsuda, W., Furuta, T., Nakamura, K.C., Hioki, H., Fujiyama, F., Arai, R. & Kaneko, T. (2009) Single nigrostriatal dopaminergic neurons form widely spread and highly dense axonal arborizations in the neostriatum. *J Neurosci*, **29**, 444-453.

Matsumura, M., Nambu, A., Yamaji, Y., Watanabe, K., Imai, H., Inase, M., Tokuno, H. & Takada, M. (2000) Organization of somatic motor inputs from the frontal lobe to the pedunculopontine tegmental nucleus in the macaque monkey. *Neuroscience*, **98**, 97-110.

Mazzone, P., Lozano, A., Stanzione, P., Galati, S., Scarnati, E., Peppe, A. & Stefani, A. (2005) Implantation of human pedunculopontine nucleus: a safe and clinically relevant target in Parkinson's disease. *Neuroreport*, **16**, 1877-1881.

Mena-Segovia, J. & Bolam, J.P. (2011) Phasic modulation of cortical high-frequency oscillations by pedunculopontine neurons. *Prog Brain Res*, **193**, 85-92.

Mena-Segovia, J., Bolam, J.P. & Magill, P.J. (2004a) Pedunculopontine nucleus and basal ganglia: distant relatives or part of the same family? *Trends in Neurosciences*, **27**, 585-588.

Mena-Segovia, J., Favila, R. & Giordano, M. (2004b) Long-term effects of striatal lesions on c-Fos immunoreactivity in the pedunculopontine nucleus. *Eur J Neurosci*, **20**, 2367-2376.

Mena-Segovia, J., Micklem, B.R., Nair-Roberts, R.G., Ungless, M.A. & Bolam, J.P. (2009) GABAergic neuron distribution in the pedunculopontine nucleus defines functional subterritories. *J Comp Neurol*, **515**, 397-408.

Mena-Segovia, J., Ross, H.M., Magill, P.J. & Bolam, J.P. (2005) The pedunculopontine nucleus: Towards a functional integration with the basal ganglia. In Bolam, J.P., Ingham, C., Magill, P.J. (eds) *The Basal Ganglia VIII*. Springer Science and Business Media, New York, pp. 533-544.

Mena-Segovia, J., Ross, H.M., Magill, P.J. & Bolam, J.P. (2006) Correlation of morphological and physiological properties of cholinergic and non-cholinergic neurons in the pedunculopontine nucleus (PPN). Society for Neuroscience 2006, Atlanta, GA. Program No. 450.6. 2006. Neuroscience Meeting Planner: Online.

Mena-Segovia, J., Sims, H.M., Magill, P.J. & Bolam, J.P. (2008a) Cholinergic brainstem neurons modulate cortical gamma activity during slow oscillations. *J Physiol*, **586**, 2947-2960.

Mena-Segovia, J., Winn, P. & Bolam, J.P. (2008b) Cholinergic modulation of midbrain dopaminergic systems. *Brain Res Rev*, **58**, 265-271.

Mesulam, M.M., Geula, C., Bothwell, M.A. & Hersh, L.B. (1989) Human reticular formation: cholinergic neurons of the pedunculopontine and laterodorsal tegmental nuclei and some cytochemical comparisons to forebrain cholinergic neurons. *J Comp Neurol*, **283**, 611-633.

Mesulam, M.M., Mufson, E.J., Wainer, B.H. & Levey, A.I. (1983) Central cholinergic pathways in the rat: an overview based on an alternative nomenclature (Ch1-Ch6). *Neuroscience*, **10**, 1185-1201.

Mimura, Y., Mogi, K., Kawano, M., Fukui, Y., Takeda, J., Nogami, H. & Hisano, S. (2002) Differential expression of two distinct vesicular glutamate transporters in the rat retina. *Neuroreport*, **13**, 1925-1928.

Mitani, A., Ito, K., Hallanger, A.E., Wainer, B.H., Kataoka, K. & McCarley, R.W. (1988) Cholinergic projections from the laterodorsal and pedunculopontine tegmental nuclei to the pontine gigantocellular tegmental field in the cat. *Brain Res*, **451**, 397-402.

Mitchell, I.J., Clarke, C.E., Boyce, S., Robertson, R.G., Peggs, D., Sambrook, M.A. & Crossman, A.R. (1989) Neural mechanisms underlying parkinsonian symptoms based upon regional uptake of 2-deoxyglucose in monkeys exposed to 1-methyl-4-phenyl-1,2,3,6-tetrahydropyridine. *Neuroscience*, **32**, 213-226.

Moriizumi, T. & Hattori, T. (1992) Separate neuronal populations of the rat globus pallidus projecting to the subthalamic nucleus, auditory cortex and pedunculopontine tegmental area. *Neuroscience*, **46**, 701-710.

Moro, E., Hamani, C., Poon, Y.Y., Al-Khairallah, T., Dostrovsky, J.O., Hutchison, W.D. & Lozano, A.M. (2010) Unilateral pedunculopontine stimulation improves falls in Parkinson's disease. *Brain*, **133**, 215-224.

Morris, M.E., Iansek, R., Matyas, T.A. & Summers, J.J. (1994) The pathogenesis of gait hypokinesia in Parkinson's disease. *Brain*, **117 (Pt 5)**, 1169-1181.

Morris, M.E., Matyas, T.A., Iansek, R. & Summers, J.J. (1996) Temporal stability of gait in Parkinson's disease. *Phys Ther*, **76**, 763-777; discussion 778-780.

Moss, J.B., J.P. (2009) The realationship between dopaminergic axons and glutamatergic synapses in the striatum: structural considerations. In Iversen, L., Iversen, S., Dunnett, S., Bjorklund, A. (eds) *Dopamine Handbook*. Oxford University Press, New York, pp. 49-59.

Motts, S.D. & Schofield, B.R. (2009) Sources of cholinergic input to the inferior colliculus. *Neuroscience*, **160**, 103-114.

Mouatt-Prigent, A., Agid, Y. & Hirsch, E.C. (1994) Does the calcium binding protein calretinin protect dopaminergic neurons against degeneration in Parkinson's disease? *Brain Res*, **668**, 62-70.

Muthusamy, K.A., Aravamuthan, B.R., Kringelbach, M.L., Jenkinson, N., Voets, N.L., Johansen-Berg, H., Stein, J.F. & Aziz, T.Z. (2007) Connectivity of the human pedunculopontine nucleus region and diffusion tensor imaging in surgical targeting. *J Neurosurg*, **107**, 814-820.

Nagerl, U.V., Novo, D., Mody, I. & Vergara, J.L. (2000) Binding kinetics of calbindin-D(28k) determined by flash photolysis of caged Ca(2+). *Biophys J*, **79**, 3009-3018.

Nakamura, Y., Tokuno, H., Moriizumi, T., Kitao, Y. & Kudo, M. (1989) Monosynaptic nigral inputs to the pedunculopontine tegmental nucleus neurons which send their axons to the medial reticular formation in the medulla oblongata. An electron microscopic study in the cat. *Neurosci Lett*, **103**, 145-150.

Nakano, K., Hasegawa, Y., Tokushige, A., Nakagawa, S., Kayahara, T. & Mizuno, N. (1990) Topographical projections from the thalamus, subthalamic nucleus and pedunculopontine tegmental nucleus to the striatum in the Japanese monkey, Macaca fuscata. *Brain Res*, **537**, 54-68.

Nandi, D., Aziz, T.Z., Giladi, N., Winter, J. & Stein, J.F. (2002a) Reversal of akinesia in experimental parkinsonism by GABA antagonist microinjections in the pedunculopontine nucleus. *Brain*, **125**, 2418-2430.

Nandi, D., Aziz, T.Z., Liu, X. & Stein, J.F. (2002b) Brainstem motor loops in the control of movement. *Mov Disord*, **17 Suppl 3**, S22-27.

Nandi, D., Jenkinson, N., Stein, J. & Aziz, T. (2008) The pedunculopontine nucleus in Parkinson's disease: primate studies. *Br J Neurosurg*, **22 Suppl 1**, S4-8.

Nandi, D., Liu, X., Winter, J.L., Aziz, T.Z. & Stein, J.F. (2002c) Deep brain stimulation of the pedunculopontine region in the normal non-human primate. *J Clin Neurosci*, **9**, 170-174.

Nauta, H.J. & Cole, M. (1978) Efferent projections of the subthalamic nucleus: an autoradiographic study in monkey and cat. *J Comp Neurol*, **180**, 1-16.

Ni, B., Du, Y., Wu, X., DeHoff, B.S., Rosteck, P.R., Jr. & Paul, S.M. (1996) Molecular cloning, expression, and chromosomal localization of a human brain-specific Na(+)-dependent inorganic phosphate cotransporter. *J Neurochem*, **66**, 2227-2238.

Ni, B., Rosteck, P.R., Jr., Nadi, N.S. & Paul, S.M. (1994) Cloning and expression of a cDNA encoding a brain-specific Na(+)-dependent inorganic phosphate cotransporter. *Proc Natl Acad Sci U S A*, **91**, 5607-5611.

Noda, T. & Oka, H. (1984) Nigral inputs to the pedunculopontine region: intracellular analysis. *Brain Res*, **322**, 332-336.

Noda, T. & Oka, H. (1986) Distribution and morphology of tegmental neurons receiving nigral inhibitory inputs in the cat: an intracellular HRP study. *J Comp Neurol*, **244**, 254-266.

Nomura, S., Mizuno, N. & Sugimoto, T. (1980) Direct projections from the pedunculopontine tegmental nucleus to the subthalamic nucleus in the cat. *Brain Res*, **196**, 223-227.

Oakman, S.A., Faris, P.L., Cozzari, C. & Hartman, B.K. (1999) Characterization of the extent of pontomesencephalic cholinergic neurons' projections to the thalamus: comparison with projections to midbrain dopaminergic groups. *Neuroscience*, **94**, 529-547.

Oakman, S.A., Faris, P.L., Kerr, P.E., Cozzari, C. & Hartman, B.K. (1995) Distribution of pontomesencephalic cholinergic neurons projecting to substantia nigra differs significantly from those projecting to ventral tegmental area. *J Neurosci*, **15**, 5859-5869.

Olszewski, J., and D. Baxter (1982) *Cytoarchitecture of the Human Brain Ste*m*, 2nd ed.* S. Basel, New York.

Oorschot, D.E. (1996) Total number of neurons in the neostriatal, pallidal, subthalamic, and substantia nigra nuclei of the rat basal ganglia: a stereological study using the Cavalieri and optical disector methods. *J Comp Neurol*, **366**, 580-599.

Orieux, G., Francois, C., Feger, J., Yelnik, J., Vila, M., Ruberg, M., Agid, Y. & Hirsch, E.C. (2000) Metabolic activity of excitatory parafascicular and pedunculopontine inputs to the subthalamic nucleus in a rat model of Parkinson's disease. *Neuroscience*, **97**, 79-88.

Pahapill, P.A. & Lozano, A.M. (2000) The pedunculopontine nucleus and Parkinson's disease. *Brain*, **123 (Pt 9)**, 1767-1783.

Paladini, C.A., Celada, P. & Tepper, J.M. (1999) Striatal, pallidal, and pars reticulata evoked inhibition of nigrostriatal dopaminergic neurons is mediated by $GABA_A$ receptors *in vivo*. *Neuroscience*, **89**, 799-812.

Pallanck, L. & Greenamyre, J.T. (2006) Neurodegenerative disease: pink, parkin and the brain. *Nature*, **441**, 1058.

Panov, A., Dikalov, S., Shalbuyeva, N., Taylor, G., Sherer, T. & Greenamyre, J.T. (2005) Rotenone model of Parkinson disease: multiple brain mitochondria dysfunctions after short term systemic rotenone intoxication. *J Biol Chem*, **280**, 42026-42035.

Parent, A., Cote, P.Y. & Lavoie, B. (1995) Chemical anatomy of primate basal ganglia. *Prog Neurobiol*, **46**, 131-197.

Parent, A., Fortin, M., Cote, P.Y. & Cicchetti, F. (1996) Calcium-binding proteins in primate basal ganglia. *Neurosci Res*, **25**, 309-334.

Parent, M. & Descarries, L. (2008) Acetylcholine innervation of the adult rat thalamus: distribution and ultrastructural features in dorsolateral geniculate, parafascicular, and reticular thalamic nuclei. *J Comp Neurol*, **511**, 678-691.

Parent, M., Levesque, M. & Parent, A. (2001) Two types of projection neurons in the internal pallidum of primates: single-axon tracing and three-dimensional reconstruction. *J Comp Neurol*, **439**, 162-175.

Paxinos, G.H., Xu-Feng (1995) *Atlas of the human brainstem*. Academic Press, London.

Perese, D.A., Ulman, J., Viola, J., Ewing, S.E. & Bankiewicz, K.S. (1989) A 6-hydroxydopamine-induced selective parkinsonian rat model. *Brain Res*, **494**, 285-293.

Pierantozzi, M., Palmieri, M.G., Galati, S., Stanzione, P., Peppe, A., Tropepi, D., Brusa, L., Pisani, A., Moschella, V., Marciani, M.G., Mazzone, P. & Stefani, A. (2008) Pedunculopontine nucleus deep brain stimulation changes spinal cord excitability in Parkinson's disease patients. *J Neural Transm*, **115**, 731-735.

Plaha, P. & Gill, S.S. (2005) Bilateral deep brain stimulation of the pedunculopontine nucleus for Parkinson's disease. *Neuroreport*, **16**, 1883-1887.

Pochet, R., Parmentier, M., Lawson, D.E. & Pasteels, J.L. (1985) Rat brain synthesizes two 'vitamin D-dependent' calcium-binding proteins. *Brain Res*, **345**, 251-256.

Przedborski, S., Levivier, M., Jiang, H., Ferreira, M., Jackson-Lewis, V., Donaldson, D. & Togasaki, D.M. (1995) Dose-dependent lesions of the dopaminergic nigrostriatal pathway induced by intrastriatal injection of 6-hydroxydopamine. *Neuroscience*, **67**, 631-647.

Ranson, S.W. (1939) The anatomy of the nervous system from the standpoint of development and function. W. B. Saunders, Philadelphia.

Redgrave, P., Mitchell, I.J. & Dean, P. (1987) Descending projections from the superior colliculus in rat: a study using orthograde transport of wheatgerm-agglutinin conjugated horseradish peroxidase. *Exp Brain Res*, **68**, 147-167.

Reese, N.B., Garcia-Rill, E. & Skinner, R.D. (1995) The pedunculopontine nucleus--auditory input, arousal and pathophysiology. *Prog Neurobiol*, **47**, 105-133.

Resibois, A. & Rogers, J.H. (1992) Calretinin in rat brain: an immunohistochemical study. *Neuroscience*, **46**, 101-134.

Rohrbacher, J., Ichinohe, N. & Kitai, S.T. (2000) Electrophysiological characteristics of substantia nigra neurons in organotypic cultures: spontaneous and evoked activities. *Neuroscience*, **97**, 703-714.

Rolland, A.S., Tande, D., Herrero, M.T., Luquin, M.R., Vazquez-Claverie, M., Karachi, C., Hirsch, E.C. & Francois, C. (2009) Evidence for a dopaminergic innervation of the pedunculopontine nucleus in monkeys, and its drastic reduction after MPTP intoxication. *J Neurochem*, **110**, 1321-1329.

Ros, H., Magill, P.J., Moss, J., Bolam, J.P. & Mena-Segovia, J. (2010) Distinct types of non-cholinergic pedunculopontine neurons are differentially modulated during global brain states. *Neuroscience*, **170**, 78-91.

Rye, D.B., Lee, H.J., Saper, C.B. & Wainer, B.H. (1988) Medullary and spinal efferents of the pedunculopontine tegmental nucleus and adjacent mesopontine tegmentum in the rat. *J Comp Neurol*, **269**, 315-341.

Rye, D.B., Saper, C.B., Lee, H.J. & Wainer, B.H. (1987) Pedunculopontine tegmental nucleus of the rat: cytoarchitecture, cytochemistry, and some extrapyramidal connections of the mesopontine tegmentum. *J Comp Neurol*, **259**, 483-528.

Sachs, C. & Jonsson, G. (1975) Mechanisms of action of 6-hydroxydopamine. *Biochem Pharmacol*, **24**, 1-8.

Saitoh, K., Hattori, S., Song, W.J., Isa, T. & Takakusaki, K. (2003) Nigral GABAergic inhibition upon cholinergic neurons in the rat pedunculopontine tegmental nucleus. *Eur J Neurosci*, **18**, 879-886.

Sakai, K., el Mansari, M. & Jouvet, M. (1990) Inhibition by carbachol microinjections of presumptive cholinergic PGO-on neurons in freely moving cats. *Brain Res*, **527**, 213-223.

Sakata-Haga, H., Kanemoto, M., Maruyama, D., Hoshi, K., Mogi, K., Narita, M., Okado, N., Ikeda, Y., Nogami, H., Fukui, Y., Kojima, I., Takeda, J. & Hisano, S. (2001) Differential localization and colocalization of two neuron-types of sodium-dependent inorganic phosphate cotransporters in rat forebrain. *Brain Res*, **902**, 143-155.

Saper, C.B. & Loewy, A.D. (1982) Projections of the pedunculopontine tegmental nucleus in the rat: evidence for additional extrapyramidal circuitry. *Brain Res*, **252**, 367-372.

Satoh, K. & Fibiger, H.C. (1986) Cholinergic neurons of the laterodorsal tegmental nucleus: efferent and afferent connections. *J Comp Neurol*, **253**, 277-302.

Scarnati, E., Campana, E. & Pacitti, C. (1984) Pedunculopontine-evoked excitation of substantia nigra neurons in the rat. *Brain Res*, **304**, 351-361.

Scarnati, E., Di Loreto, S., Proia, A. & Gallie, G. (1988) The functional role of the pedunculopontine nucleus in the regulation of the electrical activity of entopeduncular neurons in the rat. *Arch Ital Biol*, **126**, 145-163.

Scarnati, E., Proia, A., Di Loreto, S. & Pacitti, C. (1987) The reciprocal electrophysiological influence between the nucleus tegmenti pedunculopontinus and the substantia nigra in normal and decorticated rats. *Brain Research*, **423**, 116-124.

Schafer, M.K., Varoqui, H., Defamie, N., Weihe, E. & Erickson, J.D. (2002) Molecular cloning and functional identification of mouse vesicular glutamate transporter 3 and its expression in subsets of novel excitatory neurons. *J Biol Chem*, **277**, 50734-50748.

Schofield, B.R. & Motts, S.D. (2009) Projections from auditory cortex to cholinergic cells in the midbrain tegmentum of guinea pigs. *Brain Res Bull*, **80**, 163-170.

Schwaller, B., Meyer, M. & Schiffmann, S. (2002) 'New' functions for 'old' proteins: the role of the calcium-binding proteins calbindin D-28k, calretinin and parvalbumin, in cerebellar physiology. Studies with knockout mice. *Cerebellum*, **1**, 241-258.

Schwarting, R.K. & Huston, J.P. (1996a) The unilateral 6-hydroxydopamine lesion model in behavioral brain research. Analysis of functional deficits, recovery and treatments. *Prog Neurobiol*, **50**, 275-331.

Schwarting, R.K. & Huston, J.P. (1996b) Unilateral 6-hydroxydopamine lesions of meso-striatal dopamine neurons and their physiological sequelae. *Prog Neurobiol*, **49**, 215-266.

Semba, K. & Fibiger, H.C. (1992) Afferent connections of the laterodorsal and the pedunculopontine tegmental nuclei in the rat: a retro- and antero-grade transport and immunohistochemical study. *J Comp Neurol*, **323**, 387-410.

Semba, K., Reiner, P.B. & Fibiger, H.C. (1990) Single cholinergic mesopontine tegmental neurons project to both the pontine reticular formation and the thalamus in the rat. *Neuroscience*, **38**, 643-654.

Semba, K., Reiner, P.B., McGeer, E.G. & Fibiger, H.C. (1988) Brainstem afferents to the magnocellular basal forebrain studied by axonal transport, immunohistochemistry, and electrophysiology in the rat. *J Comp Neurol*, **267**, 433-453.

Sequier, J.M., Hunziker, W., Andressen, C. & Celio, M.R. (1990) Calbindin D-28k Protein and mRNA Localization in the Rat Brain. *Eur J Neurosci*, **2**, 1118-1126.

Sesack, S.R., Deutch, A.Y., Roth, R.H. & Bunney, B.S. (1989) Topographical organization of the efferent projections of the medial prefrontal cortex in the rat: an anterograde tract-tracing study with Phaseolus vulgaris leucoagglutinin. *J Comp Neurol*, **290**, 213-242.

Shink, E., Sidibe, M. & Smith, Y. (1997) Efferent connections of the internal globus pallidus in the squirrel monkey: II. Topography and synaptic organization of pallidal efferents to the pedunculopontine nucleus. *J Comp Neurol*, **382**, 348-363.

Sidibé, M., Paré, J.-F. & Smith, Y. (2002) Nigral and pallidal inputs to functionally segregated thalamostriatal neurons in the centromedian/parafascicular intralaminar nuclear complex in monkey. *J. Comp Neurol*, **447**, 286-299.

Skinner, R.D. & Garcia-Rill, E. (1984) The mesencephalic locomotor region (MLR) in the rat. *Brain Res*, **323**, 385-389.

Skinner, R.D., Kinjo, N., Henderson, V. & Garcia-Rill, E. (1990a) Locomotor projections from the pedunculopontine nucleus to the spinal cord. *Neuroreport*, **1**, 183-186.

Skinner, R.D., Kinjo, N., Ishikawa, Y., Biedermann, J.A. & Garcia-Rill, E. (1990b) Locomotor projections from the pedunculopontine nucleus to the medioventral medulla. *Neuroreport*, **1**, 207-210.

Smith, Y., Bolam, J.P. & Von Krosigk, M. (1990) Topographical and Synaptic Organization of the GABA-Containing Pallidosubthalamic Projection in the Rat. *Eur J Neurosci*, **2**, 500-511.

Smith, Y., Pare, D., Deschenes, M., Parent, A. & Steriade, M. (1988) Cholinergic and non-cholinergic projections from the upper brainstem core to the visual thalamus in the cat. *Exp Brain Res*, **70**, 166-180.

Smith, Y., Parent, A., Seguela, P. & Descarries, L. (1987) Distribution of GABA-immunoreactive neurons in the basal ganglia of the squirrel monkey (Saimiri sciureus). *J Comp Neurol*, **259**, 50-64.

Sofroniew, M.V., Eckenstein, F., Thoenen, H. & Cuello, A.C. (1982) Topography of Choline Acetyltransferase-Containing Neurons in the Forebrain of the Rat. *Neurosci Lett*, **33**, 7-12.

Sofroniew, M.V., Priestley, J.V., Consolazione, A., Eckenstein, F. & Cuello, A.C. (1985) Cholinergic projections from the midbrain and pons to the thalamus in the rat, identified by combined retrograde tracing and choline acetyltransferase immunohistochemistry. *Brain Res*, **329**, 213-223.

Sommer, W., Bjelke, B., Ganten, D. & Fuxe, K. (1993) Antisense oligonucleotide to c-fos induces ipsilateral rotational behaviour to d-amphetamine. *Neuroreport*, **5**, 277-280.

Somogyi, P. & Klausberger, T. (2005) Defined types of cortical interneurone structure space and spike timing in the hippocampus. *J Physiol*, **562**, 9-26.

Spann, B.M. & Grofova, I. (1989) Origin of ascending and spinal pathways from the nucleus tegmenti pedunculopontinus in the rat. *J Comp Neurol*, **283**, 13-27.

Spann, B.M. & Grofova, I. (1991) Nigropedunculopontine projection in the rat: an anterograde tracing study with Phaseolus Vulgaris-leucoagglutinin (PHA-L). *J Comp Neurol*, **311**, 375-388.

Staiger, J.F., Masanneck, C., Schleicher, A. & Zuschratter, W. (2004) Calbindin-containing interneurons are a target for VIP-immunoreactive synapses in rat primary somatosensory cortex. *J Comp Neurol*, **468**, 179-189.

Starr, P.A., Vitek, J.L. & Bakay, R.A. (1998) Deep brain stimulation for movement disorders. *Neurosurg Clin N Am*, **9**, 381-402.

Steeves, J.D. & Jordan, L.M. (1984) Autoradiographic demonstration of the projections from the mesencephalic locomotor region. *Brain Res*, **307**, 263-276.

Stefani, A., Lozano, A.M., Peppe, A., Stanzione, P., Galati, S., Tropepi, D., Pierantozzi, M., Brusa, L., Scarnati, E. & Mazzone, P. (2007) Bilateral deep brain stimulation of the pedunculopontine and subthalamic nuclei in severe Parkinson's disease. *Brain*, **130**, 1596-1607.

Steininger, T.L., Rye, D.B. & Wainer, B.H. (1992) Afferent projections to the cholinergic pedunculopontine tegmental nucleus and adjacent midbrain extrapyramidal area in the albino rat. I. Retrograde tracing studies. *J Comp Neurol*, **321**, 515-543.

Steininger, T.L., Wainer, B.H., Blakely, R.D. & Rye, D.B. (1997) Serotonergic dorsal raphe nucleus projections to the cholinergic and noncholinergic neurons of the pedunculopontine tegmental region: a light and electron microscopic anterograde tracing and immunohistochemical study. *J Comp Neurol*, **382**, 302-322.

Steriade, M., Amzica, F. & Contreras, D. (1996) Synchronization of fast (30-40 Hz) spontaneous cortical rhythms during brain activation. *J Neurosci*, **16**, 392-417.

Steriade, M., Datta, S., Pare, D., Oakson, G. & Curro Dossi, R.C. (1990a) Neuronal activities in brain-stem cholinergic nuclei related to tonic activation processes in thalamocortical systems. *J Neurosci*, **10**, 2541-2559.

Steriade, M., Pare, D., Datta, S., Oakson, G. & Curro Dossi, R. (1990b) Different cellular types in mesopontine cholinergic nuclei related to ponto-geniculo-occipital waves. *J Neurosci*, **10**, 2560-2579.

Steriade, M., Pare, D., Parent, A. & Smith, Y. (1988) Projections of cholinergic and non-cholinergic neurons of the brainstem core to relay and associational thalamic nuclei in the cat and macaque monkey. *Neuroscience*, **25**, 47-67.

Stornetta, R.L., Sevigny, C.P. & Guyenet, P.G. (2002a) Vesicular glutamate transporter DNPI/VGLUT2 mRNA is present in C1 and several other groups of brainstem catecholaminergic neurons. *J Comp Neurol*, **444**, 191-206.

Stornetta, R.L., Sevigny, C.P., Schreihofer, A.M., Rosin, D.L. & Guyenet, P.G. (2002b) Vesicular glutamate transporter DNPI/VGLUT2 is expressed by both C1 adrenergic and nonaminergic presympathetic vasomotor neurons of the rat medulla. *J Comp Neurol*, **444**, 207-220.

Sugimoto, T. & Hattori, T. (1984) Organization and efferent projections of nucleus tegmenti pedunculopontinus pars compacta with special reference to its cholinergic aspects. *Neuroscience*, **11**, 931-946.

Sugimoto, T., Mizukawa, K., Hattori, T., Konishi, A., Kaneko, T. & Mizuno, N. (1984) Cholinergic neurons in the nucleus tegmenti pedunculopontinus pars compacta and the caudoputamen of the rat: a light and electron microscopic immunohistochemical study using a monoclonal antibody to choline acetyltransferase. *Neurosci Lett*, **51**, 113-117.

Sukhatme, V.P., Cao, X.M., Chang, L.C., Tsai-Morris, C.H., Stamenkovich, D., Ferreira, P.C., Cohen, D.R., Edwards, S.A., Shows, T.B., Curran, T. & et al. (1988) A zinc finger-encoding gene coregulated with c-fos during growth and differentiation, and after cellular depolarization. *Cell*, **53**, 37-43.

Takakusaki, K., Habaguchi, T., Nagaoka, T. & Sakamoto, T. (1997) Stimulus effects of pedunculopontine tegmental nucleus (PPTN) on hindlimb motoneurons in cats. *Soc. Neurosci. Abstr.*, **23**, 762.

Takakusaki, K., Saitoh, K., Harada, H. & Kashiwayanagi, M. (2004) Role of basal ganglia-brainstem pathways in the control of motor behaviors. *Neurosci Res*, **50**, 137-151.

Takakusaki, K., Shiroyama, T., Yamamoto, T. & Kitai, S.T. (1996) Cholinergic and noncholinergic tegmental pedunculopontine projection neurons in rats revealed by intracellular labeling. *J Comp Neurol*, **371**, 345-361.

Takamori, S., Rhee, J.S., Rosenmund, C. & Jahn, R. (2000) Identification of a vesicular glutamate transporter that defines a glutamatergic phenotype in neurons. *Nature*, **407**, 189-194.

Tsai-Morris, C.H., Cao, X.M. & Sukhatme, V.P. (1988) 5' flanking sequence and genomic structure of Egr-1, a murine mitogen inducible zinc finger encoding gene. *Nucleic Acids Res*, **16**, 8835-8846.

Ungerstedt, U. (1968) 6-Hydroxy-dopamine induced degeneration of central monoamine neurons. *Eur J Pharmacol*, **5**, 107-110.

Varoqui, H., Schafer, M.K., Zhu, H., Weihe, E. & Erickson, J.D. (2002) Identification of the differentiation-associated Na+/PI transporter as a novel vesicular glutamate transporter expressed in a distinct set of glutamatergic synapses. *J Neurosci*, **22**, 142-155.

Vertes, R.P. (1991) A PHA-L analysis of ascending projections of the dorsal raphe nucleus in the rat. *J Comp Neurol*, **313**, 643-668.

Vincent, S.R. (2000) The ascending reticular activating system--from aminergic neurons to nitric oxide. *J Chem Neuroanat*, **18**, 23-30.

Vincent, S.R., Satoh, K., Armstrong, D.M. & Fibiger, H.C. (1983) NADPH-diaphorase: a selective histochemical marker for the cholinergic neurons of the pontine reticular formation. *Neurosci Lett*, **43**, 31-36.

Vincent, S.R., Satoh, K., Armstrong, D.M., Panula, P., Vale, W. & Fibiger, H.C. (1986) Neuropeptides and NADPH-diaphorase activity in the ascending cholinergic reticular system of the rat. *Neuroscience*, **17**, 167-182.

Wainer, B.H., Bolam, J.P., Freund, T.F., Henderson, Z., Totterdell, S. & Smith, A.D. (1984) Cholinergic synapses in the rat brain: a correlated light and electron microscopic immunohistochemical study employing a monoclonal antibody against choline acetyltransferase. *Brain Res*, **308**, 69-76.

Wakabayashi, K., Takahashi, H., Obata, K. & Ikuta, F. (1992) Immunocytochemical localization of synaptic vesicle-specific protein in Lewy body-containing neurons in Parkinson's disease. *Neurosci Lett*, **138**, 237-240.

Wang, H.L. & Morales, M. (2008) Corticotropin-releasing factor binding protein within the ventral tegmental area is expressed in a subset of dopaminergic neurons. *J Comp Neurol*, **509**, 302-318.

Wang, H.L. & Morales, M. (2009) Pedunculopontine and laterodorsal tegmental nuclei contain distinct populations of cholinergic, glutamatergic and GABAergic neurons in the rat. *Eur J Neurosci*, **29**, 340-358.

Webster, H.H. & Jones, B.E. (1988) Neurotoxic lesions of the dorsolateral pontomesencephalic tegmentum-cholinergic cell area in the cat. II. Effects upon sleep-waking states. *Brain Res*, **458**, 285-302.

Winn, P. (2006) How best to consider the structure and function of the pedunculopontine tegmental nucleus: evidence from animal studies. *J Neurol Sci*, **248**, 234-250.

Winn, P. (2008) Experimental studies of pedunculopontine functions: are they motor, sensory or integrative? *Parkinsonism Relat Disord*, **14 Suppl 2**, S194-198.

Woolf, N.J. & Butcher, L.L. (1986) Cholinergic systems in the rat brain: III. Projections from the pontomesencephalic tegmentum to the thalamus, tectum, basal ganglia, and basal forebrain. *Brain Res Bull*, **16**, 603-637.

Wouterlood, F.G., Aliane, V., Boekel, A.J., Hur, E.E., Zaborszky, L., Barroso-Chinea, P., Hartig, W., Lanciego, J.L. & Witter, M.P. (2008) Origin of calretinin-containing, vesicular glutamate transporter 2-coexpressing fiber terminals in the entorhinal cortex of the rat. *J Comp Neurol*, **506**, 359-370.

Yamamoto, K., Mamelak, A.N., Quattrochi, J.J. & Hobson, J.A. (1990) A cholinoceptive desynchronized sleep induction zone in the anterodorsal pontine tegmentum: spontaneous and drug-induced neuronal activity. *Neuroscience*, **39**, 295-304.

Yasui, Y., Cechetto, D.F. & Saper, C.B. (1990) Evidence for a cholinergic projection from the pedunculopontine tegmental nucleus to the rostral ventrolateral medulla in the rat. *Brain Res*, **517**, 19-24.

Zrinzo, L., Zrinzo, L.V., Tisch, S., Limousin, P.D., Yousry, T.A., Afshar, F. & Hariz, M.I. (2008) Stereotactic localization of the human pedunculopontine nucleus: atlas-based coordinates and validation of a magnetic resonance imaging protocol for direct localization. *Brain*, **131**, 1588-1598.

Zweig, R.M., Jankel, W.R., Hedreen, J.C., Mayeux, R. & Price, D.L. (1989) The pedunculopontine nucleus in Parkinson's disease. *Ann Neurol*, **26**, 41-46.